17-AAG Mediated HSP90 Inhibition as an Effective Therapy for Lymphoma Stem Cells

by

Bryan W. Newman

A dissertation submitted in partial fulfillment
of the requirements for the degree of
Doctor of Philosophy
(Pharmaceutical Science)
in The University of Michigan
2012

Doctoral Committee:

Associate Professor Duxin Sun, Chair

Professor Gordon L. Amidon

Professor Peter X. Ma

Professor Max S. Wicha

To my parents, sisters, and all of my family, whose love, prayers, and support have made this possible.

Acknowledgements

First and foremost, I would like to thank my advisor, Dr. Duxin Sun, for all of his guidance and encouragement throughout my graduate career. His mentorship has led me to become an effective scientist, and has instilled within me a sense of leadership, humbleness, and eagerness to help others. I will always be grateful to him for teaching me these lessons.

I would like to thank my other committee members, Dr. Max S. Wicha, Dr. Gordon L. Amidon, and Dr. Peter X. Ma, for their helpful insights and support of my projects. I want to specially thank Drs. Yan Liu and Yin Wang for their tremendous help and support with my lymphoma studies. Special thanks also goes to the Wicha lab members Dr. Sarah J. Conley, for her help with experimental design and manuscript editing, and Drs. Hasan Korkaya, Suling Liu, and Sean McDermott, for their graciously provided cancer stem cell technical training and reagents. Thanks to Assistant Professor Felix Feng and his lab members Kari Wilder-Romans and Wei Chen for their assistance with my radiation studies. I would also like to thank past and present lab members Hsiu-Fang Lee, Yanke Yu, Tao Zhang, Peng Zou, Xiaoqin Li, Yasuhiro Tsume, Dr. Yiqun Jiang, Zhenkun Zhu, Yanyan Li, Joseph Burnett, Jamie Connarn, and Hayley Paholak for their support. Lastly I would like to thank all my friends and colleagues in the department of Pharmaceutical Science, which have made my graduate studies a wonderful experience.

Table of Contents

List of Figures

Abstract

Peripheral T-Cell Lymphomas (PTCL) are rare cancers that lack effective therapies, resulting in poor long-term survival in patients. Cancer stem cells (CSCs) represent a subpopulation within tumors that have been implicated in drug resistance, recurrence, and metastasis, all of which influence the long-term survival of patients. Therefore, to increase patient response, it will be necessary to identify inhibitors that efficiently eliminate CSCs. Initial methods for targeting CSCs have relied on disrupting stem cell proliferation, a process called self-renewal. However, multiple pathways can govern the self-renewal process, potentially providing redundancy to treatments which target only one of these pathways. A better approach would be to block multiple self-renewal pathways simultaneously through inhibition of the molecular chaperone Heat Shock Protein 90 (HSP90) with 17-AAG. As human PTCL is comprised of many tumor subtypes, a transgenic mouse model of T-cell lymphoma was used to examine the efficacy of 17-AAG in treating lymphoma CSCs. Strikingly, lymphoma and Acute Myeloid Leukemia (AML) CSCs were selectively sensitive to 17-AAG treatment, as low concentrations of 17-AAG induced apoptosis and ablated their ability to form colonies, while having little effect on the differentiated tumor bulk. These effects were found to result from the loss of HIF1a function, which is crucial for the maintenance of both mouse lymphoma and AML CSCs. In addition, the non-CSCs were shown to express higher levels of Heat Shock Factor-1 (HSF1), a transcription factor which regulates

chaperone genes such as HSP90 and HSP70. Knockdown of HSF1 resulted in reduced mRNA expression of HSP90α, reduced colony formation, and sensitization of non-CSCs to 17-AAG treatment. This implicates high HSF1 expression as a potential 17-AAG resistance mechanism. Lastly, to broaden the scope of 17-AAG as a CSC-targeting agent, 17-AAG was tested for the ability to sensitize breast CSCs to radiation, a conventional treatment. Interestingly, radioresistance and sensitization to radiation with 17-AAG was not universally observed in CSCs within and between breast cancer lines. Taken together, these results validate 17-AAG mediated HSP90 inhibition as a method for treating lymphoma CSCs, and merits clinical reevaluation as a CSC-sensitizer to conventional cancer therapy.

Chapter 1

Background and Introduction

Current Classifications of T-Cell Lymphoma

Hematopoietic cancers are divided into two main categories: leukemia and lymphoma. While leukemia is characterized by the presence of white blood cells circulating in the blood, lymphomas conventionally reside within the nodal system of the lymphatics, although extranodal lymphomas have also been described. Lymphomas are further subdivided into two main classes: Hodgkin's and Non-Hodgkin's Lymphoma (NHL). Hodgkin's lymphoma is classified by the presence of "Reed-Sternberg" cells, first observed by Dorothy Reed and Carl Sternberg [1]. Unlike Hodgkin's lymphoma, Non-Hodgkin's lymphoma can originate from a variety of white blood cells. Approximately 12% of NHLs originate from T-cells, with the remaining NHLs originating from B-cells [2]. Within T-Cell Lymphomas, the World Health Organization distinguishes 4 subcategories, depending on the cancers clinical presentation and preferred site of growth.

Nodal TCL

T cell lymphomas within lymph nodes are classified as Peripheral T-cell lymphomas (PTCL). These are further divided into subtypes including Angioimmunoblastic T-cell lymphomas (AITL) (18.5% of PTCL) [3] and Anaplastic

Large Cell Lymphoma (ALCL), which are further divided based on the expression of ALK fusion proteins (ALK+ 6.6% of PTCL, ALK- 5.5% of PTCL) [3]. Finally, a large subset of PTCLs are designated as Not Otherwise Specified (NOS) (25.9% of PTCL) [3, 4]. To date, the most well characterized TCL is an ALCL which expresses fusion proteins containing the constitutively active ALK tyrosine kinase. ALK+ ALCL make up 50-85% of ALCL cases, and hold the best prognosis of TCLs. In vitro studies of ALK+ ALCL has shown that the JAK-STAT3 pathway is a crucial mediator of ALK signaling, enhancing cellular proliferation and survival [5]. Despite lacking expression of ALK fusion proteins, ALK- ALCL cells show a similar gene transcription profile as ALK+ ALCL. The cells of origin, as well as the signaling pathways governing PTCLs, have been an area of considerable investigation. Evidence suggests ALK- ALCL originates from transformed activated cytotoxic T-cells [6]. However, the mechanism for this transformation has not yet been defined [5]. Further studies have identified follicular helper T cells as potential transformed cells of origin in AITL [7-9]. While several expression markers, such as CXCL13, can be used to accurately identify neoplastic cells in AITL, aberrant signaling pathways responsible for transformation and proliferation have not been identified [5, 10]. With the exception of Platelet-derived Growth Factor Receptor (PDGFRA) tyrosine kinase [11, 12] and Spleen Tyrosine Kinase (SYK) [13, 14] overexpression and activation, identifying neoplastic cells and their transformative mechanisms remains a challenge in PTCL-NOS [5]. Comprised of both small and large lymphoma cells, PTCL-NOS has variable expression of antigens associated with T-cells, with loss of CD7 occurring more frequently than CD3. Most cases of PTCL-NOS have CD4 expression, and contain cells with increased expression of proteins involved in

metastasis (LAMB1, COL1A2, FN1) and decreased expression of pro-apoptotic proteins [11].

Extranodal TCL

T-cell lymphomas that are extranodal are comprised of hepatosplenic γδ T-Cell lymphoma (1.4% PTCL), enteropathy-associated T-Cell lymphoma (4.7%), NK/T-cell lymphoma (nasal type) (10% of PTCL), and subcutaneous panniculitis-like TCL (0.9% PTCL). Extranodal TCLs are commonly disseminated and rarely associate with lymph nodes. Hemophagocytic syndrome commonly occurs with extraonodal TCL [15, 16]. NK/TCL is most prevalent in Asia, Mexico, and South America [17]. While much is still unclear regarding how NK/TCL is initiated, the partial loss of chromosome 6 appears to be a frequent occurrence [18, 19]. This region contains notable tumor suppressors (PRDM1, ATG5, AIM1, and HACE1), the loss of which could provide a mechanism for transformation [20, 21]. Additionally, several signaling pathways (PDGFRA, AKT, JAK, STAT, NF-kB) have been shown to be activated in NK/TCL, providing potential therapeutic targets [21, 22]. Enteropathy-associated TCL (ETL) involves the formation of ulcerated jejunal lesions containing intestinal intraepithelial lymphocytes (IEL), which can cause perforation of the small intestines. ETL is divided into two categories, type I (coeliac-associated) and type II (coeliac-unassociated) [5]. ETL type I is viewed as a complication of gluten insensitivity, and presents with necrotic tumors containing inflammatory cells. Several chromosomal aberrations (amplifications, deletions, partial trisomy), and the up regulation of proinflammatory cytokine IL-15 have been implicated in transformation of IELs [23-27]. Interestingly, both types of ETL have alterations in

chromosome 9 with regions near the genes for NOTCH1 and ABL1 [28]. Some TCLs such as hepatosplenic γδ and panniculis TCLs are characterized by the receptors they express. Hepatosplenic γδ TCL is a rare TLC predominately affecting men. To date, the isochromosome 7q as well as chronic immune suppression have been suggested as potential mechanisms triggering the initiation of hepatosplenic TLC [5, 29-32]. Finally, panniculitis-like TCL is characterized by T-cells with the αβ T-cell Receptor (TCR). Five year survival following treatment with this disease is high (82%), and efforts to understand tumor initiation are ongoing [5, 33].

Cutaneous TCL

The cutaneous form of TCL (CTCL) also presents as extranodal, and similar to other categories of TCL, encompasses an assortment of tumor types. The majority of CTCL (approximately 66%) are either mycosis fungoides (MF) or Sézary's syndrome (SS) [33, 34]. MF CTCL originates from the transformation of an effector memory T-helper cell, which exhibits the characteristic cerebriform nucleus [33]. SS is the more aggressive leukemic variant of CTCL, and originates from central memory T-helper cells that can be found in peripheral blood [35]. Numerous signaling pathways have been implicated in the initiation of this disease. Both MF and SS exhibit increased expression of NOTCH1 [36]. Activation of both NF-kB and STAT3 have also been detected in MF [37-40]. In SS, the loss of the cell cycle checkpoint proteins p16/INK4A and p14/ARF lead to decreased p53 activity and uncontrolled proliferation [41, 42]. The second most common type of CTCL are primary CD30+ lymphoproliferative disorders. These include two types: primary cutaneous anaplastic large cell lymphoma (C-ALCL), and

lymphomatoid papulosis, representing two extremes of the CTCL disease spectrum. In C-ALCL, transformed CD4+ T-cells are present, and lack expression of ALK fusion proteins. Lymphomatoid papulosis is characterized by recurring, self-healing papular nodules. Compared to other TCLs, lymphomatoid papulosis has a high success rate following therapy, and usually requires a low-dose methotrexate for achieving stable remission [43, 44].

Leukemic-like TCL

The majority of leukemic-like TCL are comprised of human T-lymphotropic virus type 1 (HTLV-1) associated adult T-cell lymphoma, T-cell chronic large granular lymphocytic leukemia (TGL), aggressive natural killer-cell leukemia (ANKL), and T-cell prolymphocytic leukemia [4]. In HTLV-1 adult TCL, T-cells become activated with uncontrolled proliferation when the HTLV-1 viral protein is activated within the cell. The aggressive form of this disease carries a poor prognosis due to tumor cell drug resistance and the suppression of the immune system, which can allow fatal infections to occur [45-48]. In addition, aberrant activation of NOTCH1 has been implicated in adult TCL [49]. TGLs account for 2-5% of PTCLs, and involve T-cells that have been activated through either aberrant self-recognition or viral interaction [50-54]. As seen with other diseases described above, dysregulated signaling through JAK/STAT, NF-kB, PI3K/AKT, MAPK/ERK/Ras, and Fas pathways are believed to drive persistence of this disease [54-58]. TGL is one of the less aggressive TCLs, with median survival greater than 10 years [59]. ANKL is characterized by uncontrolled NK proliferation within the peripheral blood and bone marrow [60]. The initiation of this disease is believed to result

from a defective response to the Epstein-Barr Virus (EBV). Loss of chromosome 6q is typical with ANKL [61]. Similarly, T-cell prolymphocytic leukemia has been associated with EBV infection [62]. In addition, activation of the AKT-associated protooncogene TCL-1 [63, 64], and loss of the tumor repressor ATM are a prevalent occurrence in patients diagnosed with T-cell prolymphocytic leukemia [65, 66]. As with most PTCLs, prognosis with this disease remains poor, despite newly developed therapies [67].

Survival and Treatment Options

In the United States, 1 in 100,000 people will develop PTCL each year [68]. In general, the prognosis for patients diagnosed with TCL is poorer compared to patients with aggressive forms of BCL [3]. Overall survival (OS) and failure-free survival (FFS) in patients with the most prevalent for of PTCL, PTCL-NOS is between 10% to 20% at a 10-15 year follow up [4]. As NHL is predominately comprised of B-Cell lymphomas, most large controlled clinical trials have been carried out to test therapeutics on BCLs rather than TCLs. Thus, patients diagnosed with TCL are, for lack of a better option, typically given therapies proven effective against BCL [4].

CHOP Therapy

The first line of therapy for PTCL, which is also the standard care for BCL patients, is the administration of CHOP (cyclophosphamide, doxorubicin, vincristine, and prednisone). Cyclophosphamide is a prodrug that, once converted in the liver to nitrogen mustards, can cause DNA alkylation and crosslinking [69-71]. Doxorubicin is a classical anthracycline also used in the treatment of solid tumors, known to intercalate within

DNA, inhibiting DNA synthesis and replication [72, 73]. Vincristine is a vinca alkaloid that has been demonstrated to block microtubule synthesis through its reversible interaction with the tubulin subunits [74]. Prednisone is an anti-inflammatory agent that works via inhibiting the glucocorticoid receptor to reduce the painful swelling that typically accompanies lymphomas. Taken together, patients treated with CHOP have a 5 year OS of 37.5% [75]. The International Peripheral T-cell Lymphoma project also reported an OS and FFS of 32% and 22%, respectively [76].

Combinations with CHOP Therapy

Immunotherapy in addition to CHOP has been assessed using an anti-CD52 humanized monoclonal antibody known as Alemtuzumab. CD52 is an antigen on both normal and malignant T- and B-cells, making it a suitable target for patients suffering from lymphomas. When given as a single agent, Alemtuzumab had an overall response rate of 36% in relapsed PTCL [77]. Unfortunately, due to the expression of CD52 on normal T- and B- cells, the use of Alemtuzumab results in dramatic immune suppression, resulting in increased opportunistic infections in patients. This immune suppression is believed to be the reason for the high treatment-related mortality. In combination with CHOP, Alemtuzumab therapy had an overall response rate of 80% and a 1-year event free survival of 43%, mirroring results typically seen with CHOP therapy alone [78]. A phase II trial testing the combination of these therapies was stopped early due to unacceptable treatment-related deaths. Another trial conducted by the GITIL utilized a single pretreatment with Alemtuzumab prior to beginning CHOP cycles. This resulted in

fewer side effects, and a complete response and estimated 2-year FFS of 71% and 48% respectively [79].

Other antibodies under development for PTCLs include MDX-060 and Zanolimumab. MDX-060 recognizes CD30, a surface antigen preferentially expressed on tumor cells, such as ALCL and some PTCL-NOS. While MDX-060 has only been used as a single therapy in trials thus far, reports of stable disease with low issues of toxicity make this antibody a likely candidate for a combination study in future trials [80, 81]. Zanolimumab is a human monoclonal antibody which targets the CD4 antigen on T-helper cells. Reponses seen with Zanolimumab were modest (24%), however low toxicity with this therapy also make it a candidate for CHOP combination [82].

CHOP has also been combined with Denileukin-diftitox, a genetically engineered fusion protein tethering the A and B fragments of diphtheria toxin to the binding domain of IL-2. This leads to the uptake of the fusion protein by IL-2R expressing immune cells [83]. Initial trials with this therapy found an overall response rate and median progression free survival (PFS) of 48% and 6 months, respectively [84]. Combining Denileukin-diftitox with a CHOP regimen resulted in high response rates in AITL (80%) and ALCL (87%), but demonstrated little improvement in patients with PTCL (47%) [85]. The combination of gemcitabine and etoposide has been used in addition to CHOP. Gemcitabine is a nucleoside analogue that exerts its tumor inhibition through two mechanisms: incorporation of the active metabolite into DNA during replication, and inhibition of the ribonucleotide reductase enzyme. Efficacy seen with Gemcitabine as a single agent ranges from 20-69% [86-88]. When used in combination with CHOP and

etoposide, overall response rates were 77%, but were accompanied by grade 4 neutropenia, suggesting dose optimization is still needed [89].

Alternatives to CHOP Based Therapies

Inhibitors of Histone Deacetylases (HDAC) have recently been assessed as therapeutics in TCL patients. Chromatin structure is governed by the balance of two classes of enzymes: HDACs and Histone Acetyltransferases (HAT). Acetylation of histones via HATs leads to DNA unwinding, allowing increased access of transcriptional factors to genes that would otherwise be sequestered by their local histone. Opposing this action are HDACs, which remove acetyl groups from histones, facilitating sequestering of the DNA. Thus, treatment with HDAC inhibitors results in increased acetylation and subsequent gene transcription, resulting in cell cycle arrest and death in malignant cells [86]. Phase I/II clinical trials testing the HDAC inhibitor Romidepsin have shown an overall response rate of 28% in patients with relapsed/refractory PTCL [90, 91].

Another drug that has been tested on patients diagnosed with PTCL is Pralatrexate. A structural analogue of methotrexate, Pralatrexate functions as an antimetabolite, interfering with DNA synthesis through inhibition of Dihydofolate Reductase. Initial Phase I/II studies indicated TCLs were selectively sensitive to Pralatrexate therapy. Patients with relapsed/refractory PTCL showed an overall response rate of 29%, with toxicity limited to mucositis, thrombocytopenia, and neutropenia [92, 93].

In addition to chemotherapy, autologous stem cell transplantation (ASCT) has been tested in patients with PTCL. For this treatment, patients are first treated with

standard therapy in order to achieve disease remission prior to removing hematopoietic stem cells from the patient's blood and/or bone marrow for long-term storage. Patients are then treated with high intensity chemotherapy or radiation to eliminate all of the remaining malignant cells. As this also depletes the patient's own healthy stem cells, previously stored stem cells are then reintroduced to the patient to replenish their blood system [94]. Patients with relapsing BCLs that are refractory to standard treatment exhibit an increase in 5-year disease free survival (46%) with ASCT therapy compared to chemotherapy alone (12%) [95]. Given these promising results in BCLs, subsequent studies have examined this therapy in PTCLs. In one phase II trial, patients were first treated with mega-CHOP (dose-escalated CHOP) before ASCT. After 2 years, OS and PFS were 73% and 53%, respectively [96]. In an additional larger clinical trial, CHOP therapy combined with ASCT resulted in a 3 year overall and disease free survival of 48% and 53% respectively [97]. ASCT has also been utilized in PTCL patients who have relapsed following standard therapy, with 30% to 50% achieving long term disease free survival. However, the greatest predictor of ASCT response is the level of remission achieved by the initial debulking therapy. If the PTCL is refractory to CHOP therapy prior to ASCT, OS remains poor [98-100].

Conclusions from TCL Therapies Thus Far

As TCL is a very heterogeneous disease, encompassing many subtypes which demonstrate varied responses to treatment, development of effective first line therapies remains a complicated problem. As a result, prognosis and survival for many of the TCL subtypes remains poor. The use of promising BCL therapies in TCL patients has not

resulted in significant long term survival. Despite reported response rates of 50-70% in most TCL clinical trials, OS remains low at 10-30% [101-105]. Testing new therapies for TCL is complicated by the difficulty in accruing adequate patient numbers to effectively examine new combination therapies. Aside from the few regulating pathways described above, inadequate understanding of the mechanisms driving the majority of TCLs, in particular PTCL-NOS, impedes the development of novel targeted therapies. Improved therapies that can specifically target these regulatory mechanisms is necessary to increase therapeutic response rates and improve overall patient survival. In this regard, utilization of TCL preclinical models, namely murine models, may allow for more rapid delineation of T-cell transformative events, and thereby identify novel drug targets.

Identification and Characterization of TGB Mice

Increased cancer rates have been observed in patients who undergo dramatic immune suppression, including HIV infection or induced suppression in organ transplant patients [106-108]. In contrast, most transgenic mice lacking innate T-cell immunity, do not exhibit increased incidence of cancer [109]. By taking advantage of the allelic exclusion that exists in lymphocytes, random integration of T-cell Receptor (TCR) αβ chains into the genome allowed for the development of mouse strains lacking T-cell immunity [110]. Similar to previous observations, the majority of TCR transgenic mice resulted in little to no increase in cancer incidence, with the exception of occasional thyomas [111]. However, Wang et al. discovered that one strain of transgenic mice, designated as TGB, developed an aggressive TCL with a 6-month median survival [112].

Closer examination of the TGB mouse TCL revealed that TCR integration had occurred within intron 1 of the Epm2a gene, resulting in the reduced expression of its gene product laforin. In addition, mice heterozygous for the TCR transgene also succumbed to TCL. Examination of the Epm2a promoter region showed signs of silencing by hypermethylation in heterozygous mice that had progressed to disease. To determine if loss of laforin was sufficient to initiate tumor growth, the authors transfected normal mouse bone marrow cells with siRNA to Epm2a, recapitulating the loss of laforin in TGB mice. Epm2a knockdown in these cells increased growth and survival in vitro. Furthermore, when mice were injected with cells that had Epm2a knocked down, they succumbed to disease closely resembling TGB mice with TCL. Lastly, complementation of Epm2a in transgenic mice reduced the incidence of TGB TCL and prolonged its onset. Wang et al. concluded from these results that laforin is a tumor suppressor, whose loss is sufficient to initiate tumor formation [112].

Laforin functions as a protein phosphatase, and in the context of TGB TCL, regulates the function of the kinase GSK-3β [112]. As a crucial regulator of the Wnt/β-catenin signaling network, GSK-3β antagonizes β-catenin through phosphorylation at Serines 33 and 37 leading to its degradation via the proteasomal pathway [113-116]. In their study, Wang et al. demonstrated that under normal conditions, laforin prevents GSK-3β inactivation via AKT-mediated phosphorylation at the Serine 9 position [111]. This functions to prevent aberrant activation of the Wnt/ β-catenin pathway, which has been linked to the promotion of numerous types of solid and hematological cancers [117]. In terms of TGB TCL, Wang et al. showed that with the loss of laforin expression, a dramatic increase in inactivated, serine 9 phosphorylated GSK-3β occurred, accompanied

by the nuclear translocation of β-catenin. Lastly, little to no expression of the Epm2a gene, as well as the high nuclear accumulation of β-catenin were observed in human TCL cell lines, demonstrating that the molecular phenotype in TGB TCL was also present in human TCL [112]. Taken together, TGB TCL comprises an aggressive disease with committed, mature T-cells under the control of aberrantly activated β-catenin signaling.

Influence of Cancer Stem Cells in Solid and Hematological Malignancies

Although response rates in some TCLs can be as high as 70%, these malignancies ultimately recur in a majority of patients, resulting in low OS rates. In addition, current therapeutic strategies for relapsed and refractory TCL are limited, emphasizing the need for novel agents. The lack of effective therapy for patients whose disease has progressed is not unique to TCL, or hematological cancers in general. Treatment for patients with relapsed or progressive solid tumors is largely palliative, with few curative strategies. Due to the lack of efficacy of most cancer therapies, new lines of research have reassessed the classical models of tumor initiation and growth, as well as the accepted strategies for patient treatment.

For the majority of the past century, cancer was thought of as a disease of the proliferative cell, where a tumor could be described as a clonally associated cellular mass with aberrantly enhanced growth, and whose origin was the result of stochastically driven accumulation of mutational events. Under this mindset, the majority of efforts in treating cancers consisted of using agents which could exploit the rapid proliferation of cancer cells to induce cell death [118]. As molecular biology has increased the understanding of signaling pathways governing the proliferation and survival in many malignancies, new

targeted-therapies have been developed. However, these new therapies still target the cells which comprise the tumor bulk. With the exception of treatment-resistant clones, these drugs were expected to be effective in all tumor cells carrying the targeted genetic lesion [118]. However, results from clinical trials testing these new agents have brought these assumptions into question. Surgery, radiation and chemotherapy can all be used to effectively inhibit the proliferative population in many types of cancers. However, tumor relapse and metastatic progression remain major challenges to overall patient outcome, despite strong responses to initial treatment [119].

The failure of current cancer therapies to address relapse and disease progression has driven oncology research to reexamine tumor composition, namely its heterogeneity. Stemming from pioneering work in the late 1930s with single cell tumorigenicity [120], and the early 1970s with classification of tumor heterogeneity in human AML samples [121, 122], the notion that all tumor cells behaved and performed a similar function has been changing. In contrast to previous models, the cancer stem cell (CSC) theory put forth that tumors are initiated and sustained by a rare population of cells which possess the capacity for self-renewal and can give rise to more differentiated cells that form the bulk of the tumor. The CSC hypothesis was firmly established after the hierarchical arrangement of AML was elucidated, validating that a subpopulation comprising 0.1-1% of the tumor bulk contained the tumorigenic capacity when reimplanted in mice [123-125]. Since these pioneering observations, a number of hematological and solid cancers have been shown to contain tumor initiating/cancer stem cells such as CML, ALL, multiple myeloma, brain, breast, colon, and prostate [126-134].

The origin of CSCs continues to be a topic of debate. The number of normal stem cells in the body is maintained through asymmetric cell division (ACD), generating one new identical stem cell (via self-renewal) and a progenitor cell [135]. The progenitor cell (lacking self-renewal) can continue down the differentiation pathway, as directed by its genetic programming and the surrounding microenvironment [136]. ACD helps maintain an adequate ratio of stem to differentiated cells within a tissue. Symmetric cell division (SCD) in stem cells is also possible, and has been associated with wound healing [135]. As SCD is capable of expanding the stem cell pool, this process is tightly regulated primarily via self-renewal pathways, including the Wnt, Sonic Hedgehog, and NOTCH pathways. Hematopoietic, gut, and epidermal stem cells have been shown to rely on Wnt signaling for control of self-renewal [137, 138]. The binding of Wnt ligands to the Frizzled receptor leads to the nuclear translocation of the transcription factor β-catenin, and subsequent transcription of genes related to self-renewal [139]. In the Sonic Hedgehog pathway, hedgehog ligands (Sonic Hedgehog/Shh; Desert Hedgehog/Dhh; Indian Hedgehog/Ihh) can be secreted from neighboring cells to bind the transmembrane receptors (Hip1 and Patched). This leads to the release of the Gli transcription factors, which translocate to the nucleus and transcribe genes involved in proliferation and angiogenesis [140-142]. The NOTCH pathway has been shown to be vital for cell fate decision in a variety of tissues, particularly in hematopoietic stem cells [143, 144]. NOTCH signaling occurs through the association of NOTCH ligands (DLL1, DLL3, DLL4, Jagged1, Jagged2) with one of four NOTCH receptors (NOTCH1-4) [145]. This interaction causes the cleavage of the NOTCH and the release of the NOTCH intracellular domain (NICD), which translocates to the nucleus to initiate gene

transcription [143]. Aberrant activation of these self-renewal pathways has been observed in a variety of cancers. Activated Wnt signaling in epidermal stem cells resulted in the development of skin cancer, as demonstrated using transgenic mice [146]. Upregulation of the transcription factor β-catenin has also been noted in breast cancer [147]. Activation of the Sonic Hedgehog pathway has been reported in brain, prostate and pancreatic cancers [148, 149]. Many of components of the pathway are known oncogenes (Smo, Shh, Gli1, Gli2) and tumor suppressors (Patched) [141]. As with the Sonic Hedgehog pathway, numerous hematopoietic and solid cancers have been associated with activating mutations and amplifications of NOTCH signaling pathway components [150, 151]. It has been reported that in 50% of breast cancers, the NOTCH inhibitor Numb is downregulated [152, 153]. Also striking is that 50% of T-cell acute lymphoblastic leukemias have mutations in the NOTCH1 gene [154]. While identification of aberrant regulation of these pathways has provided initial targets for therapy, it remains unanswered whether CSCs originate from normal stem cells via the loss of self-renewal control or from progenitor/mature cells via reactivation of self-renewal [155-157].

The CSC hypothesis has provided an alternate theory for explaining the current failures seen in the clinic. CSCs have been shown to possess a whole host of cellular defenses against damage originating from innate physiological processes as well as drug- or radiological-related processes [158]. Cellular efflux pumps expressed on the plasma membrane can lower intracellular drug concentrations by actively removing therapeutic agents from the cell. Similar to normal stem cells, CSCs have been found to overexpress these transporter proteins, thereby increasing their resistance to agents which the tumor

bulk might be sensitive [159-162]. In addition, CSCs exhibit enhanced DNA repair, and overexpress anti-apoptotic proteins, both of which increase CSC tolerance to damage that would normally induce cell death, allowing more time for repair [163, 164]. These resistance mechanisms allow CSCs to escape therapies which normally induce dramatic death of cells within the tumor bulk, thereby permitting relapse to occur after cessation of treatment [119, 165, 166]. Lastly, along with their supposed role in relapse, CSCs have also been implicated in metastatic spread of the disease [167]. It is well-known that the formation of metastatic lesions is a highly dynamic and inefficient process. The percentage of cancer patients that exhibit circulating tumor cells can be as high as 90%, while distant metastasis form in only a portion of all patients (20-30%) [168-171]. This suggests that only a minority of tumor cells are capable of both migration and tumor initiation. These concepts have been described in a recent model by Li et al, in which the initial cellular CSC transformation selects the type of cancer formed, and the degree of spread mediated by these CSCs [172]. Utilizing cues from the environment that favor stem cell retention, such as low oxygen [173, 174], circulating CSCs traffic to distant sites and reestablish tumors that carry many of the same genetic lesions seen in the primary tumor. These observations highlight the role that CSCs play in tumor biology, and their clinical implications.

Given the association of CSCs with tumorigenesis, resistance to therapy, recurrence and metastatic spread, development of an effective CSC-specific treatment will profoundly impact the severity of cancer. A number of approaches have been used to target CSCs, ranging from inhibition of oncogenic proteins associated with self-renewal either directly (NOTCH via γ-secretase; Sonic Hedgehog via Smoothened) [175,

176] or indirectly (Her2, bcr/abl) [177, 178], to sensitization to conventional radiotherapy [163, 179]. It is important to note that inhibitors that are designed to block self-renewal pathways may present unwanted patient toxicity, as both normal stem cells and CSCs are likely to be targeted. Therefore, discovery of novel agents that can specifically eliminate CSCs over their normal counterparts is still currently needed.

CSCs in TGB Lymphoma

As discussed earlier, Wang et al showed that the committed, mature TGB lymphoma cells that comprised the tumor bulk were driven by the constitutively activated β-catenin pathway, caused by the loss of the GSK-3β phosphatase, laforin. In order to determine if the TGB lymphoma cells had a CSC subpopulation similar to other hematological and solid cancers, several dilutions of cells with and without the expression of both c-Kit and Sca1 were injected into mice [180]. Hematopoietic cells expressing both c-Kit and Sca1 have been shown to contain stem-cell characteristics, such as reconstitution of bone marrow following sublethal radiation, thus demonstrating the ability of these markers to identify stem cell populations [181]. Indeed, as little as $1x10^2$ c-Kit^+Sca1^+ TGB lymphoma cells could reinitiate lymphoma after transplantation into healthy B10.BR mice. In contrast, $1x10^4$ c-Kit^-Sca1^-cells were needed for lymphoma engraftment, indicating an enhanced tumorigenic potential of the c-kit^+Sca1^+ subpopulation. When cultured in vitro, the c-Kit^+Sca1^+ subpopulation remained at 0.5-1.5% of the tumor cells, and was capable of replenishing the c-Kit^-Sca1^- population indefinitely. Lastly, these CSCs could serially transplant the lymphoma in vivo, demonstrating self-renewal.

To investigate the molecular mechanisms driving the tumorigenic subpopulation, Wang et al screened a number of pathway inhibitors, targeting AKT, mTOR, NF-kB, JNK, and HIF1α, among others [180]. Of the compounds tested, Echinomycin (a HIF1α inhibitor) dramatically reduced the ability of the c-Kit^{+}Sca1^{+} cells to form colonies. These CSCs were astonishingly sensitive to HIF1α inhibition, with doses as low as 20 pM inducing apoptotic cell death. When tested in vivo, all mice given Echinomycin (10 μg/kg) survived up to 252 days, with no signs of lymphoma as assessed during necropsy. In contrast, all vehicle-treated mice succumbed to lymphoma between 6-10 weeks post tumor cell implantation. These results demonstrated that HIF1α activity was at the center of TGB lymphoma CSC maintenance and survival.

Hypoxia Inducible Factor 1a (HIF1α) is a member of the Hypoxia Inducible Factor proteins that regulate gene response during times of low oxygen (O2 pressure between 5-10 mmHg). HIF1α is a heterodimer, consisting of the constitutively expressed HIF1β and the oxygen regulated HIF1α. Under normoxia, prolyl hydroxylases modify HIF1α using O2 as a substrate. Hydroxylated HIF1α is a substrate for the von Hippel-Lindau (VHL) E3 ubiquitin ligase, which ubiquitinates HIF1α under normoxic conditions, resulting in proteasomal degradation. Under hypoxia, HIF1α is no longer hydroxylated, allowing it to associate with HIF1β to form a transcriptional complex [182, 183]. Many stem cell associated genes have been linked to HIF1α activity. The efflux pumps MDR1 and BCRP are regulated through HIF1α mediated transcription [184, 185]. In addition, stem cell maintenance and self-renewal have also been associated with HIF1α. The NOTCH pathway, a highly conserved signaling mechanism important for a

number of tissue stem cell populations [186-189], has been shown to be enhanced through direct interaction of HIF1α [190].

To explore the mechanism controlling the difference seen following HIF1α inhibition between TGB lymphoma CSCs and the tumor bulk, c-Kit^{+}Sca1^{+} and c-Kit^{-} Sca1^{-} cells were isolated via flow cytometry, and the mRNA and protein expression levels were analyzed. Strikingly, HIF1α protein expression was found exclusively within the CSC subpopulation. This result explained the observed selectivity of the Echinomycin treatment, as the reduced efficacy of HIF1α ablation in the committed c-Kit^{-}Sca1^{-} cells coincided with the lack of HIF1α expression in these cells. As discussed above, cellular levels of HIFs are regulated by the level of oxygen in the environment. As the expression of HIF1α in TGB lymphoma CSCs was detected under normoxia, Wang et al determined the expression levels of HIF regulatory proteins in order to understand this discrepancy. As predicted, CSCs were found to lack expression of VHL, whereas non-CSCs expressed high levels of VHL. In line with the necessity for HIF1α activity for CSC survival, ectopic expression of VHL in the TGB CSCs eliminated this population, and reduced their tumorigenicity in vivo. With a deficient mechanism for degrading HIF1α, TGB lymphoma CSCs maintain HIF1α expression under normoxia, and rely on its activity for maintenance.

While the committed tumor bulk was found to rely on aberrantly activated β-catenin signaling, inhibition of this pathway was not found to influence TGB lymphoma CSC self-renewal. In contrast, treatment with the γ-secretase inhibitor L-685458, an agent targeting the NOTCH signaling pathway, was found to block CSC colony formation. Transfection of a dominant-negative form of the NOTCH intracellular

transcription complex also reduced the number of TGB lymphoma CSCs and their tumorigenicity in vivo. This suggested that aberrantly activated NOTCH signaling may be how HIF1α maintains self-renewal in the TGB lymphoma CSCs. It was later demonstrated that inhibition of HIF1α led to the reduced expression of Hes1, a NOTCH target gene. Moreover, a HIF1α binding site was identified near Hes1 binding sites within the Hes1 promoter. These Hes1 sites function as a negative feedback mechanism to control the level of Hes1 expression [191, 192]. Hes1 promoter repression, via ectopically expressed Hes1 or NOTCH intracellular domain, was reduced through expression of an oxygen resistant HIF1α mutant. Lastly, HIF1α was found to compete with Hes1 for promoter binding, as assessed through chromatin immunoprecipitation. Taken together, these results suggest the interaction of HIF1α with NOTCH facilitated maintenance of TGB lymphoma CSC self-renewal [180].

Through the sustained expression of HIF1α, and subsequent maintenance of NOTCH transcriptional activity, TGB lymphoma CSCs can be maintained in vitro indefinitely. Aberrant activity of the NOTCH pathway has previously been shown to promote cellular transformation. Forced activation in T-cell progenitors resulted in the onset of acute T-cell lymphoblastic leukemia [193]. In addition, other hematopoietic CSCs have also been shown to require functional HIF1α for survival. Acute Myeloid Leukemia (AML) $CD34^{+}CD38^{-}$ cells (CSCs) also demonstrate an increase in HIF1α expression over the non-CSCs. In addition, HIF1α inhibition reduced the tumorigenicity of the AML CSCs both in vitro and in vivo [180]. As seen throughout the study by Wang et al, successful ablation of HIF1α activity is capable of reducing the number and tumorigenic capacity of hematological CSCs, both in vitro and in vivo. Therefore,

chemical agents that can effectively reduce HIF1α activity will provide attractive candidates for CSC targeting agents.

Rationale for a Multi-Targeting Approach to Treat TCL CSCs

As discussed earlier, TCLs are comprised of a heterogeneous mix of classified cancers. For the most part, the molecular mechanisms driving the malignant phenotypes of TCLs have been inadequately determined. Treatment options for TCL have traditionally produced modest efficacy at best, and have done little to improve OS rates despite any initial response to therapies. While new therapeutic strategies continue to be explored, failure to improve suggests current strategies for fighting TCL have been misdirected. Despite the growing list of CSC-driven solid and hematological cancers, CSC-driven TCL has not been well characterized. Only recently has evidence for BCL CSCs been reported [194, 195]. Given the capacity of CSCs to resist treatment, current therapies for TCL likely fail to significantly reduce TCL CSCs, allowing them to survive and reinitiate tumor growth. Therefore, improving overall survival in TCL will likely require both novel therapies for TCL and resistant TCL CSCs.

As CSCs utilize multiple self-renewal pathways, targeting individual pathways may prove ineffective. An alternate method of targeting CSCs would utilize a strategy to effectively target multiple self-renewal pathways simultaneously. This approach was first conceptualized following reports of the overexpression of a central molecular chaperone, Heat Shock Protein 90 (HSP90), in various types of cancer cells [196]. Consistent with this phenomenon, cases of NHLs have been shown to express elevated levels of HSP90. In particular, TCLs were found to exhibit moderate (precursor T-cell

lymphoblastic leukemia/lymphoma--31%; PTCL-NOS--23%; AITL--12%) to high levels (ALCL-ALK$^+$--75%; ALCL-ALK$^-$--42%) of HSP90 expression [197]. In addition, the level of HSP90 expression was found to increase as tumor grade increased in TCLs. HSP90 has also been found to be heavily associated with co-chaperone proteins in cancer cells [198]. This has been attributed to the rampant genomic instability seen within tumors [199, 200], and suggests a critical reliance of the malignant cells on HSP90. Most importantly, CSC-related proteins (Her2, AKT, HIF1α) [201-204] have been shown to require HSP90 for activity. Taken together, these observations suggest HSP90 inhibition may be a suitable method for targeting TCL CSCs.

Heat Shock Protein 90

Protein function is dictated by its spatial conformation, formed through the proper folding of the amino acid sequence comprising its backbone. While the specific amino acids dictate the final structural conformation, the complex and rapidly changing environment within a cell can interfere with proper protein folding [205]. This chaotic environment is further exacerbated in cancer cells, where stress from hypoxia, acidosis, and the effects of therapies are constantly challenging the cellular milieu [206]. Evolution has solved this protein folding dilemma with molecular chaperones, proteins which facilitate the folding and stability of both normal and oncogenic proteins through low-affinity interactions [207, 208]. The importance of chaperones in this sense can be inferred from the highly conserved nature of chaperone genetic sequences amongst eukaryotic cells.

HSP90 is one of the most well characterized molecular chaperones. Constituting between 1-2% of cytosolic proteins, HSP90 is considered a key mediator of the folding, maturation, and stability of over 200 target proteins [209-211]. These client proteins can influence a wide range of functions, such as tyrosine kinases (Her2, EGFR), signaling pathway mediators (AKT, IKK), DNA damage sensors (p53), chimeric signaling proteins (bcr/abl, NPM/ALK), regulators of cell cycle progression (CDK4, CDK6), and transcription factors (HIF1α) [207, 212-217]. In order to carry out its functions, HSP90 relies on more than 20 accessory proteins (known as co-chaperones) to help facilitate ATPase and HSP90 cycle turnover, in addition to client recruitment and loading onto HSP90 [211, 218].

As stated above, the sequence and structure of HSP90 is highly conserved. This permits the extrapolation of structural information from the HSP90 and Grp94 (an isoform of HSP90 expressed in the endoplasmic reticulum) crystal structures for insights into the structure of human HSP90 [219, 220]. Within the cell, HSP90 is a dimeric protein, consisting of two monomers, each containing 3 regions: N-terminal, middle, and C-terminal domains. The N-terminal domain includes an essential ATP-binding pocket that facilitates the HSP90 folding mechanism [221, 222]. The discrimination and identification of client proteins is carried out by the middle domain [223]. Lastly, the C-terminal domain of HSP90 has been shown to harbor several functions. Dimerization of the two HSP90 monomers is mainly facilitated by the C-terminal domain, as the N-terminal regions are only weakly associated. A conserved five amino acid sequence (MEEVD) is contained within the C-terminal domain, which facilitates the association of

HSP90 with the co-chaperone Hop. Lastly, the C-terminal domain can allosterically regulate the N-terminal domain via a nucleotide binding pocket [223-226].

The HSP90 chaperone cycle consists of transitions between open and closed protein conformations [212]. Throughout each cycle, the transition between open and closed states allows for the rearrangement of different co-chaperones that associate with HSP90. To begin the cycle, the two N-terminal domains of the dimer are in a separated, open state, which is maintained through interaction with Hop at both the N-terminal and C-terminal domains [227-229]. A client protein is recruited to HSP90/Hop via the HSP70/HSP40 co-chaperone complex, which associates with HSP90 through the interaction of HSP70 with Hop [225]. While in this intermediate complex, the client protein is transferred from HSP70 to the middle domain of HSP90. At this point, ATP is bound to each of the N-terminal binding pockets. Next, Hop disassociates from the HSP90 complex, due to reduced affinity following binding of ATP and the co-chaperone p23 [230, 231]. In this mature complex, the N-terminal and middle domain are brought together to form the closed state of the chaperone complex. At this stage, both HSP90 and p23 facilitate folding of the client protein [230, 231]. To complete the cycle, additional co-chaperones, such as aha1 (activator of HSP90 ATPase) and the peptidyl-prolyl cis-trans isomerases Cpr6/Cyp40, bind to the chaperone complex and induce ATP hydrolysis [232-234]. Conversion of ATP to ADP + Pi allows the HSP90 dimer to reopen, and the newly or refolded client protein disassociates from the chaperone complex. Upon returning to its open state, HSP90 reassociates with Hop in place of p23, and thus completes the cycle [235].

Methods for HSP90 Inhibition

The first HSP90 inhibitors identified belong to a class of antibiotics called benzoquinone ansamycins. Initial work with the ansamycin herbimycin led some to believe these compounds mainly function as tyrosine kinase inhibitors [236]. HSP90 inhibition was not associated with these compounds until the discovery of geldanamycin. First identified in the 1970s, geldanamycin was found to disrupt the HSP90 chaperone cycle through competitive binding with ATP for the N-terminal domain ATP binding pockets [237-240]. Without ATP binding, geldanamycin prevents the HSP90 chaperone from adopting its closed conformation, thus preventing its protein folding mechanism. Client proteins which dissociate from HSP90 in an immature, unfolded state are marked for proteasomal degradation via ubiquitin ligase enzymes [241-243]. However, the success of geldanamycin was limited in vivo, as preclinical mouse models showed geldanamycin treatment led to severe liver toxicity [244]. To date, three geldanamycin analogues have been synthesized to reduce toxicity while maintaining efficacy against HSP90.

Synthesized in 1995, 17-AAG (17-N-allylamino-17-demethoxygeldanamycin) was the first analogue tested that showed inhibition of HSP90 with a more favorable toxicity profile [245]. Using in vitro assays, 17-AAG arrested cancer cell growth and induced apoptosis. When used to treat cancer xenografts in preclinical models, 17-AAG was capable of reducing tumor growth rates [246-248]. A number of phase I clinical trials have been carried out to determine the maximum tolerated dose (MTD) and dosing schedule for 17-AAG. In one trial, Goetz et al identified that 431 mg/m^2 given on days 1, 8, and 15 of a 28 day cycle was efficacious for patients with advanced cancers. However,

this dose presented dose limiting toxicities in two patients, such as hyperbilirubinaemia, transaminitis, and nausea/vomiting requiring hospitalization [249]. A second phase I trial found an MTD of 450 mg/m^2 using the same dose regiment. Diarrhea and transaminitis were also seen at this dose. Of note, two patients with metastatic melanoma achieved disease stabilization, which Banerji et al assigned to a possible cytostatic effect from the 17-AAG treatment [250]. Initial Phase II clinical trials have focused on cancers driven by known oncogenic clients, such as bcr/abl and Her2 [251, 252]. While some Phase II trials have demonstrated somewhat modest responses, particularly in metastatic melanoma, others have been relatively successful.[253]. A Phase II trial in advanced metastatic Her2 positive breast cancer patients found the combination of Herceptin (Trastuzumab) with weekly infusion of 17-AAG produced a response rate and overall clinical benefit of 22% and 59% of patients [254]. While these results are promising, issues with toxicities from both 17-AAG and its formulation have made it difficult to assess the agent's full clinical potential [237, 251, 253, 255].

A new compound, 17-DMAG, has been synthesized to improve upon the formulation of 17-AAG [256]. The water solubility of 17-DMAG is greatly increased over 17-AAG, easing the difficulty of formulation. In addition, higher potency was seen with 17-DMAG treatment in preclinical models, as compared to 17-AAG. However, this increase in potency was also accompanied by an increase in toxicity [256, 257]. In contrast to 17-AAG, complete response and stable disease have been reported with 17-DMAG treatment [258]. Another analogue still in clinical development is IPI-504 [259]. This compound is a stabilized soluble hydroquinone form of 17-AAG, and therefore does not require NQO1-mediated reduction [260]. While a clinical study evaluating IPI-504 in

gastrointestinal stromal tumors was terminated due to hepatotoxicity, recent reports of IPI-504 therapy in non-small cell lung cancer patients which carry ALK mutations have been promising [261, 262].

In addition to the anamycins and their derivatives, other antibiotics identified from the Monocillium nordinii and Monosporium bonorden fungi have been shown to have efficacy against HSP90 [263]. Radicicol was demonstrated to potently inhibit HSP90, via a similar mechanism as 17-AAG. However, although radicicol is effective in targeting HSP90 in vitro, this agent was not as effective in treating mice bearing tumor xenografts. This was later attributed to poor chemical stability of radicicol in vivo. Synthesis of new analogues, along with removal of an epoxide moiety within radicicol, were done to improve stability in vivo. While these radicicol analogues have shown efficacy against human tumor xenografts, a candidate for clinical development has not yet been reached [264, 265].

Utilizing the crystal structures of HSP90 and its N-terminal domain ATP binding pocket, structure based drug design has yielded several novel scaffolds which have improved binding capability of new compounds over classical HSP90 inhibitors. CNF2024/BIIB021 was the first synthetic compound developed using a purine scaffold. Several Phase I trials with CNF2024/BIIB021 have been conducted, with the MTD reported as 800 mg. One patient with B cell lymphocytic leukemia had a 39% reduction in lymph node volume. Also promising were the responses seen in solid tumors, with 68% reporting stable disease [266, 267]. Using a 6,7-dihydro-indazol-4-one scaffold, SNX-5422 was developed and has been used in a Phase I trial for refractory solid tumors and lymphomas. One dose limiting toxicity (nonseptic arthritis) and no objective

response were reported from the trial. While 47% of patients had stable disease with SNX-5422 treatment, this compound is no longer under development due to ocular toxicity reported in a separate phase I trial [268]. Another novel scaffold was identified using high-throughput screening. AUY922 has been used in a recent phase I trial in patients with advanced solid tumors. With an MTD of 70 mg/m^2, AUY922 treatment resulted in disease stabilization in 16 of 96 patients. Grade 3 dose limiting toxicities consisted of atrial flutter, fatigue, diarrhea, asthenia, and darkening of vision [269].

With the discovery of an ATP binding pocket in the C-terminal domain of HSP90, efforts to identify potent allosteric HSP90 inhibitors have been ongoing. The first compound to demonstrate HSP90 inhibition through binding at the C-terminal ATP site was novobiocin [270]. As a high concentration of novobiocin (700 μM) was needed to bind the C-terminal HSP90 domain, new derivatives (DHN1, DHN2) have been developed with much greater affinity. DHN2 was found to bind the C-terminal domain with higher affinity than DHN1. Additionally, between the three inhibitors, DHN2 showed the least affinity for DNA Gyrase, a common off-target protein which can bind novobiocin [271]. While development of novobiocin derivatives continues to improve efficacy against HSP90, no candidate has been selected for clinical evaluation [272-274].

17-AAG mediated HSP90 Inhibition Remains a Viable Approach for TCL CSCs

Results from clinical trials of HSP90 inhibitors have shown this method of treatment is most effective in tumor types which are solely driven by an HSP90 client protein, and cannot rely on alternate pathways for survival. Tumor cells that are not "addicted" to any particular HSP90 client may show marginal efficacy to HSP90

inhibition, leading to little or no response in clinical trials. Indeed, in patients with non small cell lung cancer (NSCLC), overall response to HSP90 inhibition was very low (7%). However, two partial responses and one stable disease were seen in the three patients with NSCLC that carried ALK fusion proteins (HSP90 clients) [262]. This selective sensitivity was also seen in a separate NSCLC trial, where four of the eight patients with NSCLC that contained ALK fusion proteins showed objective responses [275]. Moreover, patients with metastatic Her2+ breast cancer that received a combination of 17-AAG and Herceptin demonstrated an overall response rate of 22% and a clinical benefit rate (CR + PR + SD) of 59% [254]. As illustrated by these trials, HSP90 inhibition can be effective in tumor types that are critically reliant on particular client proteins for survival.

In addition to differential efficacy in various tumor types, sensitivity to HSP90 inhibition may be heterogeneous among cells within a single tumor. In the context of the CSC hypothesis, it is important to consider that the most responsive cells to HSP90 inhibition might not be part of the tumor bulk. CSCs are uniquely driven by the aberrant activation of self-renewal pathways. As known HSP90 clients (Her2, AKT, HIF1α) are required for maintenance of self-renewal, this addiction to self-renewal could be exploited by HSP90-targeted agents. Indeed, several reports have shown that HSP90 inhibition can effectively target CSCs [276, 277]. In particular, glioma stem cells, derived from both cell lines and patients with glioblastoma metaforte, were reduced in growth rate and client protein expression with 17-AAG-targeted treatment [203]. Finally, unpublished data from our lab has shown that inhibition of breast CSCs in vivo can be achieved using low doses of 17-AAG, thereby avoiding toxicity issues which have

plagued this treatment. These reports suggest that the efficacy of HSP90 inhibitors should be reevaluated, given the possibility that they can successfully eliminate CSCs.

To examine this prospect, we plan to investigate the efficacy of 17-AAG treatment for elimination of CSCs. Maximum efficacy with HSP90 inhibition requires that both the tumor cell critically relies on a client facilitated pathway, and the client protein's function solely depends on HSP90. As discussed earlier, the TGB lymphoma CSCs are reliant on the sustained activity of the HSP90 client HIF1α for maintenance of self-renewal. Thus, we hypothesize that 17-AAG will effectively eliminate the CSCs by inducing HIF1α degradation through HSP90 inhibition.

Specific Aims:

1.) To determine the efficacy of 17-AAG-mediated treatment in TGB lymphoma CSCs, in vitro and in vivo.
2.) To identify the mechanism for sensitivity and/or selectivity seen in TGB lymphoma CSCs over the differentiated cell population.
3.) To validate a combination therapy consisting of 17-AAG plus a conventional cancer treatment in an alternate, solid tumor CSC model.

References

1. Kuppers, R. and K. Rajewsky, *The origin of Hodgkin and Reed/Sternberg cells in Hodgkin's disease.* Annu Rev Immunol, 1998. **16**: p. 471-93.
2. O'Leary, H. and K.J. Savage, *The spectrum of peripheral T-cell lymphomas.* Curr Opin Hematol, 2009. **16**(4): p. 292-8.
3. Vose, J., J. Armitage, and D. Weisenburger, *International peripheral T-cell and natural killer/T-cell lymphoma study: pathology findings and clinical outcomes.* J Clin Oncol, 2008. **26**(25): p. 4124-30.
4. Foss, F.M., et al., *Peripheral T-cell lymphoma.* Blood, 2011. **117**(25): p. 6756-67.
5. de Leval, L. and P. Gaulard, *Pathology and biology of peripheral T-cell lymphomas.* Histopathology, 2011. **58**(1): p. 49-68.
6. Piva, R., et al., *Gene expression profiling uncovers molecular classifiers for the recognition of anaplastic large-cell lymphoma within peripheral T-cell neoplasms.* J Clin Oncol, 2010. **28**(9): p. 1583-90.
7. de Leval, L., et al., *The gene expression profile of nodal peripheral T-cell lymphoma demonstrates a molecular link between angioimmunoblastic T-cell lymphoma (AITL) and follicular helper T (TFH) cells.* Blood, 2007. **109**(11): p. 4952-63.
8. Piccaluga, P.P., et al., *Gene expression analysis of angioimmunoblastic lymphoma indicates derivation from T follicular helper cells and vascular endothelial growth factor deregulation.* Cancer Res, 2007. **67**(22): p. 10703-10.
9. Vinuesa, C.G., et al., *Follicular B helper T cells in antibody responses and autoimmunity.* Nat Rev Immunol, 2005. **5**(11): p. 853-65.
10. Yu, H., A. Shahsafaei, and D.M. Dorfman, *Germinal-center T-helper-cell markers PD-1 and CXCL13 are both expressed by neoplastic cells in angioimmunoblastic T-cell lymphoma.* Am J Clin Pathol, 2009. **131**(1): p. 33-41.
11. Piccaluga, P.P., et al., *Gene expression analysis of peripheral T cell lymphoma, unspecified, reveals distinct profiles and new potential therapeutic targets.* J Clin Invest, 2007. **117**(3): p. 823-34.
12. Piccaluga, P.P., et al., *Expression of platelet-derived growth factor receptor alpha in peripheral T-cell lymphoma not otherwise specified.* Lancet Oncol, 2005. **6**(6): p. 440.
13. Feldman, A.L., et al., *Overexpression of Syk tyrosine kinase in peripheral T-cell lymphomas.* Leukemia, 2008. **22**(6): p. 1139-43.
14. Wilcox, R.A., et al., *Inhibition of Syk protein tyrosine kinase induces apoptosis and blocks proliferation in T-cell non-Hodgkin's lymphoma cell lines.* Leukemia, 2010. **24**(1): p. 229-32.
15. Jaffe, E.S., *Pathobiology of peripheral T-cell lymphomas.* Hematology Am Soc Hematol Educ Program, 2006: p. 317-22.
16. Jaffe, E.S., L. Krenacs, and M. Raffeld, *Classification of cytotoxic T-cell and natural killer cell lymphomas.* Semin Hematol, 2003. **40**(3): p. 175-84.
17. Bossard, C., et al., *Expression of the granzyme B inhibitor PI9 predicts outcome in nasal NK/T-cell lymphoma: results of a Western series of 48 patients treated with first-line polychemotherapy within the Groupe d'Etude des Lymphomes de l'Adulte (GELA) trials.* Blood, 2007. **109**(5): p. 2183-9.

18. Nakashima, Y., et al., *Genome-wide array-based comparative genomic hybridization of natural killer cell lymphoma/leukemia: different genomic alteration patterns of aggressive NK-cell leukemia and extranodal Nk/T-cell lymphoma, nasal type.* Genes Chromosomes Cancer, 2005. **44**(3): p. 247-55.
19. Taborelli, M., et al., *Chromosome band 6q deletion pattern in malignant lymphomas.* Cancer Genet Cytogenet, 2006. **165**(2): p. 106-13.
20. Iqbal, J., et al., *Genomic analyses reveal global functional alterations that promote tumor growth and novel tumor suppressor genes in natural killer-cell malignancies.* Leukemia, 2009. **23**(6): p. 1139-51.
21. Huang, Y., et al., *Gene expression profiling identifies emerging oncogenic pathways operating in extranodal NK/T-cell lymphoma, nasal type.* Blood, 2010. **115**(6): p. 1226-37.
22. Coppo, P., et al., *STAT3 transcription factor is constitutively activated and is oncogenic in nasal-type NK/T-cell lymphoma.* Leukemia, 2009. **23**(9): p. 1667-78.
23. Mention, J.J., et al., *Interleukin 15: a key to disrupted intraepithelial lymphocyte homeostasis and lymphomagenesis in celiac disease.* Gastroenterology, 2003. **125**(3): p. 730-45.
24. Malamut, G., et al., *IL-15 triggers an antiapoptotic pathway in human intraepithelial lymphocytes that is a potential new target in celiac disease-associated inflammation and lymphomagenesis.* J Clin Invest, 2010. **120**(6): p. 2131-43.
25. Zettl, A., et al., *Chromosomal gains at 9q characterize enteropathy-type T-cell lymphoma.* Am J Pathol, 2002. **161**(5): p. 1635-45.
26. Verkarre, V., et al., *Recurrent partial trisomy 1q22-q44 in clonal intraepithelial lymphocytes in refractory celiac sprue.* Gastroenterology, 2003. **125**(1): p. 40-6.
27. Deleeuw, R.J., et al., *Whole-genome analysis and HLA genotyping of enteropathy-type T-cell lymphoma reveals 2 distinct lymphoma subtypes.* Gastroenterology, 2007. **132**(5): p. 1902-11.
28. Cejkova, P., et al., *Amplification of NOTCH1 and ABL1 gene loci is a frequent aberration in enteropathy-type T-cell lymphoma.* Virchows Arch, 2005. **446**(4): p. 416-20.
29. Wlodarska, I., et al., *Fluorescence in situ hybridization study of chromosome 7 aberrations in hepatosplenic T-cell lymphoma: isochromosome 7q as a common abnormality accumulating in forms with features of cytologic progression.* Genes Chromosomes Cancer, 2002. **33**(3): p. 243-51.
30. Belhadj, K., et al., *Hepatosplenic gammadelta T-cell lymphoma is a rare clinicopathologic entity with poor outcome: report on a series of 21 patients.* Blood, 2003. **102**(13): p. 4261-9.
31. Rosh, J.R., et al., *Hepatosplenic T-cell lymphoma in adolescents and young adults with Crohn's disease: a cautionary tale?* Inflamm Bowel Dis, 2007. **13**(8): p. 1024-30.
32. Shale, M., et al., *Hepatosplenic T cell lymphoma in inflammatory bowel disease.* Gut, 2008. **57**(12): p. 1639-41.
33. Willemze, R. and C.J. Meijer, *Classification of cutaneous T-cell lymphoma: from Alibert to WHO-EORTC.* J Cutan Pathol, 2006. **33 Suppl 1**: p. 18-26.

34. Criscione, V.D. and M.A. Weinstock, *Incidence of cutaneous T-cell lymphoma in the United States, 1973-2002.* Arch Dermatol, 2007. **143**(7): p. 854-9.
35. Campbell, J.J., et al., *Sezary syndrome and mycosis fungoides arise from distinct T-cell subsets: a biologic rationale for their distinct clinical behaviors.* Blood, 2010. **116**(5): p. 767-71.
36. Kamstrup, M.R., et al., *Notch1 as a potential therapeutic target in cutaneous T-cell lymphoma.* Blood, 2010. **116**(14): p. 2504-12.
37. Izban, K.F., et al., *Constitutive expression of NF-kappa B is a characteristic feature of mycosis fungoides: implications for apoptosis resistance and pathogenesis.* Hum Pathol, 2000. **31**(12): p. 1482-90.
38. Sors, A., et al., *Down-regulating constitutive activation of the NF-kappaB canonical pathway overcomes the resistance of cutaneous T-cell lymphoma to apoptosis.* Blood, 2006. **107**(6): p. 2354-63.
39. Nielsen, M., et al., *Constitutive activation of a slowly migrating isoform of Stat3 in mycosis fungoides: tyrphostin AG490 inhibits Stat3 activation and growth of mycosis fungoides tumor cell lines.* Proc Natl Acad Sci U S A, 1997. **94**(13): p. 6764-9.
40. Sommer, V.H., et al., *In vivo activation of STAT3 in cutaneous T-cell lymphoma. Evidence for an antiapoptotic function of STAT3.* Leukemia, 2004. **18**(7): p. 1288-95.
41. Scarisbrick, J.J., et al., *Frequent abnormalities of the p15 and p16 genes in mycosis fungoides and sezary syndrome.* J Invest Dermatol, 2002. **118**(3): p. 493-9.
42. Laharanne, E., et al., *CDKN2A-CDKN2B deletion defines an aggressive subset of cutaneous T-cell lymphoma.* Mod Pathol, 2010. **23**(4): p. 547-58.
43. Willemze, R., et al., *WHO-EORTC classification for cutaneous lymphomas.* Blood, 2005. **105**(10): p. 3768-85.
44. Vonderheid, E.C., A. Sajjadian, and M.E. Kadin, *Methotrexate is effective therapy for lymphomatoid papulosis and other primary cutaneous CD30-positive lymphoproliferative disorders.* J Am Acad Dermatol, 1996. **34**(3): p. 470-81.
45. Franchini, G., *Molecular mechanisms of human T-cell leukemia/lymphotropic virus type I infection.* Blood, 1995. **86**(10): p. 3619-39.
46. Matsuoka, M. and K.T. Jeang, *Human T-cell leukaemia virus type 1 (HTLV-1) infectivity and cellular transformation.* Nat Rev Cancer, 2007. **7**(4): p. 270-80.
47. Shimoyama, M., *Chemotherapy of ATL*, in *Adult T-cell Leukaemia*, K. Takatsuki, Editor 1994, Oxford University Press: Oxford, UK. p. 221-237.
48. Taylor, G.P. and M. Matsuoka, *Natural history of adult T-cell leukemia/lymphoma and approaches to therapy.* Oncogene, 2005. **24**(39): p. 6047-57.
49. Liu, H., M.Y. Chiang, and W.S. Pear, *Critical roles of NOTCH1 in acute T-cell lymphoblastic leukemia.* Int J Hematol, 2011. **94**(2): p. 118-25.
50. Sokol, L. and T.P. Loughran, Jr., *Large granular lymphocyte leukemia.* Oncologist, 2006. **11**(3): p. 263-73.
51. Zambello, R., et al., *Analysis of the T cell receptor in the lymphoproliferative disease of granular lymphocytes: superantigen activation of clonal CD3+ granular lymphocytes.* Cancer Res, 1995. **55**(24): p. 6140-5.

52. Kanchan, K. and T.P. Loughran, Jr., *Antigen-driven clonal T cell expansion in disorders of hematopoiesis.* Leuk Res, 2003. **27**(4): p. 291-2.
53. O'Keefe, C.L., et al., *Molecular analysis of TCR clonotypes in LGL: a clonal model for polyclonal responses.* J Immunol, 2004. **172**(3): p. 1960-9.
54. Yang, J., et al., *Antigen activation and impaired Fas-induced death-inducing signaling complex formation in T-large-granular lymphocyte leukemia.* Blood, 2008. **111**(3): p. 1610-6.
55. Schade, A.E., M.W. Wlodarski, and J.P. Maciejewski, *Pathophysiology defined by altered signal transduction pathways: the role of JAK-STAT and PI3K signaling in leukemic large granular lymphocytes.* Cell Cycle, 2006. **5**(22): p. 2571-4.
56. Epling-Burnette, P.K., et al., *Inhibition of STAT3 signaling leads to apoptosis of leukemic large granular lymphocytes and decreased Mcl-1 expression.* J Clin Invest, 2001. **107**(3): p. 351-62.
57. Epling-Burnette, P.K., et al., *ERK couples chronic survival of NK cells to constitutively activated Ras in lymphoproliferative disease of granular lymphocytes (LDGL).* Oncogene, 2004. **23**(57): p. 9220-9.
58. Lamy, T., et al., *Dysregulation of CD95/CD95 ligand-apoptotic pathway in CD3(+) large granular lymphocyte leukemia.* Blood, 1998. **92**(12): p. 4771-7.
59. Dearden, C., *Large granular lymphocytic leukaemia pathogenesis and management.* Br J Haematol, 2011. **152**(3): p. 273-83.
60. Ham, M.F. and Y.H. Ko, *Natural killer cell neoplasm: biology and pathology.* Int J Hematol, 2010. **92**(5): p. 681-9.
61. Ko, Y.H., et al., *Aggressive natural killer cell leukemia: is Epstein-Barr virus negativity an indicator of a favorable prognosis?* Acta Haematol, 2008. **120**(4): p. 199-206.
62. Lan, K., et al., *Detection of Epstein-Barr virus in T-cell prolymphocytic leukemia cells in vitro.* J Clin Virol, 2008. **43**(3): p. 260-5.
63. Herling, M., et al., *High TCL1 expression and intact T-cell receptor signaling define a hyperproliferative subset of T-cell prolymphocytic leukemia.* Blood, 2008. **111**(1): p. 328-37.
64. Laine, J., et al., *The protooncogene TCL1 is an AKT kinase coactivator.* Mol Cell, 2000. **6**(2): p. 395-407.
65. Stilgenbauer, S., et al., *Biallelic mutations in the ATM gene in T-prolymphocytic leukemia.* Nat Med, 1997. **3**(10): p. 1155-9.
66. Stoppa-Lyonnet, D., et al., *Inactivation of the ATM gene in T-cell prolymphocytic leukemias.* Blood, 1998. **91**(10): p. 3920-6.
67. Khot, A. and C. Dearden, *T-cell prolymphocytic leukemia.* Expert Rev Anticancer Ther, 2009. **9**(3): p. 365-71.
68. Morton, L.M., et al., *Lymphoma incidence patterns by WHO subtype in the United States, 1992-2001.* Blood, 2006. **107**(1): p. 265-76.
69. Brock, N., et al., *Basis and new developments in the field of oxazaphosphorines.* Cancer Invest, 1988. **6**(5): p. 513-32.
70. Chen, C.S., et al., *Activation of the anticancer prodrugs cyclophosphamide and ifosfamide: identification of cytochrome P450 2B enzymes and site-specific mutants with improved enzyme kinetics.* Mol Pharmacol, 2004. **65**(5): p. 1278-85.

71. Rooseboom, M., J.N. Commandeur, and N.P. Vermeulen, *Enzyme-catalyzed activation of anticancer prodrugs.* Pharmacol Rev, 2004. **56**(1): p. 53-102.
72. Fornari, F.A., et al., *Interference by doxorubicin with DNA unwinding in MCF-7 breast tumor cells.* Mol Pharmacol, 1994. **45**(4): p. 649-56.
73. Momparler, R.L., et al., *Effect of adriamycin on DNA, RNA, and protein synthesis in cell-free systems and intact cells.* Cancer Res, 1976. **36**(8): p. 2891-5.
74. Zhou, X.J. and R. Rahmani, *Preclinical and clinical pharmacology of vinca alkaloids.* Drugs, 1992. **44 Suppl 4**: p. 1-16; discussion 66-9.
75. Abouyabis, A.N., et al., *Incidence and outcomes of the peripheral T-cell lymphoma subtypes in the United States.* Leuk Lymphoma, 2008. **49**(11): p. 2099-107.
76. Weisenburger, D.D., et al., *Peripheral T-cell lymphoma, not otherwise specified: a report of 340 cases from the International Peripheral T-cell Lymphoma Project.* Blood, 2011. **117**(12): p. 3402-8.
77. Enblad, G., et al., *A pilot study of alemtuzumab (anti-CD52 monoclonal antibody) therapy for patients with relapsed or chemotherapy-refractory peripheral T-cell lymphomas.* Blood, 2004. **103**(8): p. 2920-4.
78. Kim, J.G., et al., *Alemtuzumab plus CHOP as front-line chemotherapy for patients with peripheral T-cell lymphomas: a phase II study.* Cancer Chemother Pharmacol, 2007. **60**(1): p. 129-34.
79. Gallamini, A., et al., *Alemtuzumab (Campath-1H) and CHOP chemotherapy as first-line treatment of peripheral T-cell lymphoma: results of a GITIL (Gruppo Italiano Terapie Innovative nei Linfomi) prospective multicenter trial.* Blood, 2007. **110**(7): p. 2316-23.
80. Ansell, S.M., et al., *Phase I/II study of an anti-CD30 monoclonal antibody (MDX-060) in Hodgkin's lymphoma and anaplastic large-cell lymphoma.* J Clin Oncol, 2007. **25**(19): p. 2764-9.
81. O'Leary, H.M. and K.J. Savage, *Novel therapies in peripheral T-cell lymphomas.* Curr Hematol Malig Rep, 2008. **3**(4): p. 213-20.
82. d'Amore, F., et al., *Phase II trial of zanolimumab (HuMax-CD4) in relapsed or refractory non-cutaneous peripheral T cell lymphoma.* Br J Haematol, 2010. **150**(5): p. 565-73.
83. Foss, F.M., *DAB(389)IL-2 (ONTAK): a novel fusion toxin therapy for lymphoma.* Clin Lymphoma, 2000. **1**(2): p. 110-6; discussion 117.
84. Dang, N.H., et al., *Phase II study of denileukin diftitox for relapsed/refractory B-Cell non-Hodgkin's lymphoma.* J Clin Oncol, 2004. **22**(20): p. 4095-102.
85. Foss, F.M., Sjak-Shie, A., Goy, A., Advani, R., Jacobsen, E.D., *Phase II study of denileukin diftitox with CHOP chemotherapy in newly diagnosed PTCL: CONCEPT trial [Abstract]*. J Clin Oncol, 2010. **28**(15s): p. 8045.
86. O'Leary, H.M. and K.J. Savage, *Novel therapies in peripheral T-cell lymphomas.* Curr Oncol Rep, 2008. **10**(5): p. 404-11.
87. Sallah, S., J.Y. Wan, and N.P. Nguyen, *Treatment of refractory T-cell malignancies using gemcitabine.* Br J Haematol, 2001. **113**(1): p. 185-7.
88. Zinzani, P.L., et al., *Therapy with gemcitabine in pretreated peripheral T-cell lymphoma patients.* Ann Oncol, 1998. **9**(12): p. 1351-3.

89. Kim, J.G., et al., *CHOP plus etoposide and gemcitabine (CHOP-EG) as front-line chemotherapy for patients with peripheral T cell lymphomas.* Cancer Chemother Pharmacol, 2006. **58**(1): p. 35-9.
90. Piekarz, R.L., et al., *Inhibitor of histone deacetylation, depsipeptide (FR901228), in the treatment of peripheral and cutaneous T-cell lymphoma: a case report.* Blood, 2001. **98**(9): p. 2865-8.
91. Piekarz, R., Frye, R., Wright, J., et al. , *Update of the NCI multi-institutional phase II trial of romidepsin, FK228, for patients with cutaneous or peripheral T-cell lymphoma [ASCO abstract]*. J Clin Oncol, 2007. **25**: p. 8027.
92. O'Connor, O.A., et al., *Phase II-I-II study of two different doses and schedules of pralatrexate, a high-affinity substrate for the reduced folate carrier, in patients with relapsed or refractory lymphoma reveals marked activity in T-cell malignancies.* J Clin Oncol, 2009. **27**(26): p. 4357-64.
93. O'Connor, O.A., et al., *Pralatrexate in patients with relapsed or refractory peripheral T-cell lymphoma: results from the pivotal PROPEL study.* J Clin Oncol, 2011. **29**(9): p. 1182-9.
94. Appelbaum, F., Forman, S., Negrin, R., Blume, K., *Thomas' Hematopoietic Cell Transplantation*. 4 ed2009: Wiley-Blackwell. 1752.
95. Philip, T., et al., *Autologous bone marrow transplantation as compared with salvage chemotherapy in relapses of chemotherapy-sensitive non-Hodgkin's lymphoma.* N Engl J Med, 1995. **333**(23): p. 1540-5.
96. Rodriguez, J., et al., *Frontline autologous stem cell transplantation in high-risk peripheral T-cell lymphoma: a prospective study from The Gel-Tamo Study Group.* Eur J Haematol, 2007. **79**(1): p. 32-8.
97. Reimer, P., et al., *Autologous stem-cell transplantation as first-line therapy in peripheral T-cell lymphomas: results of a prospective multicenter study.* J Clin Oncol, 2009. **27**(1): p. 106-13.
98. Feyler, S., et al., *The role of high-dose therapy and stem cell rescue in the management of T-cell malignant lymphomas: a BSBMT and ABMTRR study.* Bone Marrow Transplant, 2007. **40**(5): p. 443-50.
99. Kyriakou, C., et al., *High-dose therapy and autologous stem-cell transplantation in angioimmunoblastic lymphoma: complete remission at transplantation is the major determinant of Outcome-Lymphoma Working Party of the European Group for Blood and Marrow Transplantation.* J Clin Oncol, 2008. **26**(2): p. 218-24.
100. Chen, A.I., et al., *Long-term results of autologous hematopoietic cell transplantation for peripheral T cell lymphoma: the Stanford experience.* Biol Blood Marrow Transplant, 2008. **14**(7): p. 741-7.
101. Reiser, M., et al., *T-cell non-Hodgkin's lymphoma in adults: clinicopathological characteristics, response to treatment and prognostic factors.* Leuk Lymphoma, 2002. **43**(4): p. 805-11.
102. Siegert, W., et al., *Treatment of angioimmunoblastic lymphadenopathy (AILD)-type T-cell lymphoma using prednisone with or without the COPBLAM/IMVP-16 regimen. A multicenter study. Kiel Lymphoma Study Group.* Ann Intern Med, 1992. **117**(5): p. 364-70.
103. Coiffier, B., et al., *Peripheral T-cell lymphomas have a worse prognosis than B-cell lymphomas: a prospective study of 361 immunophenotyped patients treated*

with the LNH-84 regimen. The GELA (Groupe d'Etude des Lymphomes Agressives). Ann Oncol, 1990. **1**(1): p. 45-50.
104. Evens, A.M. and R.B. Gartenhaus, *Treatment of T-cell non-Hodgkin's lymphoma.* Curr Treat Options Oncol, 2004. **5**(4): p. 289-303.
105. Besson, C., et al., *Treatment of adult T-cell leukemia-lymphoma by CHOP followed by therapy with antinucleosides, alpha interferon and oral etoposide.* Leuk Lymphoma, 2002. **43**(12): p. 2275-9.
106. Boshoff, C. and R. Weiss, *AIDS-related malignancies.* Nat Rev Cancer, 2002. **2**(5): p. 373-82.
107. Penn, I., *Sarcomas in organ allograft recipients.* Transplantation, 1995. **60**(12): p. 1485-91.
108. Penn, I., *Malignant melanoma in organ allograft recipients.* Transplantation, 1996. **61**(2): p. 274-8.
109. Rygaard, J. and C.O. Povlsen, *Is immunological surveillance not a cell-mediated immune function?* Transplantation, 1974. **17**(1): p. 135-6.
110. Geiger, T., L.R. Gooding, and R.A. Flavell, *T-cell responsiveness to an oncogenic peripheral protein and spontaneous autoimmunity in transgenic mice.* Proc Natl Acad Sci U S A, 1992. **89**(7): p. 2985-9.
111. Reimann, J., et al., *TCR/CD3 ligation of a TCR-transgenic T lymphoma blocks its proliferation in vitro but does not affect its growth in vivo.* Exp Clin Immunogenet, 1994. **11**(4): p. 197-208.
112. Wang, Y., et al., *Epm2a suppresses tumor growth in an immunocompromised host by inhibiting Wnt signaling.* Cancer Cell, 2006. **10**(3): p. 179-90.
113. Aberle, H., et al., *beta-catenin is a target for the ubiquitin-proteasome pathway.* EMBO J, 1997. **16**(13): p. 3797-804.
114. Orford, K., et al., *Serine phosphorylation-regulated ubiquitination and degradation of beta-catenin.* J Biol Chem, 1997. **272**(40): p. 24735-8.
115. Winston, J.T., et al., *The SCFbeta-TRCP-ubiquitin ligase complex associates specifically with phosphorylated destruction motifs in IkappaBalpha and beta-catenin and stimulates IkappaBalpha ubiquitination in vitro.* Genes Dev, 1999. **13**(3): p. 270-83.
116. Morin, P.J., *beta-catenin signaling and cancer.* Bioessays, 1999. **21**(12): p. 1021-30.
117. Gehrke, I., R.K. Gandhirajan, and K.A. Kreuzer, *Targeting the WNT/beta-catenin/TCF/LEF1 axis in solid and haematological cancers: Multiplicity of therapeutic options.* Eur J Cancer, 2009. **45**(16): p. 2759-67.
118. Dick, J.E., *Stem cell concepts renew cancer research.* Blood, 2008. **112**(13): p. 4793-807.
119. Blagosklonny, M.V., *Why therapeutic response may not prolong the life of a cancer patient: selection for oncogenic resistance.* Cell Cycle, 2005. **4**(12): p. 1693-8.
120. Furth, J., Kahn, M., *The transmission of leukemia of mice with a single cell.* Am J Cancer, 1937. **31**: p. 276-282.
121. Clarkson, B.D., *Review of recent studies of cellular proliferation in acute leukemia.* Natl Cancer Inst Monogr, 1969. **30**: p. 81-120.

122. Clarkson, B., *The survival value of the dormant state in neoplastic and normal cell populations*. Control of Proliferation in Animal Cells, ed. A.R. Baserga1974, Cold Spring Harbor Laboratory. 27.
123. Lapidot, T., et al., *A cell initiating human acute myeloid leukaemia after transplantation into SCID mice.* Nature, 1994. **367**(6464): p. 645-8.
124. Bonnet, D. and J.E. Dick, *Human acute myeloid leukemia is organized as a hierarchy that originates from a primitive hematopoietic cell.* Nat Med, 1997. **3**(7): p. 730-7.
125. Sutherland, H.J., A. Blair, and R.W. Zapf, *Characterization of a hierarchy in human acute myeloid leukemia progenitor cells.* Blood, 1996. **87**(11): p. 4754-61.
126. Holyoake, T., et al., *Isolation of a highly quiescent subpopulation of primitive leukemic cells in chronic myeloid leukemia.* Blood, 1999. **94**(6): p. 2056-64.
127. George, A.A., et al., *Detection of leukemic cells in the CD34(+)CD38(-) bone marrow progenitor population in children with acute lymphoblastic leukemia.* Blood, 2001. **97**(12): p. 3925-30.
128. Matsui, W., et al., *Characterization of clonogenic multiple myeloma cells.* Blood, 2004. **103**(6): p. 2332-6.
129. Singh, S.K., et al., *Identification of a cancer stem cell in human brain tumors.* Cancer Res, 2003. **63**(18): p. 5821-8.
130. Singh, S.K., et al., *Identification of human brain tumour initiating cells.* Nature, 2004. **432**(7015): p. 396-401.
131. Al-Hajj, M., et al., *Prospective identification of tumorigenic breast cancer cells.* Proc Natl Acad Sci U S A, 2003. **100**(7): p. 3983-8.
132. Stingl, J., et al., *Purification and unique properties of mammary epithelial stem cells.* Nature, 2006. **439**(7079): p. 993-7.
133. O'Brien, C.A., et al., *A human colon cancer cell capable of initiating tumour growth in immunodeficient mice.* Nature, 2007. **445**(7123): p. 106-10.
134. Collins, A.T., et al., *Prospective identification of tumorigenic prostate cancer stem cells.* Cancer Res, 2005. **65**(23): p. 10946-51.
135. Morrison, S.J. and J. Kimble, *Asymmetric and symmetric stem-cell divisions in development and cancer.* Nature, 2006. **441**(7097): p. 1068-74.
136. Smalley, M. and A. Ashworth, *Stem cells and breast cancer: A field in transit.* Nat Rev Cancer, 2003. **3**(11): p. 832-44.
137. Brittan, M. and N.A. Wright, *Gastrointestinal stem cells.* J Pathol, 2002. **197**(4): p. 492-509.
138. Reya, T., et al., *A role for Wnt signalling in self-renewal of haematopoietic stem cells.* Nature, 2003. **423**(6938): p. 409-14.
139. Schweizer, L. and H. Varmus, *Wnt/Wingless signaling through beta-catenin requires the function of both LRP/Arrow and frizzled classes of receptors.* BMC Cell Biol, 2003. **4**: p. 4.
140. Cohen, M.M., Jr., *The hedgehog signaling network.* Am J Med Genet A, 2003. **123A**(1): p. 5-28.
141. Lewis, M.T. and J.M. Veltmaat, *Next stop, the twilight zone: hedgehog network regulation of mammary gland development.* J Mammary Gland Biol Neoplasia, 2004. **9**(2): p. 165-81.

142. Pasca di Magliano, M. and M. Hebrok, *Hedgehog signalling in cancer formation and maintenance.* Nat Rev Cancer, 2003. **3**(12): p. 903-11.
143. Mumm, J.S. and R. Kopan, *Notch signaling: from the outside in.* Dev Biol, 2000. **228**(2): p. 151-65.
144. Krause, D.S., *Regulation of hematopoietic stem cell fate.* Oncogene, 2002. **21**(21): p. 3262-9.
145. Reedijk, M., et al., *High-level coexpression of JAG1 and NOTCH1 is observed in human breast cancer and is associated with poor overall survival.* Cancer Res, 2005. **65**(18): p. 8530-7.
146. Honeycutt, K.A. and D.R. Roop, *c-Myc and epidermal stem cell fate determination.* J Dermatol, 2004. **31**(5): p. 368-75.
147. Bafico, A., et al., *An autocrine mechanism for constitutive Wnt pathway activation in human cancer cells.* Cancer Cell, 2004. **6**(5): p. 497-506.
148. Olsen, C.L., et al., *Hedgehog-interacting protein is highly expressed in endothelial cells but down-regulated during angiogenesis and in several human tumors.* BMC Cancer, 2004. **4**: p. 43.
149. Karhadkar, S.S., et al., *Hedgehog signalling in prostate regeneration, neoplasia and metastasis.* Nature, 2004. **431**(7009): p. 707-12.
150. Wang, Z., et al., *Emerging role of Notch in stem cells and cancer.* Cancer Lett, 2009. **279**(1): p. 8-12.
151. Bolos, V., J. Grego-Bessa, and J.L. de la Pompa, *Notch signaling in development and cancer.* Endocr Rev, 2007. **28**(3): p. 339-63.
152. Pece, S., et al., *Loss of negative regulation by Numb over Notch is relevant to human breast carcinogenesis.* J Cell Biol, 2004. **167**(2): p. 215-21.
153. Politi, K., N. Feirt, and J. Kitajewski, *Notch in mammary gland development and breast cancer.* Semin Cancer Biol, 2004. **14**(5): p. 341-7.
154. Weng, A.P., et al., *Activating mutations of NOTCH1 in human T cell acute lymphoblastic leukemia.* Science, 2004. **306**(5694): p. 269-71.
155. Shackleton, M., et al., *Heterogeneity in cancer: cancer stem cells versus clonal evolution.* Cell, 2009. **138**(5): p. 822-9.
156. Gupta, P.B., C.L. Chaffer, and R.A. Weinberg, *Cancer stem cells: mirage or reality?* Nat Med, 2009. **15**(9): p. 1010-2.
157. Bomken, S., et al., *Understanding the cancer stem cell.* Br J Cancer, 2010. **103**(4): p. 439-45.
158. Jordan, C.T., M.L. Guzman, and M. Noble, *Cancer stem cells.* N Engl J Med, 2006. **355**(12): p. 1253-61.
159. Abbott, B.L., *ABCG2 (BCRP): a cytoprotectant in normal and malignant stem cells.* Clin Adv Hematol Oncol, 2006. **4**(1): p. 63-72.
160. Scharenberg, C.W., M.A. Harkey, and B. Torok-Storb, *The ABCG2 transporter is an efficient Hoechst 33342 efflux pump and is preferentially expressed by immature human hematopoietic progenitors.* Blood, 2002. **99**(2): p. 507-12.
161. Dean, M., T. Fojo, and S. Bates, *Tumour stem cells and drug resistance.* Nat Rev Cancer, 2005. **5**(4): p. 275-84.
162. Eyler, C.E. and J.N. Rich, *Survival of the fittest: cancer stem cells in therapeutic resistance and angiogenesis.* J Clin Oncol, 2008. **26**(17): p. 2839-45.

163. Bao, S., et al., *Glioma stem cells promote radioresistance by preferential activation of the DNA damage response.* Nature, 2006. **444**(7120): p. 756-60.
164. Rich, J.N., *Cancer stem cells in radiation resistance.* Cancer Res, 2007. **67**(19): p. 8980-4.
165. Tang, C., B.T. Ang, and S. Pervaiz, *Cancer stem cell: target for anti-cancer therapy.* FASEB J, 2007. **21**(14): p. 3777-85.
166. Maitland, N.J. and A.T. Collins, *Prostate cancer stem cells: a new target for therapy.* J Clin Oncol, 2008. **26**(17): p. 2862-70.
167. Wicha, M.S., *Cancer stem cells and metastasis: lethal seeds.* Clin Cancer Res, 2006. **12**(19): p. 5606-7.
168. Cheng, L., et al., *The clinical and therapeutic implications of cancer stem cell biology.* Expert Rev Anticancer Ther, 2011. **11**(7): p. 1131-43.
169. Sheu, C.C., et al., *Development of a membrane array-based multimarker assay for detection of circulating cancer cells in patients with non-small cell lung cancer.* Int J Cancer, 2006. **119**(6): p. 1419-26.
170. Riethdorf, S., et al., *Detection and HER2 expression of circulating tumor cells: prospective monitoring in breast cancer patients treated in the neoadjuvant GeparQuattro trial.* Clin Cancer Res, 2010. **16**(9): p. 2634-45.
171. Schuster, R., et al., *Circulating tumor cells as prognostic factor for distant metastases and survival in patients with primary uveal melanoma.* Clin Cancer Res, 2007. **13**(4): p. 1171-8.
172. Li, F., et al., *Beyond tumorigenesis: cancer stem cells in metastasis.* Cell Res, 2007. **17**(1): p. 3-14.
173. Griffiths, E.A., et al., *Is the hypoxia-inducible factor pathway important in gastric cancer?* Eur J Cancer, 2005. **41**(18): p. 2792-805.
174. Muller, A., et al., *Involvement of chemokine receptors in breast cancer metastasis.* Nature, 2001. **410**(6824): p. 50-6.
175. Tatarek, J., et al., *Notch1 inhibition targets the leukemia-initiating cells in a Tal1/Lmo2 mouse model of T-ALL.* Blood, 2011. **118**(6): p. 1579-90.
176. Kiselyov, A.S., *Targeting the hedgehog signaling pathway with small molecules.* Anticancer Agents Med Chem, 2006. **6**(5): p. 445-9.
177. Li, X., et al., *Intrinsic resistance of tumorigenic breast cancer cells to chemotherapy.* J Natl Cancer Inst, 2008. **100**(9): p. 672-9.
178. Copland, M., et al., *Dasatinib (BMS-354825) targets an earlier progenitor population than imatinib in primary CML but does not eliminate the quiescent fraction.* Blood, 2006. **107**(11): p. 4532-9.
179. Zuch, D., et al., *Targeting radioresistant osteosarcoma cells with parthenolide.* J Cell Biochem, 2011.
180. Wang, Y., et al., *Targeting HIF1alpha eliminates cancer stem cells in hematological malignancies.* Cell Stem Cell, 2011. **8**(4): p. 399-411.
181. Okada, S., et al., *In vivo and in vitro stem cell function of c-kit- and Sca-1-positive murine hematopoietic cells.* Blood, 1992. **80**(12): p. 3044-50.
182. Harris, A.L., *Hypoxia--a key regulatory factor in tumour growth.* Nat Rev Cancer, 2002. **2**(1): p. 38-47.
183. Semenza, G.L., *Targeting HIF-1 for cancer therapy.* Nat Rev Cancer, 2003. **3**(10): p. 721-32.

184. Comerford, K.M., et al., *Hypoxia-inducible factor-1-dependent regulation of the multidrug resistance (MDR1) gene.* Cancer Res, 2002. **62**(12): p. 3387-94.
185. Krishnamurthy, P., et al., *The stem cell marker Bcrp/ABCG2 enhances hypoxic cell survival through interactions with heme.* J Biol Chem, 2004. **279**(23): p. 24218-25.
186. Joseph, N.M. and S.J. Morrison, *Toward an understanding of the physiological function of Mammalian stem cells.* Dev Cell, 2005. **9**(2): p. 173-83.
187. Ohlstein, B., et al., *The stem cell niche: theme and variations.* Curr Opin Cell Biol, 2004. **16**(6): p. 693-9.
188. Ohlstein, B. and A. Spradling, *The adult Drosophila posterior midgut is maintained by pluripotent stem cells.* Nature, 2006. **439**(7075): p. 470-4.
189. Wilson, A. and F. Radtke, *Multiple functions of Notch signaling in self-renewing organs and cancer.* FEBS Lett, 2006. **580**(12): p. 2860-8.
190. Gustafsson, M.V., et al., *Hypoxia requires notch signaling to maintain the undifferentiated cell state.* Dev Cell, 2005. **9**(5): p. 617-28.
191. Hirata, H., et al., *Oscillatory expression of the bHLH factor Hes1 regulated by a negative feedback loop.* Science, 2002. **298**(5594): p. 840-3.
192. Takebayashi, K., et al., *Structure, chromosomal locus, and promoter analysis of the gene encoding the mouse helix-loop-helix factor HES-1. Negative autoregulation through the multiple N box elements.* J Biol Chem, 1994. **269**(7): p. 5150-6.
193. Pear, W.S. and J.C. Aster, *T cell acute lymphoblastic leukemia/lymphoma: a human cancer commonly associated with aberrant NOTCH1 signaling.* Curr Opin Hematol, 2004. **11**(6): p. 426-33.
194. Martinez-Climent, J.A., et al., *Lymphoma stem cells: enough evidence to support their existence?* Haematologica, 2010. **95**(2): p. 293-302.
195. Jones, R.J., et al., *Circulating clonotypic B cells in classic Hodgkin lymphoma.* Blood, 2009. **113**(23): p. 5920-6.
196. Isaacs, J.S., W. Xu, and L. Neckers, *Heat shock protein 90 as a molecular target for cancer therapeutics.* Cancer Cell, 2003. **3**(3): p. 213-7.
197. Valbuena, J.R., et al., *Expression of heat-shock protein-90 in non-Hodgkin's lymphomas.* Mod Pathol, 2005. **18**(10): p. 1343-9.
198. Kamal, A., et al., *A high-affinity conformation of Hsp90 confers tumour selectivity on Hsp90 inhibitors.* Nature, 2003. **425**(6956): p. 407-10.
199. Stoler, D.L., et al., *The onset and extent of genomic instability in sporadic colorectal tumor progression.* Proc Natl Acad Sci U S A, 1999. **96**(26): p. 15121-6.
200. Hahn, W.C. and R.A. Weinberg, *Modelling the molecular circuitry of cancer.* Nat Rev Cancer, 2002. **2**(5): p. 331-41.
201. Korkaya, H., et al., *HER2 regulates the mammary stem/progenitor cell population driving tumorigenesis and invasion.* Oncogene, 2008. **27**(47): p. 6120-30.
202. Korkaya, H., et al., *Regulation of mammary stem/progenitor cells by PTEN/AKT/beta-catenin signaling.* PLoS Biol, 2009. **7**(6): p. e1000121.
203. Sauvageot, C.M., et al., *Efficacy of the HSP90 inhibitor 17-AAG in human glioma cell lines and tumorigenic glioma stem cells.* Neuro Oncol, 2009. **11**(2): p. 109-21.

204. Gallia, G.L., et al., *Inhibition of AKT inhibits growth of glioblastoma and glioblastoma stem-like cells.* Mol Cancer Ther, 2009. **8**(2): p. 386-93.
205. Bagatell, R. and L. Whitesell, *Altered Hsp90 function in cancer: a unique therapeutic opportunity.* Mol Cancer Ther, 2004. **3**(8): p. 1021-30.
206. Neckers, L., *Heat shock protein 90: the cancer chaperone.* J Biosci, 2007. **32**(3): p. 517-30.
207. Zhao, R., et al., *Navigating the chaperone network: an integrative map of physical and genetic interactions mediated by the hsp90 chaperone.* Cell, 2005. **120**(5): p. 715-27.
208. Dezwaan, D.C. and B.C. Freeman, *HSP90: the Rosetta stone for cellular protein dynamics?* Cell Cycle, 2008. **7**(8): p. 1006-12.
209. Welch, W.J., *The role of heat-shock proteins as molecular chaperones.* Curr Opin Cell Biol, 1991. **3**(6): p. 1033-8.
210. Welch, W.J. and J.R. Feramisco, *Purification of the major mammalian heat shock proteins.* J Biol Chem, 1982. **257**(24): p. 14949-59.
211. Trepel, J., et al., *Targeting the dynamic HSP90 complex in cancer.* Nat Rev Cancer, 2010. **10**(8): p. 537-49.
212. Kamal, A., M.F. Boehm, and F.J. Burrows, *Therapeutic and diagnostic implications of Hsp90 activation.* Trends Mol Med, 2004. **10**(6): p. 283-90.
213. Wiech, H., et al., *Hsp90 chaperones protein folding in vitro.* Nature, 1992. **358**(6382): p. 169-70.
214. McClellan, A.J., et al., *Diverse cellular functions of the Hsp90 molecular chaperone uncovered using systems approaches.* Cell, 2007. **131**(1): p. 121-35.
215. Falsone, S.F., et al., *A proteomic snapshot of the human heat shock protein 90 interactome.* FEBS Lett, 2005. **579**(28): p. 6350-4.
216. Bonvini, P., et al., *Nucleophosmin-anaplastic lymphoma kinase (NPM-ALK), a novel Hsp90-client tyrosine kinase: down-regulation of NPM-ALK expression and tyrosine phosphorylation in ALK(+) CD30(+) lymphoma cells by the Hsp90 antagonist 17-allylamino,17-demethoxygeldanamycin.* Cancer Res, 2002. **62**(5): p. 1559-66.
217. Mabjeesh, N.J., et al., *Geldanamycin induces degradation of hypoxia-inducible factor 1alpha protein via the proteosome pathway in prostate cancer cells.* Cancer Res, 2002. **62**(9): p. 2478-82.
218. Taipale, M., D.F. Jarosz, and S. Lindquist, *HSP90 at the hub of protein homeostasis: emerging mechanistic insights.* Nat Rev Mol Cell Biol, 2010. **11**(7): p. 515-28.
219. Ali, M.M., et al., *Crystal structure of an Hsp90-nucleotide-p23/Sba1 closed chaperone complex.* Nature, 2006. **440**(7087): p. 1013-7.
220. Dollins, D.E., et al., *Structures of GRP94-nucleotide complexes reveal mechanistic differences between the hsp90 chaperones.* Mol Cell, 2007. **28**(1): p. 41-56.
221. Pearl, L.H. and C. Prodromou, *Structure and mechanism of the Hsp90 molecular chaperone machinery.* Annu Rev Biochem, 2006. **75**: p. 271-94.
222. Dutta, R. and M. Inouye, *GHKL, an emergent ATPase/kinase superfamily.* Trends Biochem Sci, 2000. **25**(1): p. 24-8.

223. Hawle, P., et al., *The middle domain of Hsp90 acts as a discriminator between different types of client proteins.* Mol Cell Biol, 2006. **26**(22): p. 8385-95.
224. Terasawa, K., M. Minami, and Y. Minami, *Constantly updated knowledge of Hsp90.* J Biochem, 2005. **137**(4): p. 443-7.
225. Pearl, L.H., C. Prodromou, and P. Workman, *The Hsp90 molecular chaperone: an open and shut case for treatment.* Biochem J, 2008. **410**(3): p. 439-53.
226. Brandt, G.E. and B.S. Blagg, *Alternate strategies of Hsp90 modulation for the treatment of cancer and other diseases.* Curr Top Med Chem, 2009. **9**(15): p. 1447-61.
227. Richter, K., et al., *Conserved conformational changes in the ATPase cycle of human Hsp90.* J Biol Chem, 2008. **283**(26): p. 17757-65.
228. Prodromou, C., et al., *Regulation of Hsp90 ATPase activity by tetratricopeptide repeat (TPR)-domain co-chaperones.* EMBO J, 1999. **18**(3): p. 754-62.
229. Richter, K., et al., *Sti1 is a non-competitive inhibitor of the Hsp90 ATPase. Binding prevents the N-terminal dimerization reaction during the atpase cycle.* J Biol Chem, 2003. **278**(12): p. 10328-33.
230. Li, J., K. Richter, and J. Buchner, *Mixed Hsp90-cochaperone complexes are important for the progression of the reaction cycle.* Nat Struct Mol Biol, 2011. **18**(1): p. 61-6.
231. Li, J., J. Soroka, and J. Buchner, *The Hsp90 chaperone machinery: Conformational dynamics and regulation by co-chaperones.* Biochim Biophys Acta, 2012. **1823**(3): p. 624-35.
232. Meyer, P., et al., *Structural basis for recruitment of the ATPase activator Aha1 to the Hsp90 chaperone machinery.* EMBO J, 2004. **23**(6): p. 1402-10.
233. Panaretou, B., et al., *Activation of the ATPase activity of hsp90 by the stress-regulated cochaperone aha1.* Mol Cell, 2002. **10**(6): p. 1307-18.
234. McLaughlin, S.H., H.W. Smith, and S.E. Jackson, *Stimulation of the weak ATPase activity of human hsp90 by a client protein.* J Mol Biol, 2002. **315**(4): p. 787-98.
235. Hessling, M., K. Richter, and J. Buchner, *Dissection of the ATP-induced conformational cycle of the molecular chaperone Hsp90.* Nat Struct Mol Biol, 2009. **16**(3): p. 287-93.
236. Okabe, M., et al., *Effect of herbimycin A, an antagonist of tyrosine kinase, on bcr/abl oncoprotein-associated cell proliferations: abrogative effect on the transformation of murine hematopoietic cells by transfection of a retroviral vector expressing oncoprotein P210bcr/abl and preferential inhibition on Ph1-positive leukemia cell growth.* Blood, 1992. **80**(5): p. 1330-8.
237. Messaoudi, S., et al., *Recent advances in Hsp90 inhibitors as antitumor agents.* Anticancer Agents Med Chem, 2008. **8**(7): p. 761-82.
238. Roe, S.M., et al., *Structural basis for inhibition of the Hsp90 molecular chaperone by the antitumor antibiotics radicicol and geldanamycin.* J Med Chem, 1999. **42**(2): p. 260-6.
239. Stebbins, C.E., et al., *Crystal structure of an Hsp90-geldanamycin complex: targeting of a protein chaperone by an antitumor agent.* Cell, 1997. **89**(2): p. 239-50.

240. Uehara, Y., *Natural product origins of Hsp90 inhibitors.* Curr Cancer Drug Targets, 2003. **3**(5): p. 325-30.
241. Blagg, B.S. and T.D. Kerr, *Hsp90 inhibitors: small molecules that transform the Hsp90 protein folding machinery into a catalyst for protein degradation.* Med Res Rev, 2006. **26**(3): p. 310-38.
242. Neckers, L., *Chaperoning oncogenes: Hsp90 as a target of geldanamycin.* Handb Exp Pharmacol, 2006(172): p. 259-77.
243. Mimnaugh, E.G., C. Chavany, and L. Neckers, *Polyubiquitination and proteasomal degradation of the p185c-erbB-2 receptor protein-tyrosine kinase induced by geldanamycin.* J Biol Chem, 1996. **271**(37): p. 22796-801.
244. Supko, J.G., et al., *Preclinical pharmacologic evaluation of geldanamycin as an antitumor agent.* Cancer Chemother Pharmacol, 1995. **36**(4): p. 305-15.
245. Schnur, R.C., et al., *erbB-2 oncogene inhibition by geldanamycin derivatives: synthesis, mechanism of action, and structure-activity relationships.* J Med Chem, 1995. **38**(19): p. 3813-20.
246. Hostein, I., et al., *Inhibition of signal transduction by the Hsp90 inhibitor 17-allylamino-17-demethoxygeldanamycin results in cytostasis and apoptosis.* Cancer Res, 2001. **61**(10): p. 4003-9.
247. Kelland, L.R., et al., *DT-Diaphorase expression and tumor cell sensitivity to 17-allylamino, 17-demethoxygeldanamycin, an inhibitor of heat shock protein 90.* J Natl Cancer Inst, 1999. **91**(22): p. 1940-9.
248. Solit, D.B., et al., *17-Allylamino-17-demethoxygeldanamycin induces the degradation of androgen receptor and HER-2/neu and inhibits the growth of prostate cancer xenografts.* Clin Cancer Res, 2002. **8**(5): p. 986-93.
249. Goetz, M.P., et al., *Phase I trial of 17-allylamino-17-demethoxygeldanamycin in patients with advanced cancer.* J Clin Oncol, 2005. **23**(6): p. 1078-87.
250. Banerji, U., et al., *Phase I pharmacokinetic and pharmacodynamic study of 17-allylamino, 17-demethoxygeldanamycin in patients with advanced malignancies.* J Clin Oncol, 2005. **23**(18): p. 4152-61.
251. Pacey, S., et al., *Hsp90 inhibitors in the clinic.* Handb Exp Pharmacol, 2006(172): p. 331-58.
252. Dai, C. and L. Whitesell, *HSP90: a rising star on the horizon of anticancer targets.* Future Oncol, 2005. **1**(4): p. 529-40.
253. Solit, D.B., et al., *Phase II trial of 17-allylamino-17-demethoxygeldanamycin in patients with metastatic melanoma.* Clin Cancer Res, 2008. **14**(24): p. 8302-7.
254. Modi, S., et al., *HSP90 inhibition is effective in breast cancer: a phase II trial of tanespimycin (17-AAG) plus trastuzumab in patients with HER2-positive metastatic breast cancer progressing on trastuzumab.* Clin Cancer Res, 2011. **17**(15): p. 5132-9.
255. Pacey, S., et al., *A Phase II trial of 17-allylamino, 17-demethoxygeldanamycin (17-AAG, tanespimycin) in patients with metastatic melanoma.* Invest New Drugs, 2012. **30**(1): p. 341-9.
256. Eiseman, J.L., et al., *Pharmacokinetics and pharmacodynamics of 17-demethoxy 17-[[(2-dimethylamino)ethyl]amino]geldanamycin (17DMAG, NSC 707545) in C.B-17 SCID mice bearing MDA-MB-231 human breast cancer xenografts.* Cancer Chemother Pharmacol, 2005. **55**(1): p. 21-32.

257. Hollingshead, M., et al., *In vivo antitumor efficacy of 17-DMAG (17-dimethylaminoethylamino-17-demethoxygeldanamycin hydrochloride), a water-soluble geldanamycin derivative.* Cancer Chemother Pharmacol, 2005. **56**(2): p. 115-25.
258. Pacey, S., et al., *A phase I study of the heat shock protein 90 inhibitor alvespimycin (17-DMAG) given intravenously to patients with advanced solid tumors.* Clin Cancer Res, 2011. **17**(6): p. 1561-70.
259. Didelot, C., et al., *Anti-cancer therapeutic approaches based on intracellular and extracellular heat shock proteins.* Curr Med Chem, 2007. **14**(27): p. 2839-47.
260. Neckers, L. and P. Workman, *Hsp90 molecular chaperone inhibitors: are we there yet?* Clin Cancer Res, 2012. **18**(1): p. 64-76.
261. Janin, Y.L., *ATPase inhibitors of heat-shock protein 90, second season.* Drug Discov Today, 2010. **15**(9-10): p. 342-53.
262. Sequist, L.V., et al., *Activity of IPI-504, a novel heat-shock protein 90 inhibitor, in patients with molecularly defined non-small-cell lung cancer.* J Clin Oncol, 2010. **28**(33): p. 4953-60.
263. Delmotte, P. and J. Delmotte-Plaque, *A new antifungal substance of fungal origin.* Nature, 1953. **171**(4347): p. 344.
264. Dymock, B.W., et al., *Novel, potent small-molecule inhibitors of the molecular chaperone Hsp90 discovered through structure-based design.* J Med Chem, 2005. **48**(13): p. 4212-5.
265. Soga, S., et al., *Development of radicicol analogues.* Curr Cancer Drug Targets, 2003. **3**(5): p. 359-69.
266. Chiosis, G., *Discovery and development of purine-scaffold Hsp90 inhibitors.* Curr Top Med Chem, 2006. **6**(11): p. 1183-91.
267. Taldone, T., et al., *Targeting Hsp90: small-molecule inhibitors and their clinical development.* Curr Opin Pharmacol, 2008. **8**(4): p. 370-4.
268. Rajan, A., et al., *A phase I study of PF-04929113 (SNX-5422), an orally bioavailable heat shock protein 90 inhibitor, in patients with refractory solid tumor malignancies and lymphomas.* Clin Cancer Res, 2011. **17**(21): p. 6831-9.
269. Samuel, T.A., Sessa, C., Britten, C., Milligan, K.S., Mita, M.M., Banerji, U., Pluard, T.J., Stiegler, P., Quadt, C., Shapiro, G., *AUY922, a novel HSP90 inhibitor: Final results of a first-in-human study in patients with advanced solid malignancies (ABSTRACT).* J Clin Oncol, 2010. **28**(15s).
270. Marcu, M.G., et al., *The heat shock protein 90 antagonist novobiocin interacts with a previously unrecognized ATP-binding domain in the carboxyl terminus of the chaperone.* J Biol Chem, 2000. **275**(47): p. 37181-6.
271. Burlison, J.A., et al., *Novobiocin: redesigning a DNA gyrase inhibitor for selective inhibition of hsp90.* J Am Chem Soc, 2006. **128**(48): p. 15529-36.
272. Zhao, H., et al., *Engineering an antibiotic to fight cancer: optimization of the novobiocin scaffold to produce anti-proliferative agents.* J Med Chem, 2011. **54**(11): p. 3839-53.
273. Matthews, S.B., et al., *Characterization of a novel novobiocin analogue as a putative C-terminal inhibitor of heat shock protein 90 in prostate cancer cells.* Prostate, 2010. **70**(1): p. 27-36.

274. Donnelly, A. and B.S. Blagg, *Novobiocin and additional inhibitors of the Hsp90 C-terminal nucleotide-binding pocket.* Curr Med Chem, 2008. **15**(26): p. 2702-17.
275. Wong, K., Koczywas, M., Goldman, J.W., Paschold, E.H., Horn, L., Lufkin, J.M., et al., *An open-label phase II study of the Hsp90 inhibitor ganetespib (STA-9090) as monotherapy in patients with advanced non small cell lung cancer (NSCLC). (Meeting Abstract).* J Clin Oncol, 2011. **29**.
276. Peng, C., et al., *Inhibition of heat shock protein 90 prolongs survival of mice with BCR-ABL-T315I-induced leukemia and suppresses leukemic stem cells.* Blood, 2007. **110**(2): p. 678-85.
277. Sobhan, P.K., et al., *Identification of heat shock protein 90 inhibitors to sensitize drug resistant side population tumor cells using a cell based assay platform.* Cancer Lett, 2012. **317**(1): p. 78-88.

Chapter 2

17-AAG mediated HSP90 Inhibition Effectively Eliminates TGB Lymphoma Cancer Stem Cells

Abstract

Peripheral T-Cell lymphomas (PTCL) encompass a complex and typically aggressive set of cancers. The response to treatment is usually poor in patients with these diseases, resulting in low survival rates. Patient relapse and metastasis provide the greatest hurdles in improving rates of long-term survival, since very few effective treatments exist in the advanced stages of disease. Cancer stem cells (CSCs) are implicated in many solid and hematological cancers as mediators of tumor recurrence and metastasis. Therefore, new strategies are needed to effective eliminate CSCs if improvements in survival are to be achieved. In the present study, we used our TGB mouse model of lymphoma to demonstrate that previously characterized CSCs are susceptible to 17-AAG mediated HSP90 inhibition. We found that dramatically low concentrations of 17-AAG reduced both the number and self-renewal capacity of these CSCs, in addition to CSCs present in acute myeloid leukemia (AML). While the committed, mature lymphoma cells were also susceptible to 17-AAG treatment, higher concentrations were required to elicit this effect, suggesting a selective sensitivity within the CSC population. These results were recapitulated in vivo, as a near dose-dependent increase in survival is achieved with 17-AAG treatment, while also reducing the CSC capacity to initiate tumor growth in reimplantation assays. Our study demonstrates the

utility of 17-AAG mediated HSP90 inhibition in treating lymphoma CSCs, and warrants further clinical evaluation.

Introduction

Peripheral T-cell lymphomas consist of a heterogeneous assortment of hematological cancers. With an incidence rate of 1 in 100,000 individuals, PTCL are considered rare, and present an aggressive phenotype [1]. Unfortunately, their rarity has impeded our ability to both understand and design therapies specific for these cancers. Stemming from the lack of clinical trials for PTCL, typical first line therapy consists of strategies adopted from successful approaches to B-cell lymphomas, but result in much less effective outcomes. In addition, the lack of effective therapies which can manage PTCL following relapse contributes to the low overall survival rate (10-30%) [2-6]. Therefore, new directions are urgently needed for patients who suffer with PTCL, that can be both effective at managing disease and can improve overall survival.

There is substantial evidence today supporting the perspective that many cancers function as hierarchical organizations of cancer cells originating from tumor-initiating cells, typically called cancer stem cells (CSCs) [7-14]. Intrinsic resistance to both chemotherapy and fractionated radiation allows CSCs to survive strategies often successful for removing the tumor bulk, allowing disease relapse often with refractory tumors. In addition, distant metastases often contain similar genetic lesions as the primary tumor, implicating CSCs for their origin [15-18]. This suggests that effective therapies for CSCs have the potential to reduce rates of tumor relapse and metastasis, both of which have been associated with determining overall survival. Current

approaches to eliminate CSCs rely on disruption of self-renewal, a process necessary for CSC maintenance. Initiation of self-renewal is orchestrated via the signaling by a number of intrinsic (Wnt, Sonic Hedgehog, NOTCH, p53 etc.) and extrinsic (microenvironment, oxygen tension etc.) signals. This complexity offers the chance for redundancy if one signal is inhibited. Thus, simultaneous inhibition of multiple self-renewal signals by HSP90 inhibition offers the highest chance for success, as many clients of HSP90 have been shown to influence stem cell self-renewal.

Molecular chaperone proteins function to ensure the proper conformation of client proteins when cells experience stress or damage [19]. Heat shock protein 90 (HSP90) is the most studied and well known molecular chaperone that facilitates the maturation and stable conformation of several client proteins, including transcription factors Hypoxia Inducible Factor 1α (HIF1α) and p53, serine/threonine kinases (AKT, Raf-1, and Cdk4), receptor/non-receptor kinases (HER2, EGFR, Src family kinases), and steroid hormone receptors (androgen and estrogen) [20-28]. As many of these client proteins significantly contribute to tumor growth and survival, abrogation of their function with a single inhibitor has been an attractive prospect, making HSP90 an appealing molecular target for drug development [29]. One of the original and most studied HSP90 inhibitors is a derivative of the geldanamycin antibiotic, 17-N-allylamino-17-demethoxy geldanamycin (17-AAG) [30]. Through reversible binding to the ATP pocket of HSP90, 17-AAG potently disrupts its function, and ultimately induces tumor cell death.

Tumor stem cells from both AML and glioma have been shown to rely on the activity of HIF1α or 2α, respectively, for their maintenance [31-33]. Human AML CSCs are a rare population of $CD34^{+}CD38^{-}$ cells, and are thought to be responsible for the

resistance of conventional therapies [31, 34, 35]. Current efforts for targeting CSCs have focused on disruption of self-renewal [36]. However, this approach may be hampered by the redundancy in self-renewal pathways. In addition, CSCs that are quiescent may be resistant to inhibitors to self-renewal. Therefore, disrupting genes that are required for both maintaining CSCs in a stem-like state as well as self-renewal might provide a more effective therapy. We have previously reported a strain of T cell receptor transgenic mice (TGB) which spontaneously develop lymphoma with 100% incidence, due to an insertional mutation of the Emp2a gene [37]. Using this mouse lymphoma model, we identified that a small subset of cells expressing both c-Kit and Sca1 are lymphoma CSCs [32]. Here we show that these lymphoma CSCs are efficiently eliminated via apoptosis after 17-AAG HSP90 inhibition, at doses substantially lower than those required to affect the tumor bulk. 17-AAG treatment also reduced the self-renewal capacity of lymphoma CSCs, both in vitro and in vivo. Lastly, AML CSCs were similarly reduced in number and capacity for self-renewal following 17-AAG treatment. This study demonstrates that 17-AAG is an efficient CSC-killing agent, and requires reevaluation in the clinical setting.

Materials and Methods

Mice, Cells and Reagents

TCR transgenic B line (TGB) mice in the B10.BR background were maintained by heterozygous breeding pairs. B10.BR mice were used as recipients in lymphoma cell inoculation, and severe combined immunodeficiency (SCID) mice were used for human

AML maintenance. Both lines were purchased from the National Cancer Institute. All mice were kept and used for tumor implantation and treatment according to the procedures approved by the Unit of Laboratory Animal Facility (ULAM) at University of Michigan.

TGB lymphoma cells were maintained in 1% methylcellulose medium (MethoCult GF, 03434, Stem Cell Technologies) supplemented with murine cytokines (R&D Systems): 10 ng/mL recombinant IL-3 and IL-6, and 100 ng/mL stem cell factor (SCF). For some in vitro experiments, TGB lymphoma cells were transferred from 1% methylcellulose culture to an expansion medium: RPMI 1640 medium supplemented with 10% FBS, IL-3, IL-6, and SCF cytokines, 100 μM non-essential amino acids, 10 mM HEPES, and 1 mM sodium pyruvate. Human AML cells were derived from the enlarged spleen tissue of SCID mice injected with aggressive AML CSCs (AML-71) as described before [32], and maintained in SCID mice via transplantation. Short term expansion and colony formation assays of the AML CSCs were carried out similarly as our lymphoma cells, except for a substitution of human cytokines for murine cytokines. 17-AAG was purchased from LC Laboratories.

Isolation of Lymphoma CSCs and Colony Formation Assay

The lymphoma CSCs (c-Kit^{+}Sca1^{+}) are a rare population in TGB lymphoma tissue and express the surface markers c-Kit and Sca1. The CSCs were isolated from primary spleen lymphoma tissue of TGB mice by fluorescence-activated cell sorting (FACS) technology, or isolated by auto-MACS microbeads (Miltenyi Biotech) twice, after staining with antibodies to c-Kit and Sca1 (both from BD Bioscience). To maintain

the lymphoma population, lymphoma cells are grown under non-adherent conditions, using 1% methylcellulose medium supplemented with murine cytokines as described above. Using these conditions, spheroid colonies form and can be serially propagated for in vitro experiments (colony formation assay with drug treatment). In addition, to obtain lymphoma cells for implantation into B10.BR mice, cells are expanded from these colonies by first dissociating them, and then replating the cells in RPMI 1640 medium supplemented with murine cytokines for 24 hours. After the allotted time, lymphoma cells are washed and resuspended in fresh RPMI 1640 for injection into mice.

To perform the colony formation assays, lymphoma cells were seeded in a 12-well plate containing 1% methylcellulose medium supplemented with murine cytokines and 17-AAG or vehicle. After 6-8 days of culture, spheroid colonies were counted, pooled, and then replated without the addition of 17-AAG or vehicle treatment, for consecutive rounds. For tumor inoculation, the cultured lymphoma cells were expanded in vitro in RPMI1640 medium described above, 24 hours before these experiments.

MTT ([3-(4,5-dimethyl thiazol-2-yl)-2,5-diphenyl tetrazolium bromide]) Assay

The expanded lymphoma cells were seeded in the RPMI1640 culture medium at a cellular density of 2.5 x 10^5 cells/ml in a 24-well plate. Next, the cells were treated with increasing concentrations of 17-AAG and cultured for 48 hours. At the end of the treatment, the MTT assay for determining cell viability was performed according to the manufacture's protocol (Promega) and the plate was read at 490 nm.

Apoptosis Assay

The cultured lymphoma and AML cells, after treatment with 17-AAG for 24 hours, were stained with fluorescence-conjugated antibodies for the cell surface markers c-Kit and Sca1 (CD34, CD38 for AML cells), and then Annexin-V for 15 minutes at room temperature before 5 μM of DAPI was added. The apoptosis percentage of these CSCs and differentiated cells were then analyzed by flow cytometry.

In Vivo Treatment of Lymphoma with 17-AAG

Healthy, immune competent B10.BR mice were inoculated with $5x10^5$ lymphoma cells via intraperitoneal injection. Seven days following tumor implantation, the mice were I.P. injected with 17-AAG or vehicle (10% DMSO + 40% Cremophor EL:Ethanol (3:1) (v/v) + 50 % PBS) every other day for three weeks. At the cessation of treatment, mice were monitored up to 80 days post tumor cell injection. To determine the effects of 17-AAG on lymphoma initiation in vivo, secondary B10.BR recipient mice were implanted by intraperitoneal injection of $1x10^5$ lymphoma cells from the spleens of mice that had been treated with 17-AAG or vehicle. These mice were followed up to 160 days post tumor cell injection to monitor differences in tumor initiation.

Immunohistochemistry

Slides were stained using a modified protocol (Biolegend) for staining frozen sections. Spleen tissue was cryo-embedded with OCT compound (Ted Pella, Inc.) using liquid nitrogen to ensure complete freezing. Frozen blocks were cut (5-10 μm) using a cryotome, placed onto slides, and allowed to dry overnight. For fixation, slides were

covered in -20 degree C acetone for 10 min. Slides were then dried, rinsed with PBS, and incubated in 0.03% hydrogen peroxide solution (in PBS) for 10 minutes at room temperature. Next, slides were rinsed with PBS, blocked using normal goat serum, and incubated with primary antibody (goat anti-mouse Thy1, BD Biosciences) overnight at 4 degree C. Next slides were rinsed with PBS, and 200 μL of DAB reagent (Vector Labs) was added to develop color for 2-3 minutes. Slides were then stained using Hematoxylin. Afterwards, slides were rinsed in DI water then incubated in Ammonium solution to develop Hematoxylin stain. For dehydration, slides were incubated for 3 minutes in consecutive ethanol solutions (75%, 95%, 100%) before being incubated in xylene. Lastly, slides were mounted with Cytoseal XYL (xylene based). For staining of liver and lung metastasis, paraffin-embedded tissue was sectioned and prepared slides were sent to the University of Michigan Research Histology and Immunoperoxidase Laboratory for Hematoxylin and Eosin staining.

Statistics

Statistical significance was determined using unpaired Student's t-test.

Results

The Distinct Features of Lymphoma CSCs and Bulk Lymphoma Cells (non-CSCs)

We have previously demonstrated that AKT/GSK-3β/β-catenin signaling is constitutively activated in the TGB lymphoma c-Kit$^-$Sca1$^-$ cells (non-CSCs), and that HIF1α plays a critical role in the maintenance of the lymphoma c-Kit$^+$Sca1$^+$ cells (CSCs) [32, 37]. These lymphoma CSCs can efficiently initiate lymphoma when small numbers are injected into immunocompetent recipient mice (Figure 2.1A,B). Following tumor initiation, the mice ultimately succumb to the committed, highly proliferative lymphoma cells, which rapidly grow into a tumor mass in the spleen and metastasize to other organs, such as the liver and lung, leading to death within 1-2 months post-inoculation [32, 37]. These findings prompted us to devise a drug therapy which could effectively target both CSCs and non-CSCs, for the treatment of advanced lymphoma in humans. Because the CSCs and non-CSCs harbor constitutively active HIF1α and AKT (two client proteins of HSP90), respectively, we tested the HSP90 inhibitor 17-AAG for the simultaneous targeting of the two cell populations.

17-AAG Selectively Eliminates Lymphoma CSCs over non-CSCs

We next examined the ability of 17-AAG to suppress TGB lymphoma growth using the MTT cell viability assay. TGB lymphoma viability was inhibited with 17-AAG, with an IC50 of 238 nM (Figure 2.2A). In contrast, c-Kit$^+$Sca1$^+$ lymphoma cells treated with 17-AAG were significantly more sensitive to HSP90 inhibition, with an IC50

of 5.64 nM (Figure 2.2B-D). This substantial difference in the IC50 indicates a profound sensitivity of the CSC population to 17-AAG.

Previous studies have shown that treatment with 17-AAG results in programmed cell death via apoptosis [38]. To determine if 17-AAG induced apoptosis in the CSCs and/or bulk tumor cells, we stained lymphoma cells with Annexin V, a surface marker of apoptotic cells, after 17-AAG treatment. As shown in Figure 2.3, low doses of 17-AAG (10 and 25 nM) increased apoptosis of c-Kit^{+}Sca1^{+} cells by 2 to 3-fold, as compared to untreated control cells. However, 17-AAG failed to induce apoptosis of c-Kit^{-}Sca1^{-} cells at these low concentrations.

17-AAG Impairs Self-Renewal of TGB Lymphoma CSCs

As CSCs are best defined by their ability to self-renew and initiate tumor growth rather than by their surface marker expression, functional assays provide a more accurate assessment of drug-mediated therapeutic effects [39]. The in vitro generation of spheroid colonies under attachment-free conditions has been widely used as a manner to determine the number of CSCs within a population, as well as assess the ability for those CSCs to self-renew [40-42]. Formation of these colonies is dependent on the residing stem cell population, and is reduced with each stage of differentiation. To assess if 17-AAG affected CSC self-renewal, we plated lymphoma cells and treated them with increasing concentrations of 17-AAG. As a result, 10 nM 17-AAG reduced the colony formation unit (CFU) of CSCs by more than 50% (Figure 2.4), consistent with the dose necessary for induction of apoptosis. These colonies were then dissociated to the single cell level and replated in the absence of drug, to observe if self-renewal was also disrupted. Cells

from colonies previously treated with 10 nM 17-AAG were dramatically reduced in their capacity to initiate secondary colonies, indicating that 17-AAG impaired the self-renewal ability of the CSCs in vitro.

17-AAG Abrogates Lymphoma Initiation In Vivo

To investigate whether HSP90 inhibition can reduce lymphoma initiation in vivo, we injected $5x10^5$ TGB lymphoma cells intraperitoneally (I.P.) into recipient B10.BR mice. Seven days after injection, different doses of 17-AAG (5 to 40 mg/kg) or vehicle control were given to mice every other day for three weeks. Upon cessation of treatment, four mice from the 40 mg/kg 17-AAG or control group were euthanized and their spleens weighed for indication of lymphoma. Vehicle-treated mice exhibited enlarged spleens enriched in lymphoma cells that stained positive for Thy-1, a marker for T lymphoma cells (Figure 2.5A-C). The lymphoma cells had also metastasized to liver and lung tissue, as typically seen in mice with this cancer [37]. In contrast, spleens from mice which had received 17-AAG were dramatically smaller, with less infiltrating lymphoma cells in the spleen, and a lower metastatic spread into other organs, as compared to the vehicle-treated controls (Figure 2.5C). In addition, 17-AAG treated mice survived significantly longer compared to mice which received vehicle alone, demonstrating the effectiveness of 17-AAG in suppressing the lymphoma in vivo (Figure 2.5D).

A hallmark of CSC function is their ability to serially reestablish tumors in recipient mice. This CSC trait reflects their capacity for self-renewal in vivo, and provides a method for detecting agents that can disrupt this process. To examine if 17-AAG treatment impaired the self-renewal ability of TGB lymphoma CSCs in vivo, $1x10^5$

cells obtained from either 40 mg/kg 17-AAG- or vehicle-treated spleens were I.P. injected into five healthy secondary recipient B10.BR mice. All of the mice injected with vehicle-treated spleen cells eventually succumbed to lymphoma. In contrast, only one mouse that received 17-AAG-treated spleen cells died over the course of the study (Figure 2.5E). These data demonstrate that 17-AAG effectively impairs the self-renewal of the lymphoma CSCs in vivo.

17-AAG Mediated HSP90 Inhibition also Eliminates AML CSCs

To determine if 17-AAG treatment can selectively eliminate CSCs in hematopoietic cancers other than our lymphoma model, we used a separate mouse model of human AML that has been previously established [32]. Similar to our lymphoma cells, AML CSCs stably express HIF1α for their maintenance [32]. To see if 17-AAG also selectively targets AML CSCs, AML cells were treated with increasing concentrations of 17-AAG. Twenty five nM 17-AAG increased the percentage of apoptotic CSCs ($CD34^+CD38^-$) nearly 3-fold, as compared to vehicle treated CSCs. In contrast, 25 nM 17-AAG had little affect on inducing apoptosis in the non-CSCs ($CD34^+CD38^+$) (Figure 2.6A,B). Although a higher dose (100 nM) of 17-AAG induced apoptosis in both CSCs and non-CSCs, CSCs initiated apoptosis to a higher extent (35.5%) than non-CSCs (13.5%). Similar to lymphoma CSCs, a dramatically low dose (10 nM) of 17-AAG greatly reduced the capacity for AML CSCs to form colonies in sphere forming assays (Figure 2.6C). Taken together, these results demonstrate the effectiveness of HSP90 inhibition by 17-AAG for treating AML CSCs, and suggest the efficacy of this approach may extend to more types of hematological cancers.

Discussion

Peripheral T-cell lymphomas are rare and often difficult type of hematological cancers to treat. While new therapies continue to be developed for specific types of PTCL, improvement in overall survival remains poor [2, 5]. Tumor recurrence and metastatic spread, two problems that influence patient long-term survival the most, are demonstrated characteristics of tumor stem cells, which fail to respond to therapy due to their intrinsic resistance to cell damage [43]. Therefore, new strategies are needed which can target these types of cells, and potentially reduce both the rates of relapse and metastasis. As PTCL is a grouping of highly diverse conditions, many of which are difficult to study in vitro, we chose to use a mouse model of T-cell lymphoma that can be examined both in vitro and in vivo. Previous studies demonstrated that in this TCL the tumor bulk and CSC subpopulation were driven by the sustained activity of AKT/GSK-3β/β-catenin and HIF1α, respectively [32, 37]. As AKT and HIF1α are well-known HSP90 clients, we postulated that 17-AAG mediated HSP90 inhibition would effectively eliminate the TCL CSCs and the tumor bulk.

After verifying that our TCL CSCs (c-Kit^{+}Sca1^{+}) retained their tumorigenic potential over the committed, mature cells (c-Kit^{-}Sca1^{-}), we found that 17-AAG treatment, while capable of eliminating both populations, was more potently active against the CSCs. A more than 40-fold lower concentration of 17-AAG could efficiently eliminate the CSCs, as compared to the concentration required to effect the tumor bulk. In accordance with this observation, low concentrations of 17-AAG could induce apoptosis in CSCs, while failing to affect non-CSC cell death. This selective sensitivity was also seen in CSCs from AML, where lower concentrations of 17-AAG induced

apoptosis in the CSCs. Lymphoma and AML CSCs were also reduced in their capacity to initiate spheroid colonies in vitro when treated with 17-AAG. Colony formation has been a traditional technique to functionally assess changes in CSCs and their self-renewal. When colonies previously treated with 17-AAG or vehicle were replated without drug, the effect on self-renewal was even more dramatic. This demonstrated a reduction in the second generation of colonies, reflecting a loss in self-renewal not requiring the presence of 17-AAG, and instead was a permanent condition following inhibition of HSP90.

Next, we tested if the efficacy of 17-AAG treatment on lymphoma CSCs and the tumor bulk could also be seen in vivo. B10.BR mice that were implanted with TGB lymphoma cells died from the disease approximately 30 days later. In contrast, 17-AAG treatment extended the survival of implanted mice in a dose-dependent manner. While the 10 mg/kg 17-AAG treatment did have a slightly lower survival than the 5 mg/kg, this difference was not viewed as significantly different. When spleens were examined from mice treated with 17-AAG or vehicle, the number of infiltrating Thy-1 positive cells was found to be much lower in mice receiving the drug. It is also important to note that distant metastases (as determined through H&E staining) in liver and lung tissue appeared lower in mice which received 17-AAG treatment. As control of metastatic lesions in cancer patients is often rarely achieved and typically leads to death, this observation suggests 17-AAG may be an effective approach for reducing CSC-driven metastasis. To test if our therapy had any effect on CSC tumor initiation, spleen cells from 17-AAG and vehicle treated mice were reimplanted into new, secondary B10.BR mice, and monitored for overall survival. All of the vehicle treated mice (5 out of 5)

succumbed to the disease, while only one (1 out of 5) mouse from the 17-AAG implanted group died. This experiment emphasizes the potential for CSC targeting agents. Remaining CSCs that survive conventional therapy have the capability to regenerate tumor growth, often with a more aggressive phenotype. If CSCs can be both reduced in number and capacity for self-renewal, the overall probability for recurrence may also be reduced. As seen with our experiment, 17-AAG treatment diminished the tumorigenic capacity of the mouse lymphoma CSCs, further validating our claims for its efficacy in targeting CSCs.

Many HSP90 inhibitors have been developed since the discovery of geldanamycin, driven by the attractiveness of simultaneous reduction of many aberrant signaling proteins [44]. However, many 17-AAG trials failed to show significant patient response [45-49]. Inspection of tumors in some trials showed that client expression was often either insufficiently reduced or the reduction was short lived [44]. This has been attributed to suboptimal dosing regimens used to balance dose with toxicity stemming from 17-AAG's formulation [44]. While these reports cast doubt on the efficacy of 17-AAG to target HSP90, as measured by tumor growth inhibition, their failures cannot necessarily be extended to the residing CSCs. Solid tumor response is typically assessed as the percent reduction in initial tumor volume at the time of measurement. Under the Response Evaluation Criteria in Solid Tumors (RECIST) guidelines, complete response (100% reduction), partial response (>30% reduction), stable disease (no change) and disease progression (>20% increase) categorize the potential outcomes in trials with solid tumors [50]. As CSCs are often a small subpopulation of a given tumor, it is reasonable to conclude that their elimination would not substantially decrease the bulk volume.

Moreover, since the differentiated cell population remains capable of limited cell division, time would be needed before the tumor (lacking the replenishing CSCs) would reduce in volume enough to be detected.

It is also important to stress that while many of the trials testing 17-AAG as a single therapy have not be successful, several clinical trials combining 17-AAG treatment with other conventional therapies showed clinical responses. One trial with Her2+ breast cancer patients that progressed on Herceptin saw a 24% response rate and a 57% overall clinical benefit when combined with a 17-AAG treatment [51]. Similarly promising, patients with multiple myeloma progressing on bortezomib (a proteasome inhibitor) saw clinical benefit with the addition of a 17-AAG therapy [52]. These reports highlight two important criteria for the overall efficacy of HSP90 inhibition. First, the sensitivity of the client protein to HSP90 inhibition impacts overall efficacy. This strategy will be less effective in tumor types where the client protein is less sensitive to the loss of HSP90, or other molecular chaperones can potentially compensate for its loss [53]. Second, HSP90 inhibition is most effective in tumor cells which critically rely on the client protein for survival, and lack secondary mechanisms for compensation [53]. These criteria offer an explanation for the sensitivity observed in our lymphoma and AML CSCs with 17-AAG treatment. In general, stem cell maintenance is critically reliant on the continued capacity for self-renewal. Therefore, stem cells should be more sensitive to inhibitors which disrupt self-renewal rather than DNA repair or efflux pump activity. While a number of environmental factors and pathways shape the decision to initiate self-renewal, many redundant self-renewal pathways should be eliminated with HSP90 inhibition, as a number of client proteins are associated with self-renewal [54-56]. In particular, HIF1α

activity has been previously shown to be vital for maintaining CSCs from both our TGB mouse lymphoma model and AML [32]. HIF1α is a well-known HSP90 client protein, and has been shown to be susceptible to 17-AAG treatment. Taken together, these CSCs which are heavily reliant on HIF1α activity for maintenance of their self-renewal, are dramatically more sensitive to 17-AAG than the tumor bulk, as demonstrated by the effectiveness of a low 17-AAG concentration on these cells.

In summary, our work provides substantial evidence demonstrating the effectiveness of 17-AAG mediated HSP90 inhibition in eliminating CSCs from a TGB mouse lymphoma model and human AML. 17-AAG is capable of reducing the number of CSCs and their capacity for self-renewal both in vitro and in vivo. Moreover, 17-AAG was effective at dramatically lower concentrations as compared to the effective dose in mature, committed lymphoma and leukemia cells. In accordance with previous 17-AAG studies demonstrating CSC-targeting in solid tumors, our study further validates the potential of 17-AAG as an effective CSC inhibitor, and suggests CSC populations may be uniquely sensitive to this method of treatment. Most notably, the sensitivity of CSCs to 17-AAG implies that a low dose therapy may be sufficient to achieve efficacy, and therefore dramatically reduce the incidence of toxicity. This study provides further evidence that the utility of 17-AAG as a CSC-targeting agent merits reevaluation in clinical trials.

References

1. Morton, L.M., et al., *Lymphoma incidence patterns by WHO subtype in the United States, 1992-2001.* Blood, 2006. 107(1): p. 265-76.
2. Reiser, M., et al., *T-cell non-Hodgkin's lymphoma in adults: clinicopathological characteristics, response to treatment and prognostic factors.* Leuk Lymphoma, 2002. 43(4): p. 805-11.
3. Siegert, W., et al., *Treatment of angioimmunoblastic lymphadenopathy (AILD)-type T-cell lymphoma using prednisone with or without the COPBLAM/IMVP-16 regimen. A multicenter study. Kiel Lymphoma Study Group.* Ann Intern Med, 1992. 117(5): p. 364-70.
4. Coiffier, B., et al., *Peripheral T-cell lymphomas have a worse prognosis than B-cell lymphomas: a prospective study of 361 immunophenotyped patients treated with the LNH-84 regimen. The GELA (Groupe d'Etude des Lymphomes Agressives).* Ann Oncol, 1990. 1(1): p. 45-50.
5. Evens, A.M. and R.B. Gartenhaus, *Treatment of T-cell non-Hodgkin's lymphoma.* Curr Treat Options Oncol, 2004. 5(4): p. 289-303.
6. Besson, C., et al., *Treatment of adult T-cell leukemia-lymphoma by CHOP followed by therapy with antinucleosides, alpha interferon and oral etoposide.* Leuk Lymphoma, 2002. 43(12): p. 2275-9.
7. Holyoake, T., et al., *Isolation of a highly quiescent subpopulation of primitive leukemic cells in chronic myeloid leukemia.* Blood, 1999. 94(6): p. 2056-64.
8. George, A.A., et al., *Detection of leukemic cells in the CD34(+)CD38(-) bone marrow progenitor population in children with acute lymphoblastic leukemia.* Blood, 2001. 97(12): p. 3925-30.
9. Matsui, W., et al., *Characterization of clonogenic multiple myeloma cells.* Blood, 2004. 103(6): p. 2332-6.
10. Singh, S.K., et al., *Identification of a cancer stem cell in human brain tumors.* Cancer Res, 2003. 63(18): p. 5821-8.
11. Singh, S.K., et al., *Identification of human brain tumour initiating cells.* Nature, 2004. 432(7015): p. 396-401.
12. Al-Hajj, M., et al., *Prospective identification of tumorigenic breast cancer cells.* Proc Natl Acad Sci U S A, 2003. 100(7): p. 3983-8.
13. Stingl, J., et al., *Purification and unique properties of mammary epithelial stem cells.* Nature, 2006. 439(7079): p. 993-7.
14. Collins, A.T., et al., *Prospective identification of tumorigenic prostate cancer stem cells.* Cancer Res, 2005. 65(23): p. 10946-51.
15. Blagosklonny, M.V., *Why therapeutic response may not prolong the life of a cancer patient: selection for oncogenic resistance.* Cell Cycle, 2005. 4(12): p. 1693-8.
16. Tang, C., B.T. Ang, and S. Pervaiz, *Cancer stem cell: target for anti-cancer therapy.* FASEB J, 2007. 21(14): p. 3777-85.
17. Maitland, N.J. and A.T. Collins, *Prostate cancer stem cells: a new target for therapy.* J Clin Oncol, 2008. 26(17): p. 2862-70.
18. Wicha, M.S., *Cancer stem cells and metastasis: lethal seeds.* Clin Cancer Res, 2006. 12(19): p. 5606-7.

19. Neckers, L. and K. Neckers, *Heat-shock protein 90 inhibitors as novel cancer chemotherapeutic agents.* Expert Opin Emerg Drugs, 2002. 7(2): p. 277-88.
20. Blagosklonny, M.V., et al., *Mutant conformation of p53 translated in vitro or in vivo requires functional HSP90.* Proc Natl Acad Sci U S A, 1996. 93(16): p. 8379-83.
21. Isaacs, J.S., et al., *Hsp90 regulates a von Hippel Lindau-independent hypoxia-inducible factor-1 alpha-degradative pathway.* J Biol Chem, 2002. 277(33): p. 29936-44.
22. Sato, S., N. Fujita, and T. Tsuruo, *Modulation of AKT kinase activity by binding to Hsp90.* Proc Natl Acad Sci U S A, 2000. 97(20): p. 10832-7.
23. Xu, W., et al., *Hsp90, not Grp94, regulates the intracellular trafficking and stability of nascent ErbB2.* Cell Stress Chaperones, 2002. 7(1): p. 91-6.
24. Sepp-Lorenzino, L., et al., *Herbimycin A induces the 20 S proteasome- and ubiquitin-dependent degradation of receptor tyrosine kinases.* J Biol Chem, 1995. 270(28): p. 16580-7.
25. Hartson, S.D. and R.L. Matts, *Association of Hsp90 with cellular Src-family kinases in a cell-free system correlates with altered kinase structure and function.* Biochemistry, 1994. 33(30): p. 8912-20.
26. Stancato, L.F., et al., *Raf exists in a native heterocomplex with hsp90 and p50 that can be reconstituted in a cell-free system.* J Biol Chem, 1993. 268(29): p. 21711-6.
27. Veldscholte, J., et al., *Anti-androgens and the mutated androgen receptor of LNCaP cells: differential effects on binding affinity, heat-shock protein interaction, and transcription activation.* Biochemistry, 1992. 31(8): p. 2393-9.
28. Aumais, J.P., et al., *Selective interaction of hsp90 with an estrogen receptor ligand-binding domain containing a point mutation.* J Biol Chem, 1997. 272(18): p. 12229-35.
29. Zhang, H. and F. Burrows, *Targeting multiple signal transduction pathways through inhibition of Hsp90.* J Mol Med, 2004. 82(8): p. 488-99.
30. Miyata, Y., *Hsp90 inhibitor geldanamycin and its derivatives as novel cancer chemotherapeutic agents.* Curr Pharm Des, 2005. 11(9): p. 1131-8.
31. Bonnet, D. and J.E. Dick, *Human acute myeloid leukemia is organized as a hierarchy that originates from a primitive hematopoietic cell.* Nat Med, 1997. 3(7): p. 730-7.
32. Wang, Y., et al., *Targeting HIF1alpha eliminates cancer stem cells in hematological malignancies.* Cell Stem Cell, 2011. 8(4): p. 399-411.
33. Li, Z., et al., *Hypoxia-inducible factors regulate tumorigenic capacity of glioma stem cells.* Cancer Cell, 2009. 15(6): p. 501-13.
34. Reya, T., et al., *Stem cells, cancer, and cancer stem cells.* Nature, 2001. 414(6859): p. 105-11.
35. Gangemi, R., et al., *Cancer stem cells: a new paradigm for understanding tumor growth and progression and drug resistance.* Curr Med Chem, 2009. 16(14): p. 1688-703.
36. Ischenko, I., et al., *Cancer stem cells: how can we target them?* Curr Med Chem, 2008. 15(30): p. 3171-84.

37. Wang, Y., et al., *Epm2a suppresses tumor growth in an immunocompromised host by inhibiting Wnt signaling.* Cancer Cell, 2006. 10(3): p. 179-90.
38. Jares, P., D. Colomer, and E. Campo, *Genetic and molecular pathogenesis of mantle cell lymphoma: perspectives for new targeted therapeutics.* Nat Rev Cancer, 2007. 7(10): p. 750-62.
39. Clarke, M.F., et al., *Cancer stem cells--perspectives on current status and future directions: AACR Workshop on cancer stem cells.* Cancer Res, 2006. 66(19): p. 9339-44.
40. Reynolds, B.A. and S. Weiss, *Clonal and population analyses demonstrate that an EGF-responsive mammalian embryonic CNS precursor is a stem cell.* Dev Biol, 1996. 175(1): p. 1-13.
41. Reynolds, B.A. and R.L. Rietze, *Neural stem cells and neurospheres--re-evaluating the relationship.* Nat Methods, 2005. 2(5): p. 333-6.
42. Dontu, G., et al., *In vitro propagation and transcriptional profiling of human mammary stem/progenitor cells.* Genes Dev, 2003. 17(10): p. 1253-70.
43. Cheng, L., et al., *The clinical and therapeutic implications of cancer stem cell biology.* Expert Rev Anticancer Ther, 2011. 11(7): p. 1131-43.
44. Neckers, L. and P. Workman, *Hsp90 molecular chaperone inhibitors: are we there yet?* Clin Cancer Res, 2012. 18(1): p. 64-76.
45. Bagatell, R., et al., *Phase I pharmacokinetic and pharmacodynamic study of 17-N-allylamino-17-demethoxygeldanamycin in pediatric patients with recurrent or refractory solid tumors: a pediatric oncology experimental therapeutics investigators consortium study.* Clin Cancer Res, 2007. 13(6): p. 1783-8.
46. Weigel, B.J., et al., *A phase I study of 17-allylaminogeldanamycin in relapsed/refractory pediatric patients with solid tumors: a Children's Oncology Group study.* Clin Cancer Res, 2007. 13(6): p. 1789-93.
47. Ronnen, E.A., et al., *A phase II trial of 17-(Allylamino)-17-demethoxygeldanamycin in patients with papillary and clear cell renal cell carcinoma.* Invest New Drugs, 2006. 24(6): p. 543-6.
48. Solit, D.B., et al., *Phase II trial of 17-allylamino-17-demethoxygeldanamycin in patients with metastatic melanoma.* Clin Cancer Res, 2008. 14(24): p. 8302-7.
49. Heath, E.I., et al., *A phase II trial of 17-allylamino-17-demethoxygeldanamycin in patients with hormone-refractory metastatic prostate cancer.* Clin Cancer Res, 2008. 14(23): p. 7940-6.
50. Eisenhauer, E.A., et al., *New response evaluation criteria in solid tumours: revised RECIST guideline (version 1.1).* Eur J Cancer, 2009. 45(2): p. 228-47.
51. Modi, S., et al., *HSP90 inhibition is effective in breast cancer: a phase II trial of tanespimycin (17-AAG) plus trastuzumab in patients with HER2-positive metastatic breast cancer progressing on trastuzumab.* Clin Cancer Res, 2011. 17(15): p. 5132-9.
52. Richardson, P.G., et al., *Tanespimycin and bortezomib combination treatment in patients with relapsed or relapsed and refractory multiple myeloma: results of a phase 1/2 study.* Br J Haematol, 2011. 153(6): p. 729-40.
53. Kim, Y.S., et al., *Update on Hsp90 inhibitors in clinical trial.* Curr Top Med Chem, 2009. 9(15): p. 1479-92.

54. Korkaya, H., et al., *HER2 regulates the mammary stem/progenitor cell population driving tumorigenesis and invasion.* Oncogene, 2008. 27(47): p. 6120-30.
55. Korkaya, H., et al., *Regulation of mammary stem/progenitor cells by PTEN/Akt/beta-catenin signaling.* PLoS Biol, 2009. 7(6): p. e1000121.
56. Sauvageot, C.M., et al., *Efficacy of the HSP90 inhibitor 17-AAG in human glioma cell lines and tumorigenic glioma stem cells.* Neuro Oncol, 2009. 11(2): p. 109-21.

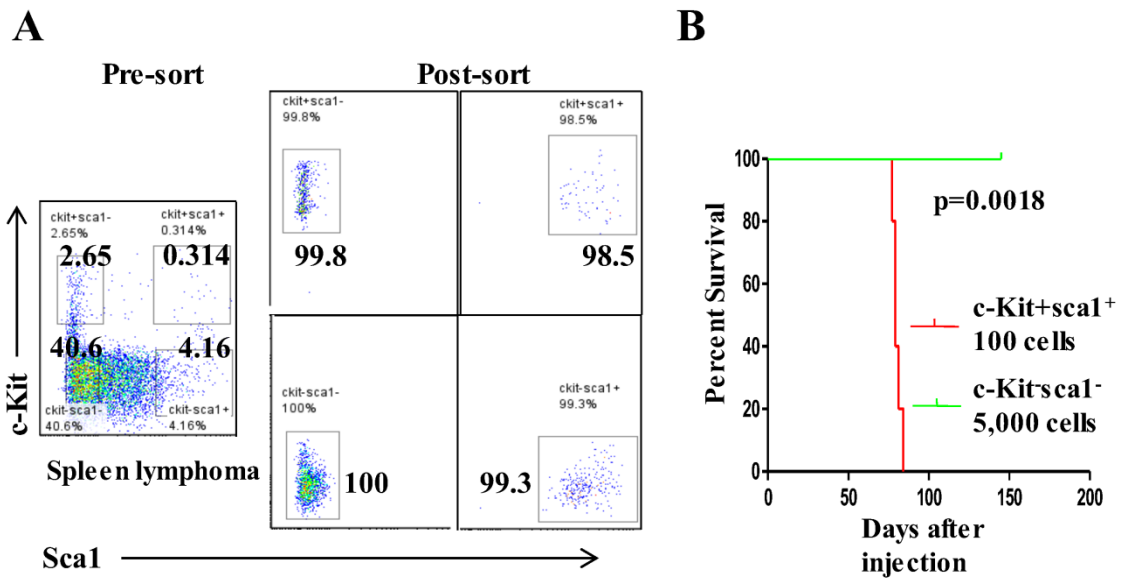

Figure 2.1 TGB Lymphoma Contains Tumorigenic Stem Cells Which Express c-Kit and Sca1. (A) Freshly isolated lymphoma cells from spleen tissues of TGB mice were stained with c-Kit and Sca1 antibodies and sorted into four subsets by BD FACSAria sorting system. (B) Sorted subsets of c-Kit^{+}Sca1^{+} and c-Kit^{-}Sca1^{-} cells were injected into B10.BR mice and the lymphoma-initiating capacity of the two subsets is expressed based on the mouse survival rate. N = 5 mice per group.

Figure 2.2 17-AAG Eliminates Lymphoma CSCs. (A) The IC50 of 17-AAG in lymphoma cells was determined by MTT assay. Cultured lymphoma cells were treated with increasing concentrations of 17-AAG for 48 hours before the MTT assay was performed. (B-D) 17-AAG selectively eliminated the c-Kit^{+}Sca1^{+} cells in a dose dependent manner. Forty eight hours after 17-AAG treatment, the lymphoma cells were stained with antibodies to c-Kit and Sca1 and analyzed by flow cytometry (B). The percentage of c-Kit^{+}Sca1^{+} cells from triplicate experiments was quantified by flow cytometry (C). The predicated IC50 of 17-AAG to c-Kit^{+}Sca1^{+} cells is shown in D.

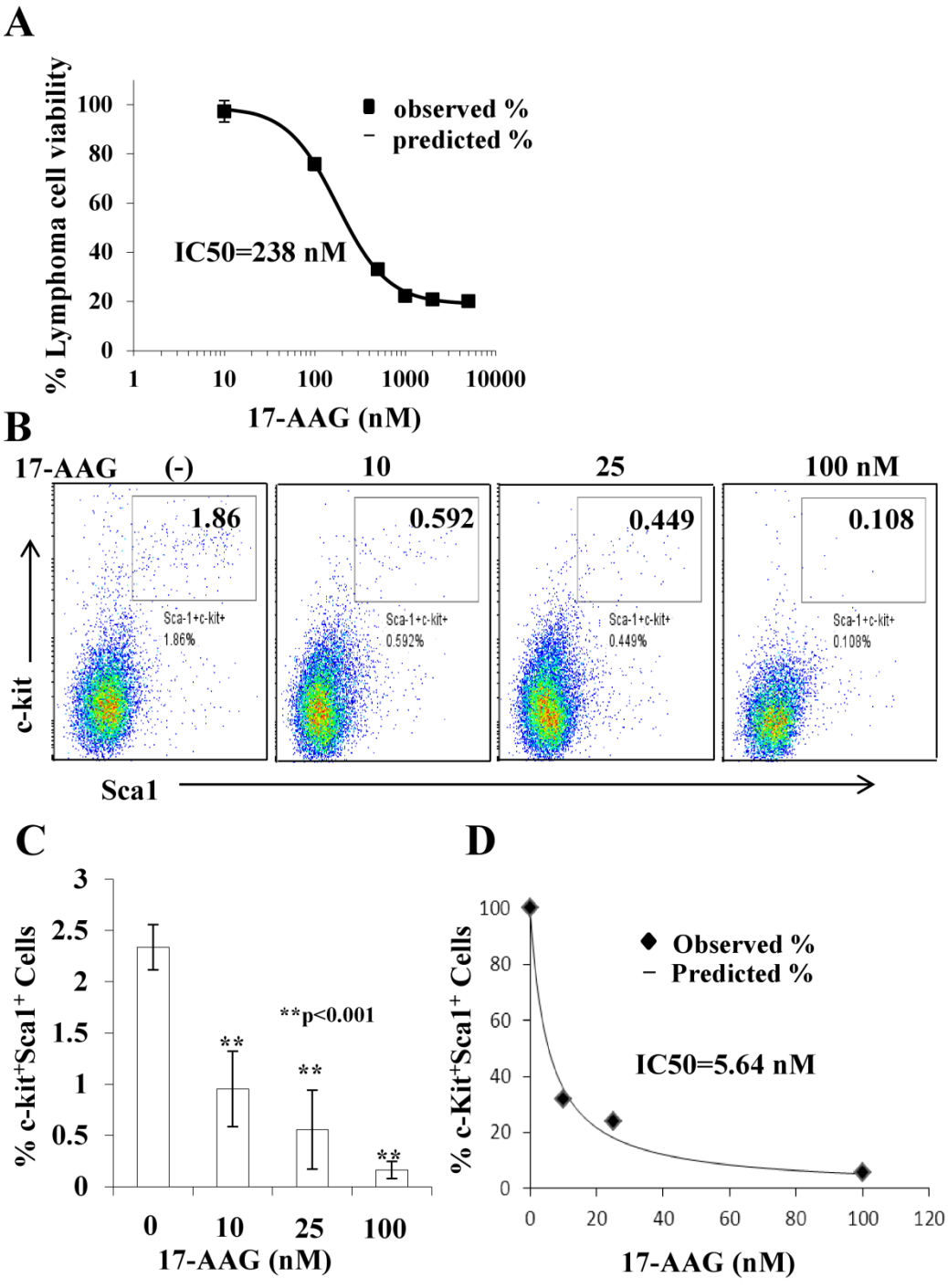
A
% Lymphoma cell viability
100
80
60
40
20
0
observed %
predicted %
IC50=238 nM
1
10
100
1000
10000
17-AAG (nM)
B
17-AAG
(-)
10
25
100 nM
1.86
0.592
0,449
0.108
Sca-1+c-kit+
1.86%
Sca-1+c-kit+
0.592%
Sca-1+c-kit+
0.449%
Sca-1+c-kit+
0.108%
c-kit
Sca1
C
% c-kit+Sca1+ Cells
3
2.5
2
1.5
1
0.5
0
**p<0.001
**
**
**
0
10
25
100
17-AAG (nM)
D
% c-Kit+Sca1+ Cells
100
80
60
40
20
0
Observed %
Predicted %
IC50=5.64 nM
0
20
40
60
80
100
120
17-AAG (nM)

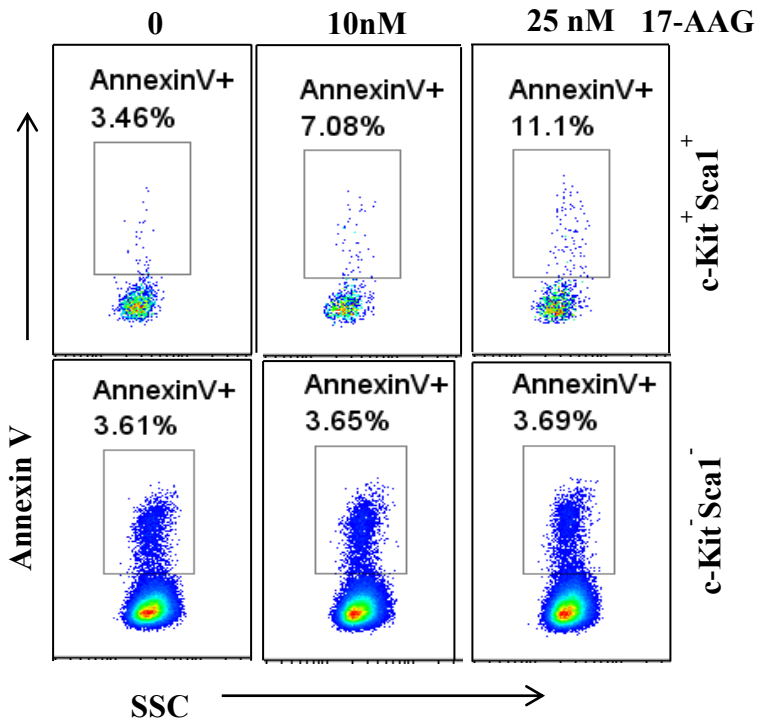

Figure 2.3 17-AAG Treatment Induces Apoptosis in Lymphoma CSCs. 17-AAG preferentially induced the apoptosis of c-Kit^{+}Sca1^{+} but not c-Kit^{-}Sca1^{-} cells. Twenty four hours after 17-AAG treatment, cultured lymphoma cells were stained with antibodies against c-Kit, Sca1, and Annexin V. c-Kit^{+}Sca1^{+} or c-Kit^{-}Sca1^{-} gated cells were then analyzed by flow cytometry for Annexin V^{+}.

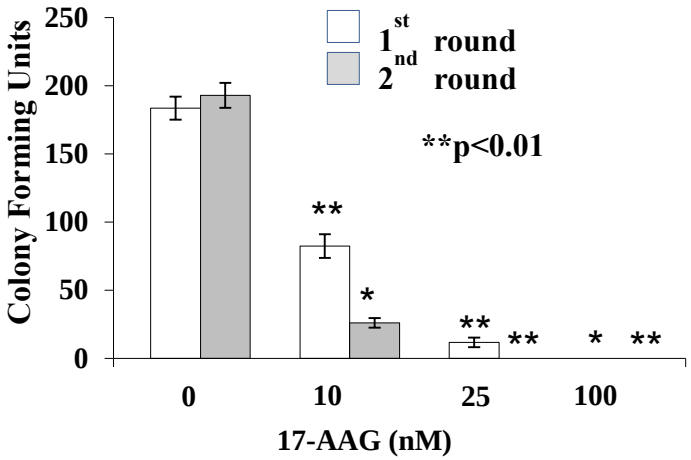

Figure 2.4 Effects of 17-AAG on Lymphoma Colony Formation. 17-AAG dramatically reduced the colony formation units (CFUs) of lymphoma CSCs. After treatment with increasing concentrations of 17-AAG, the lymphoma cells were seeded in 1% methylcellulose culture medium, and CFUs were counted, and the colony replating assay was performed after a 7 day culture. Data shown are means ± SD of colony numbers in triplicates and are representative of three independent experiments.

Figure 2.5 17-AAG Treatment is Efficacious Against TGB Lymphoma In Vivo. 17-AAG suppresses lymphoma growth in lymphoma transplanted congenic recipient mice. (A-D) B10.BR mice were inoculated with $5x10^5$ cultured lymphoma cells through I.P. injection. Seven days after implantation, randomly grouped mice were treated with different doses of 17-AAG as indicated, every other day for three weeks. After the mice were monitored for 80 days post tumor cell injection, four of the surviving mice from 40 mg/kg or vehicle control group were sacrificed to measure the spleen sizes (A) and weights (B); two mice from 25 mg/kg or control group were subjected to identification of lymphoma by an antibody to the tumor T-cell marker Thy-1 and to metastasis examination by H&E staining (C). Arrow indicates metastatic lymphoma cells (stained dark purple). The survival rate was evaluated and data shown are representative of two independent experiments (D). (E) 17-AAG reduced the self-renewal ability of lymphoma CSCs. B10.BR mice were implanted by I.P. injection with $1x10^5$ spleen cells from mice previously treated with vehicle or 17-AAG, and monitored for 160 days. The survival rate was evaluated after 160 days post spleen cell inoculation. At least 5 mice were used for each treatment group (D) and reimplantation (E).

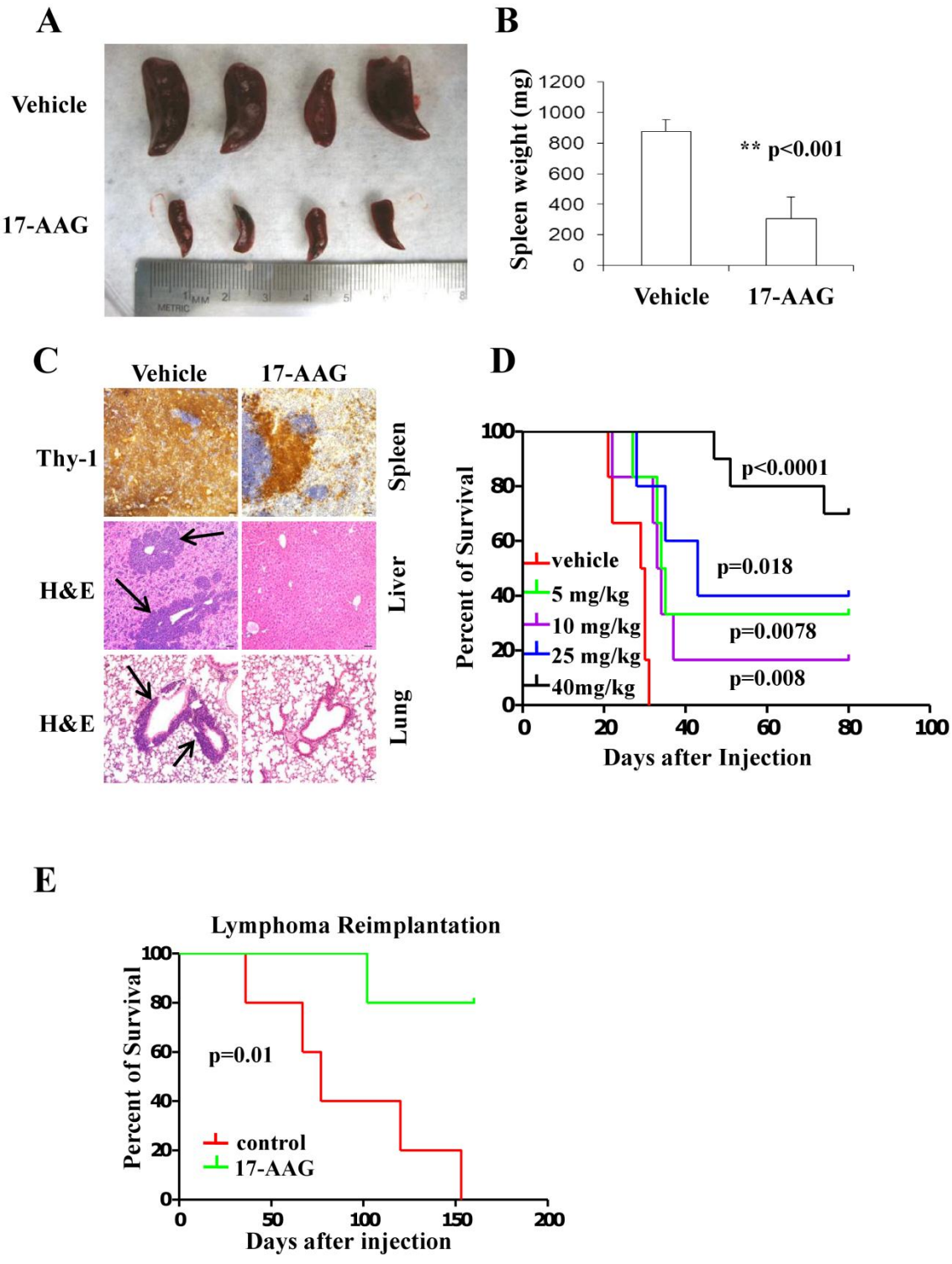
A
Vehicle
17-AAG
B
Spleen weight (mg)
1200
1000
800
600
400
200
0
** p<0.001
Vehicle
17-AAG
C
Vehicle
17-AAG
Thy-1
H&E
H&E
Spleen
Liver
Lung
D
Percent of Survival
100
80
60
40
20
0
vehicle
5 mg/kg
10 mg/kg
25 mg/kg
40mg/kg
p<0.0001
p=0.018
p=0.0078
p=0.008
0
20
40
60
80
100
Days after Injection
E
Lymphoma Reimplantation
Percent of Survival
100
80
60
40
20
0
p=0.01
control
17-AAG
0
50
100
150
200
Days after injection

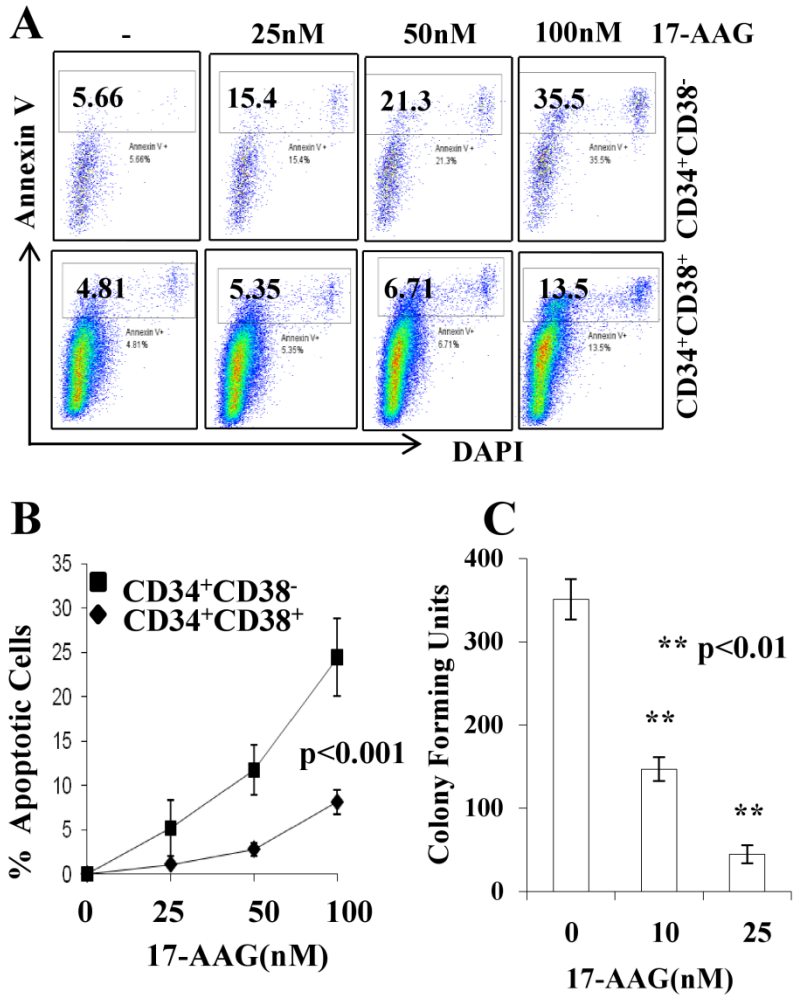

Figure 2.6 17-AAG can Selectively Eliminate AML CSCs. (A,B) Low doses of 17-AAG preferentially induced apoptosis and eliminated colony formation of AML CSCs ($CD34^+CD38^-$). After 24 hour treatment with increasing concentrations of 17-AAG, AML-71 cells were stained first with antibodies for CD34, CD38, and then with antibody for Annexin V and DAPI. The % Annexin V^+ cells in the gated $CD34^+CD38^-$ and $CD34^+CD38^+$ populations were analyzed by flow cytometry. The nuclear dye DAPI stained dead cells. The apoptotic cells in 17-AAG-treated or untreated cells from triplicate experiments are shown in B. The CFUs after 17-AAG treatment are shown in (C) Data shown are the means ± SD of the colony numbers in triplicate plates and are representative of those from at least three independent experiments.

Chapter 3

Heat Shock Factor 1 (HSF1) Mediates 17-AAG Resistance in Committed TGB Lymphoma Cells

Abstract

The clinical use of 17-AAG has resulted in both successes and failures, suggesting that the efficacy of HSP90 inhibition depends on more than just the expression of oncogenic clients. Our previous findings showed that cancer stem cells (CSCs) were highly sensitive to HSP90 inhibition, likely stemming from their dependence on the client protein HIF1α for maintenance of self-renewal. This level of inhibition was achieved at concentrations well below the IC50 of the bulk population of cells. As both the CSCs and non-CSCs are dependent on HSP90 clients and thus equally susceptible to 17-AAG, further studies were carried out to determine the mechanism for this discrepancy. We show here that 17-AAG treatment can efficiently reduce HIF1α activity in the CSCs, confirming our hypothesis for CSC susceptibility to the drug. Interestingly, Heat Shock Factor 1 (HSF1) expression was dramatically higher in the non-CSCs, suggesting a possible mode of resistance to chaperone depletion in these cells. HSF1 knockdown resulted in reduced colony formation in lymphoma and AML, further demonstrating that CSCs are critically reliant on molecular chaperones for survival. In addition, human lymphoma cells which required high concentrations (500 nM) of 17-AAG to elicit growth inhibition, were sensitized to 17-AAG treatment by HSF1 knockdown. Together these results show that HSF1 activity is both a vital part of CSC

maintenance, and a crucial mediator of resistance to 17-AAG. Furthermore, HSF1 expression may be a good prognostic indicator of susceptibility to HSP90 inhibition.

Introduction

While the use of 17-AAG in a number of phase II trials has not been successful overall, a few cases have yielded promising results. This variable response may potentially be explained by results from clinical trials testing the combination of 17-AAG with conventional therapy in Her2+ breast cancer and multiple myeloma, [1, 2]. Data from these trials suggest that the efficacy of 17-AAG treatment can be maximally achieved when both the targeted client protein is highly sensitive to HSP90 inhibition and the tumor is critically reliant on that client protein for survival. Under these circumstances, the loss of the client protein cannot be compensated for by an alternate pathway, thus making the tumor highly sensitive to HSP90 inhibition. Therefore, the specific molecular pathways that are aberrantly activated need to be taken into careful consideration when determining the potential efficacy of HSP90 inhibition across various tumor types [3]. Moreover, as tumors are regularly comprised of a heterogeneous mix of cells, the issue of varying sensitivity to 17-AAG may also extend to these different tumor subpopulations. CSCs are critically reliant on self-renewal for their maintenance [4]. These pathways have been associated with known clients of HSP90 (Her2, AKT, HIF1α) and therefore are predicted to be sensitive to HSP90 inhibition [5-8]. Indeed, CSCs in both our TGB mouse model of lymphoma as well as in AML, both of which are reliant on HIF1α activity for survival, are selectively sensitive over non-CSCs to 17-AAG

HSP90 inhibition. This is in agreement with other reports which show CSC sensitivity with 17-AAG treatment [7, 9].

Our previous data has also shown that, while not as sensitive as the CSC subpopulation, the TGB lymphoma bulk cells were also inhibited with 17-AAG treatment. These lymphoma cells aberrantly proliferate due to the loss of the laforin phosphatase, which under normal conditions maintains GSK-3β mediated suppression of β-catenin [10]. Phosphorylation of GSK-3β occurs via AKT, a well-known oncogene and HSP90 client. Therefore, 17-AAG mediated HSP90 inhibition is predicted to result in a loss of AKT, and subsequent inhibition of β-catenin signaling. As 17-AAG treatment affects both the lymphoma CSCs (via HIF1α) and the cells comprising the tumor bulk (via AKT), experiments were carried out to examine the mechanism responsible for determining the differential sensitivity between these cell populations to the drug.

17-AAG has previously been reported to target both the bulk population of cells and CSCs within glioma and AML [7, 11-13]. Unfortunately, acquired resistance to 17-AAG has been observed in both glioblastoma and melanoma through reduced expression of NAD(P)H/ quinone oxidoreductase 1 (NQO1), an enzyme responsible for the activation of 17-AAG. In addition, induction of stress response proteins, such as HSP27, and HSP70 by 17-AAG plays a large role in 17-AAG resistant cancer cells [14, 15]. The induction of these proteins relies on the transcription factor Heat Shock Factor 1 (HSF1), which regulates expression of HSP70, HSP27, and HSP90 [16-19]. Thus, targeting HSF1 has been proposed to abrogate the 17-AAG induced heat shock response [20]. This

hypothesis is supported by reports demonstrating that HSF1 is required for the initiation of both lymphoma and RAS oncogene–induced tumors [21, 22].

Results presented here show that the level of sensitivity to 17-AAG mediated HSP90 inhibition between the lymphoma CSCs and the lymphoma bulk can be attributed to the differential expression of HSF1 between these two populations. Overall expression of stress response proteins (HSP90, HSP70, HSF1) were found to be lower in CSCs as compared to the non-CSCs. While dramatically lower in expression in the CSCs, HSF1 activity is necessary in these cells, as demonstrated by the reduction in colonies formed following HSF1 knockdown. In addition, HSF1 knockdown sensitized the bulk population from human cell lines to 17-AAG treatment. These results show that HSF1 is an important contributor to the resistance to 17-AAG treatment in the differentiated population. As such, the expression level of HSF1 may serve as a prognostic indicator of tumor cell sensitivity towards HSP90 inhibition.

Materials and Methods

Mice, Cells and Reagents

TCR transgenic B line (TGB) mice in the B10.BR background were maintained by heterozygous breeding pairs. B10.BR mice were used as recipients in lymphoma cell inoculation, and severe combined immunodeficiency (SCID) mice were used for human AML maintenance. Both lines were purchased from the National Cancer Institute. All mice were kept and used for the tumor implantation and treatment according to the procedures approved by the Unit of Laboratory Animal Facility (ULAM) at University of Michigan.

TGB lymphoma cells were maintained in 1% methylcellulose medium (MethoCult GF, 03434, Stem Cell Technologies) supplemented with murine cytokines (R&D Systems): 10 ng/mL recombinant IL-3 and IL-6, and 100 ng/mL stem cell factor. For some in vitro experiments, TGB lymphoma cells were transferred from 1% methylcellulose culture to an expansion medium: RPMI 1640 medium supplemented with 10% FBS, IL-3, IL-6, and SCF cytokines, 100 μM non-essential amino acids, 10 mM HEPES, and 1 mM sodium pyruvate. Human AML cells were derived from the enlarged spleen tissue of SCID mice injected with aggressive AML CSCs (AML-71) as described before [12], and maintained in SCID mice via transplantation. Short term expansion and colony formation assays of the AML CSCs were carried out as done similarly for our lymphoma cells, except for a substitution of human cytokines for murine cytokines. The human T-cell lymphoma cell lines J45.01, Jurkat, and T-lymphoblastic leukemia line Sup-T1 were purchased from ATCC. They were cultured in RPMI medium containing 10% FBS.

17-AAG was purchased from LC Laboratories. The sources of rabbit polyclonal antibodies to the specific proteins are as follows: HSF1 (4356), HSP90 (4874), HSP70 (4874), phospho-S21/S9 GSK3α/β (9331), phospho-S473AKT (9271), AKT (9272) were purchased from Cell Signaling. Mouse antibodies to GSK3α/β (0011-A, Santa Cruz) and β-actin (AC-15, Sigma) were used in the studies.

Isolation of Lymphoma CSCs and Colony Formation Assay

The lymphoma CSCs (c-Kit^{+}Sca1^{+}) are a rare population in TGB lymphoma tissue and express the surface markers c-Kit and Sca1. The CSCs were sorted from

primary spleen lymphoma tissue of TGB mice by fluorescence-activated cell sorting (FACS), or isolated by auto-MACS microbeads (Miltenyi Biotech) twice, after staining with antibodies to c-Kit and Sca1 (both from BD Bioscience). For the detection of some downstream proteins requiring larger amounts of cells, the c-Kit$^+$ fraction (C-Kit$^+$Sca1$^+$ subset combined with c-Kit$^+$ Sca1$^-$ subset) was used. For colony formation assays, lymphoma cells were seeded in 1% methylcellulose medium containing murine cytokines in a 12-well plate. After 6-8 days of culture, colonies were counted, pooled, and then replated for consecutive rounds. For viral infection, the cultured lymphoma cells were expanded in RPMI1640 medium described above, 24 hours before these experiments.

Lentiviral Infection and Plasmids

The lentiviruses for small hairpin (Sh) RNA targeting HSF1 (Sh-HSF1) and scrambled control Sh-RNA were generated in HEK293FT cells according to the lentiviral preparation protocol (Invitrogen). Lentiviruses were made in a 150 mm falcon culture dish and 50 ml media was collected and centrifuged at 550*g* for 10 min to remove cell debris. Viral particles obtained after centrifugation at 12,857*g* overnight were suspended with 2 ml of RPMI1640 medium containing 10% FBS, aliquoted, and stored at -80^{o}C. Fifty to one hundred μl of concentrated virus per million cells was mixed with 100 μl culture medium and used for spinoculation in a U-bottom tube in a mixture containing 9 μg/ml polybrene. The spinoculation was carried out at 2,500 rpm, for 2 hours, at 30^{o}C. After spinoculation, the cell pellet was suspended gently with fresh culture medium, seeded and cultured in 1% methylcellulose for another 5-7 days before use.

The sequence of Sh-HSF1 (5-GCTCATTCAGTTCCTGATC-3) has been previously validated [23], and was cloned into a Sh-lentiviral vector as described before [12]. The Sh-HSF1 sequence is shared by mouse and human. The constructs of hypoxia responsive element (HRE) or its mutant (HRE-Mt) EGFP reporter specific for HIF1α were described before [12]. Full length coding region of HSF1 cDNA was amplified by RT-PCR using mouse bone marrow mRNA as template, and cloned into a pcDNA vector with Flag tag fused into the C-terminus of HSF1.

Western-blot

Generally, sorted CSCs or cultured lymphoma cells were lysed with 1% Triton X-100 lysis buffer containing 20 mM Tris-HCl, pH 7.4, 150 mM NaCl, 40 mM NaF, 1 mM DTT, and protease and phosphatase inhibitor cocktail (Sigma). Supernatants of the lysate were used for Western-blots and resolved on reducing and non-heated (95^{o}C, 3 min) denaturing 10% SDS-PAGE gels. Transferred membranes were blotted with primary antibody overnight at 4^{o}C with shaking, and then with secondary antibody at room temperature for 5 hrs.

Real Time PCR

Total RNAs from FACS sorted lymphoma CSCs and non-CSCs (c-Kit^{-}Sca1^{-}) were extracted using the RNeasy extraction kit (Qiagen). After reverse transcription of RNA to cDNA, real-time PCR using the converted cDNA as template was performed in triplicate using SYBR Green PCR Master Mix. The following primers were used: Hsf1, F-TTTGACCAGGGCCAGTTTG, R-TTCGGAAGCCATACATGTTGAG; Hif1α, F-

AGTCTAGAGATGCAGCAAGATCTC, R-TCATATCGAGGCTGTGTCGACTGA; Hsp90α, F-TGTTGCGGTACTACACATCTGC, R-GTCCTTGGTCTCACCTGTGATA; Hsp90β, F-CAAACAAGGAGATTTTCCTCCG, R-GCTGTCCAACTTAGAAGGGTC; Glut1, F-TGTGCTGTGCTCATGACCATC, R-ACGAGGAGCACCGTGAAGAT; β-Actin, F-GGCTGTATTCCCCTCCATCG, R-CCAGTTGGTAACAATGCCATGT. Fold differences were calculated using the Delta Delta Ct method [24] and β-actin as an endogenous standard.

Statistics

Statistical significance was determined using unpaired Student's t-test.

Results

Differential Expression of Signaling and Stress Response Proteins between Lymphoma CSCs and non-CSCs

To determine differences in the stress response between CSCs and non-CSCs, the expression levels of chaperones and the transcription factor HSF1 were examined in these cell populations. Using a BD FACSAria cell sorter, TGB lymphoma cell populations enriched for CSCs (c-Kit$^+$Sca1$^+$) and non-CSCs (c-Kit$^-$Sca1$^-$) were sorted from mouse spleen tissue enlarged with the TGB lymphoma cells as shown in Chapter 2. Quantitative real time-PCR showed that the mRNA levels of HIF1α and its target Glut1 were 4 and 8-fold higher respectively in the c-Kit$^+$Sca1$^+$cells over the c-Kit$^-$Sca1$^-$ cells. This confirmed that the c-Kit$^+$Sca1$^+$subset still maintained the unique marker of active HIF1α. The mRNA levels of chaperones HSP90α, HSP90β and HSP70, as well as HSF1 were about two-fold higher in the c-Kit$^-$Sca1$^-$ than c-Kit$^+$Sca1$^+$cells (Figure 3.1A). Consistent with the differences seen in the mRNA levels, protein levels of HSP70 were higher in the c-

Kit$^-$Sca1$^-$ cells. Strikingly, there were large differences in the protein levels of HSF1, HIF1α, and the activated status of AKT/GSK-3β pathway between the two cell populations (Figure 3.1B,C). HSF1 had over 10-fold higher expression in the c-Kit$^-$Sca1$^-$ population, compared to the c-Kit$^+$ population. Consistent with our previous results [10, 12], stable HIF1α was exclusively expressed in the CSCs, while active AKT (pS473AKT) and GSK3 (pS21/pS9GSK3α/β) were present in higher amounts in the non-CSCs compared to the CSCs. These distinct expression patterns for stable HIF1α and the active AKT/GSK-3β pathway supports our initial hypothesis for targeting CSCs and non-CSCs simultaneously with 17-AAG.

17-AAG mediated HSP90 Inhibition Leads to Ablation of HIF1α Activity in CSCs

To determine if 17-AAG interferes with HIF1α's transcriptional activity, a lentiviral reporter that utilizes HIF1α binding to specific hypoxia-inducible responsive elements (HRE) to control EGFP reporter expression was constructed [12]. Lymphoma cells were infected with this reporter, while control cells were infected with a reporter containing mutant HRE (HRE-Mt) sequences (used as a negative control for gating). Without treatment, 25.8% of HRE-EGFP positive cells were present in the c-Kit$^+$Sca1$^+$ subset, while only 0.786% were in the c-Kit$^-$Sca1$^-$ subset (Figure 3.2A). This is consistent with the expression of stable HIF1α specifically in the CSCs. With treatment, 10 nM 17-AAG reduced HRE-EGFP expression in the CSCs by 2-fold, but had little effect on the HRE-EGFP expression in non-CSCs, demonstrating the specificity of 17-AAG suppression of HIF1α activity in the CSCs. In addition to the reduction of HIF1α transcriptional activity caused by treatment 17-AAG, the mRNA levels of HIF1α and its

target Glut1 were also significantly decreased in a dose-dependent manner (Figure 3.2B). These results demonstrate that 17-AAG specifically eliminates the CSCs by inhibiting the HSP90-mediated stability and function of HIF1α at concentrations dramatically lower than the IC50 previously determined for the differentiated c-Kit$^-$Sca1$^-$ lymphoma cells.

Knockdown of HSF1 Abrogates the Colony Formation Capacity of Lymphoma CSCs

To examine the role HSF1 plays in the maintenance of CSCs, we made a hair-pin (Sh) RNA targeting HSF1. In HEK293 cells, the HSF1 ShRNA specifically knocked down ectopically expressed HSF1 by up to 80% within 24 hours after co-transfection (Figure 3.3A). In contrast, the expression of the control gene, Lef1, was not affected. Nearly half (48.1 %) of the TGB lymphoma cells were infected following transfection with the Sh-HSF1 lentivirus, as determined by the expression of an EGFP reporter within the Sh-RNA construct (Figure 3.3B). Quantitative RT-PCR revealed that Sh-HSF1 knocked down approximately 80% of the endogenous HSF1 mRNA in sorted EGFP-positive cells, relative to the mRNA levels of sorted cells expressing scrambled Sh-RNA (Sh-Sr) (Figure 3.3C). Along with the knockdown of HSF1, the mRNA of one of its target genes, HSP90α [25], was correspondingly reduced. The HSF1 shRNA significantly inhibited cell growth and eliminated the colony forming capacity of the CSCs in the absence of 17-AAG (Figure 3.3D), demonstrating that HSF1 is positioned upstream of HSP90 and controls the level of chaperones within these cells. Colony formation was not affected in the Sh-Sr infected cells, demonstrating the specificity to HSF1. Taken together, these results show that the low levels of HSF1 present in CSCs are required for their maintenance.

HSF1 Knockdown Sensitizes Lymphoma Cells to 17-AAG

To resolve the mechanism underlying 17-AAG resistance in non-CSCs, the effect of 17-AAG treatment on client protein expression was investigated in these cells. When unsorted, bulk lymphoma cells were treated with 50 nM 17-AAG, a dose capable of killing nearly all of the CSCs, the bulk population was largely unaffected, as protein levels of pS473AKT, pS21GSK3α, and pS9GSK3β remained unchanged (Figure 3.4A). In contrast, a higher dose of 100 nM 17-AAG treatment reduced the levels of pS473AKT, pS21GSK3α, and pS9GSK3β, as well as HSP90 and HSF1. In agreement with other reports in the literature, treatment of the bulk population with 100 nM 17-AAG resulted in increased HSP70 levels. Taken together, these results demonstrate that 17-AAG has less of an affect on HSP90-mediated AKT levels when HSF1 expression is high. This suggests that HSF1 can compensate for HSP90 inhibition by 17-AAG, potentially through regulating HSP70 levels. Indeed, it has been shown that knockdown of HSP70 sensitizes cancer cells to 17-AAG treatment [26].

To determine if the affect of HSF1 on cell growth is of a general significance, and not limited to the mouse lymphoma cells, HSF1 expression and the status of the AKT/GSK-3β pathway were examined in human T-lymphoblastic lymphoma/leukemia cancer lines (Sup-T1, Jurkat, and J45.01). In accordance with the results from the TGB lymphoma cells, these human lymphoma cell lines also expressed high levels of HSF1 and an activated AKT/GSK-3β pathway (Figure 3.4B). Their level of resistance to 17-AAG treatment was even more pronounced compared to TGB lymphoma cells, as 500 nM 17-AAG was required for drug efficacy. This may be due to a higher level of HSF1 expression in the human cell lines, as compared to the mouse lymphoma cells.

Knockdown of HSF1 in the human lymphoma cells with Sh-HSF1 rendered the cells sensitive to 17-AAG mediated growth inhibition, as compared to 17-AAG treatment of the Sh-Sr-expressing cells (Figure 3.4C). These results show that high expression levels of HSF1 dramatically reduce the efficacy of 17-AAG in mouse and human lymphoma cells.

HSF1 Knockdown Similarly Impairs AML CSCs

To further validate the role of HSF1 in CSC maintenance, and determine if these properties extend beyond our lymphoma model, additional studies were carried out to examine the affect of HSF1 knockdown in AML CSCs. First, in comparison to normal mouse bone marrow (BM) cells, unsorted AML cells also expressed high levels of HSF1, as well as phosphorylated AKT and GSK-3β similar to the TGB lymphoma cells (Figure 3.5A). These results suggest that AML cells may potentially respond to 17-AAG treatment via a similar mechanism as the lymphoma cells. Indeed, treatment with 17-AAG was found to decrease HIF1α mRNA, as similarly seen in the lymphoma cells (Figure 3.5B). Accordingly, knockdown of HSF1 by the Sh-HSF1 silencer abrogated colony formation of the AML CSCs, as compared to the Sh-Sr (Figure 3.5C). Lastly, to verify that the decreased colony formation in AML CSCs was through a reduction in HSP90, the lentiviral-infected AML cells were isolated by FACS, gating on EGFP-positive cells (Figure 3.5D), and the mRNA levels of HSF1 and its target gene HSP90α were determined. Knockdown of HSF1 dramatically reduced the mRNA levels of HSP90α (Figure 3.5E). Taken together, these results show that functional HSP90α and HSF1 is required for the maintenance of the AML CSCs.

Discussion

Clinical trials with the HSP90 inhibitor 17-AAG have shed light on conditions which may determine whether a given tumor type will respond to chaperone depletion. Trials with HSP90 client dependent tumor types, which had clients that were very sensitive to HSP90 inhibition, were successful when 17-AAG was used in combination with conventional treatments [3]. Extending these principles further, subpopulations of tumor cells (i.e. CSCs) may be exquisitely sensitive to HSP90 inhibition if their maintenance is dependent on chaperone client proteins within signaling pathways (i.e. self-renewal) that cannot be compensated for. Along with results presented in Chapter 2, the data presented above demonstrate that lymphoma and AML CSCs are selectively sensitive to HSP90 inhibition with 17-AAG. As seen in the current study, this susceptibility is tied to the loss of HIF1α activity from 17-AAG mediated HSP90 inhibition. Low doses of 17-AAG that were previously shown to induce CSC death through apoptosis were found to reduce both the function of HIF1α and the expression of HIF1α and Glut1 mRNA. It has previously been reported that HIF1α can regulate its own expression [27], suggesting that the abrogation of this protein by 17-AAG further reduces its own gene expression by this feedback mechanism. Moreover, these low concentrations of 17-AAG were not found to induce apoptosis or affect the signaling components of the AKT/GSK-3β/β-catenin pathway, which facilitates proliferation in the lymphoma bulk.

In order to understand the mechanism behind the discrepancy in effective dose of 17-AAG between these two lymphoma populations, we examined the expression of both

stress related and signaling proteins. As previously seen, levels of HIF1α were higher in the CSCs, while pS473AKT/pS21GSK3α/pS9GSK-3β were higher in the bulk population of lymphoma cells [10, 12]. Unexpectedly, stress related proteins, such as HSP90, HSP70 and HSF1, were more abundant in the tumor bulk than in the CSC population. This difference was most dramatic with HSF1, suggesting a possible mechanism for resistance to HSP90 inhibition in the differentiated lymphoma cells. When mouse lymphoma cells were treated with 17-AAG doses that completely eliminated the CSCs, little change in expression was observed in the phosphorylated clients. Only high concentrations of 17-AAG (100 nM) yielded a reduction in pS473AKT and other clients, demonstrating that these lymphoma cells had enhanced survival under HSP90 inhibition compared to the CSCs. This resistance to 17-AAG mediated HSP90 inhibition was not unique to our mouse lymphoma cells, as other human T-cell lymphoma cell lines (which also have high HSF1 expression) needed high concentrations of 17-AAG (500 nM) to observe loss of client proteins. Interestingly, when HSF1 was knocked down in these cell lines, lower levels of 17-AAG were capable of causing growth inhibition.

As HSP90 expression is controlled by the homotrimer of HSF1 and/or the heterotrimer of HSF1 and HSF2 [23, 28, 29], successful HSP90 inhibition by 17-AAG naturally depends on the levels and activation of HSF1. Our results suggest that low expression of HSF1 in CSCs renders them more susceptible to 17-AAG. Although HSF1 can compensate for the suppression of HSP90 by 17-AAG in the bulk population via inducing expression of HSP90 and HSP70, this likely cannot occur in the CSCs rapidly enough due to the low levels of HSF1 present in these cells. It is important to note that

loss of HSF1 can affect the expression level of HSP90α (inducible expressed) and not HSP90β (constitutively expressed) [25]. Our results support this, as HSF1 knockdown reduced HSP90α expression. In addition, HSF1 knockdown dramatically reduced the CSCs ability to form colonies. Although both HSP90 isoforms are expressed in the TGB lymphoma cells, and both can bind client proteins similarly [30], loss of colony formation following HSF1 potentially implicates HSP90α over HSP90β in the maintenance of HIF1α activity. In contrast to the CSCs, high levels of HSF1 in non-CSCs buffer the effects of 17-AAG, as more HSF1 protein allows for a more rapid stimulation of HSP90α expression in response to HSP90 inhibition. Furthermore, GSK-3β is a known repressor of DNA binding and transcriptional activity of HSF1 [31-33]. Inactivation of GSK-3β, by loss of the regulatory phosphatase laforin, is characteristic of our mouse lymphoma model, in addition to other human T-cell lymphoma cell lines [10]. Thus, high HSF1 expression coupled with the disruption of GSK-3β's ability to dampen HSF1 activity provide an explanation for the discrepancy in effective 17-AAG concentrations between the CSCs and the lymphoma bulk.

HSF1 has been previously associated with resistance to treatment [17, 34]. Inhibition of HSP90 has been shown to cause increased expression of other chaperone proteins, such as HSP70, through HSF1 gene regulations [35]. Independent of its transcriptional activity, HSF1 has been shown to reduce the effectiveness of chemotherapy through promotion of MDR1 expression [36]. Also, high HSF1 expression has been correlated with high tumor grade, and poor long-term survival [37, 38]. This study further demonstrates the ability of high HSF1 expression in the differentiated lymphoma cells to mediate resistance to 17-AAG. Furthermore, in the

context of efficacy with HSP90 inhibition, high HSF1 expression may also function as a prognostic indicator of reduced response to inhibitors such as 17-AAG.

References

1. Modi, S., et al., *HSP90 inhibition is effective in breast cancer: a phase II trial of tanespimycin (17-AAG) plus trastuzumab in patients with HER2-positive metastatic breast cancer progressing on trastuzumab.* Clin Cancer Res, 2011. **17**(15): p. 5132-9.
2. Richardson, P.G., et al., *Tanespimycin and bortezomib combination treatment in patients with relapsed or relapsed and refractory multiple myeloma: results of a phase 1/2 study.* Br J Haematol, 2011. **153**(6): p. 729-40.
3. Kim, Y.S., et al., *Update on Hsp90 inhibitors in clinical trial.* Curr Top Med Chem, 2009. **9**(15): p. 1479-92.
4. Cheng, L., et al., *The clinical and therapeutic implications of cancer stem cell biology.* Expert Rev Anticancer Ther, 2011. **11**(7): p. 1131-43.
5. Korkaya, H., et al., *HER2 regulates the mammary stem/progenitor cell population driving tumorigenesis and invasion.* Oncogene, 2008. **27**(47): p. 6120-30.
6. Korkaya, H., et al., *Regulation of mammary stem/progenitor cells by PTEN/Akt/beta-catenin signaling.* PLoS Biol, 2009. **7**(6): p. e1000121.
7. Sauvageot, C.M., et al., *Efficacy of the HSP90 inhibitor 17-AAG in human glioma cell lines and tumorigenic glioma stem cells.* Neuro Oncol, 2009. **11**(2): p. 109-21.
8. Gallia, G.L., et al., *Inhibition of Akt inhibits growth of glioblastoma and glioblastoma stem-like cells.* Mol Cancer Ther, 2009. **8**(2): p. 386-93.
9. Sobhan, P.K., et al., *Identification of heat shock protein 90 inhibitors to sensitize drug resistant side population tumor cells using a cell based assay platform.* Cancer Lett, 2012. **317**(1): p. 78-88.
10. Wang, Y., et al., *Epm2a suppresses tumor growth in an immunocompromised host by inhibiting Wnt signaling.* Cancer Cell, 2006. **10**(3): p. 179-90.
11. Bonnet, D. and J.E. Dick, *Human acute myeloid leukemia is organized as a hierarchy that originates from a primitive hematopoietic cell.* Nat Med, 1997. **3**(7): p. 730-7.
12. Wang, Y., et al., *Targeting HIF1alpha eliminates cancer stem cells in hematological malignancies.* Cell Stem Cell, 2011. **8**(4): p. 399-411.
13. Li, Z., et al., *Hypoxia-inducible factors regulate tumorigenic capacity of glioma stem cells.* Cancer Cell, 2009. **15**(6): p. 501-13.
14. McCollum, A.K., et al., *Up-regulation of heat shock protein 27 induces resistance to 17-allylamino-demethoxygeldanamycin through a glutathione-mediated mechanism.* Cancer Res, 2006. **66**(22): p. 10967-75.
15. Guo, F., et al., *Abrogation of heat shock protein 70 induction as a strategy to increase antileukemia activity of heat shock protein 90 inhibitor 17-allylamino-demethoxy geldanamycin.* Cancer Res, 2005. **65**(22): p. 10536-44.
16. Winklhofer, K.F., et al., *Geldanamycin restores a defective heat shock response in vivo.* J Biol Chem, 2001. **276**(48): p. 45160-7.
17. Bagatell, R., et al., *Induction of a heat shock factor 1-dependent stress response alters the cytotoxic activity of hsp90-binding agents.* Clin Cancer Res, 2000. **6**(8): p. 3312-8.

18. Kim, H.R., H.S. Kang, and H.D. Kim, *Geldanamycin induces heat shock protein expression through activation of HSF1 in K562 erythroleukemic cells.* IUBMB Life, 1999. **48**(4): p. 429-33.
19. Whitesell, L., R. Bagatell, and R. Falsey, *The stress response: implications for the clinical development of hsp90 inhibitors.* Curr Cancer Drug Targets, 2003. **3**(5): p. 349-58.
20. Whitesell, L. and S. Lindquist, *Inhibiting the transcription factor HSF1 as an anticancer strategy.* Expert Opin Ther Targets, 2009. **13**(4): p. 469-78.
21. Min, J.N., et al., *Selective suppression of lymphomas by functional loss of Hsf1 in a p53-deficient mouse model for spontaneous tumors.* Oncogene, 2007. **26**(35): p. 5086-97.
22. Dai, C., et al., *Heat shock factor 1 is a powerful multifaceted modifier of carcinogenesis.* Cell, 2007. **130**(6): p. 1005-18.
23. Ostling, P., et al., *Heat shock factor 2 (HSF2) contributes to inducible expression of hsp genes through interplay with HSF1.* J Biol Chem, 2007. **282**(10): p. 7077-86.
24. Livak, K.J. and T.D. Schmittgen, *Analysis of relative gene expression data using real-time quantitative PCR and the 2(-Delta Delta C(T)) Method.* Methods, 2001. **25**(4): p. 402-8.
25. Nakai, A. and T. Ishikawa, *Cell cycle transition under stress conditions controlled by vertebrate heat shock factors.* EMBO J, 2001. **20**(11): p. 2885-95.
26. Powers, M.V., P.A. Clarke, and P. Workman, *Dual targeting of HSC70 and HSP72 inhibits HSP90 function and induces tumor-specific apoptosis.* Cancer Cell, 2008. **14**(3): p. 250-62.
27. Koslowski, M., et al., *Tumor-associated CpG demethylation augments hypoxia-induced effects by positive autoregulation of HIF-1alpha.* Oncogene, 2011. **30**(7): p. 876-82.
28. Wilkerson, D.C., H.S. Skaggs, and K.D. Sarge, *HSF2 binds to the Hsp90, Hsp27, and c-Fos promoters constitutively and modulates their expression.* Cell Stress Chaperones, 2007. **12**(3): p. 283-90.
29. Akerfelt, M., R.I. Morimoto, and L. Sistonen, *Heat shock factors: integrators of cell stress, development and lifespan.* Nat Rev Mol Cell Biol, 2010. **11**(8): p. 545-55.
30. Trepel, J., et al., *Targeting the dynamic HSP90 complex in cancer.* Nat Rev Cancer, 2010. **10**(8): p. 537-49.
31. Xavier, I.J., et al., *Glycogen synthase kinase 3beta negatively regulates both DNA-binding and transcriptional activities of heat shock factor 1.* J Biol Chem, 2000. **275**(37): p. 29147-52.
32. Wigmore, S.J., et al., *De-repression of heat shock transcription factor-1 in interleukin-6- treated hepatocytes is mediated by downregulation of glycogen synthase kinase 3beta and MAPK/ERK-1.* Int J Mol Med, 2007. **19**(3): p. 413-20.
33. Batista-Nascimento, L., et al., *Deciphering human heat shock transcription factor 1 regulation via post-translational modification in yeast.* PLoS One, 2011. **6**(1): p. e15976.
34. Powers, M.V. and P. Workman, *Inhibitors of the heat shock response: biology and pharmacology.* FEBS Lett, 2007. **581**(19): p. 3758-69.

35. Neckers, L. and P. Workman, *Hsp90 molecular chaperone inhibitors: are we there yet?* Clin Cancer Res, 2012. **18**(1): p. 64-76.
36. Tchenio, T., et al., *Heat shock-independent induction of multidrug resistance by heat shock factor 1.* Mol Cell Biol, 2006. **26**(2): p. 580-91.
37. Ishiwata, J., et al., *State of heat shock factor 1 expression as a putative diagnostic marker for oral squamous cell carcinoma.* Int J Oncol, 2012. **40**(1): p. 47-52.
38. Santagata, S., et al., *High levels of nuclear heat-shock factor 1 (HSF1) are associated with poor prognosis in breast cancer.* Proc Natl Acad Sci U S A, 2011. **108**(45): p. 18378-83.

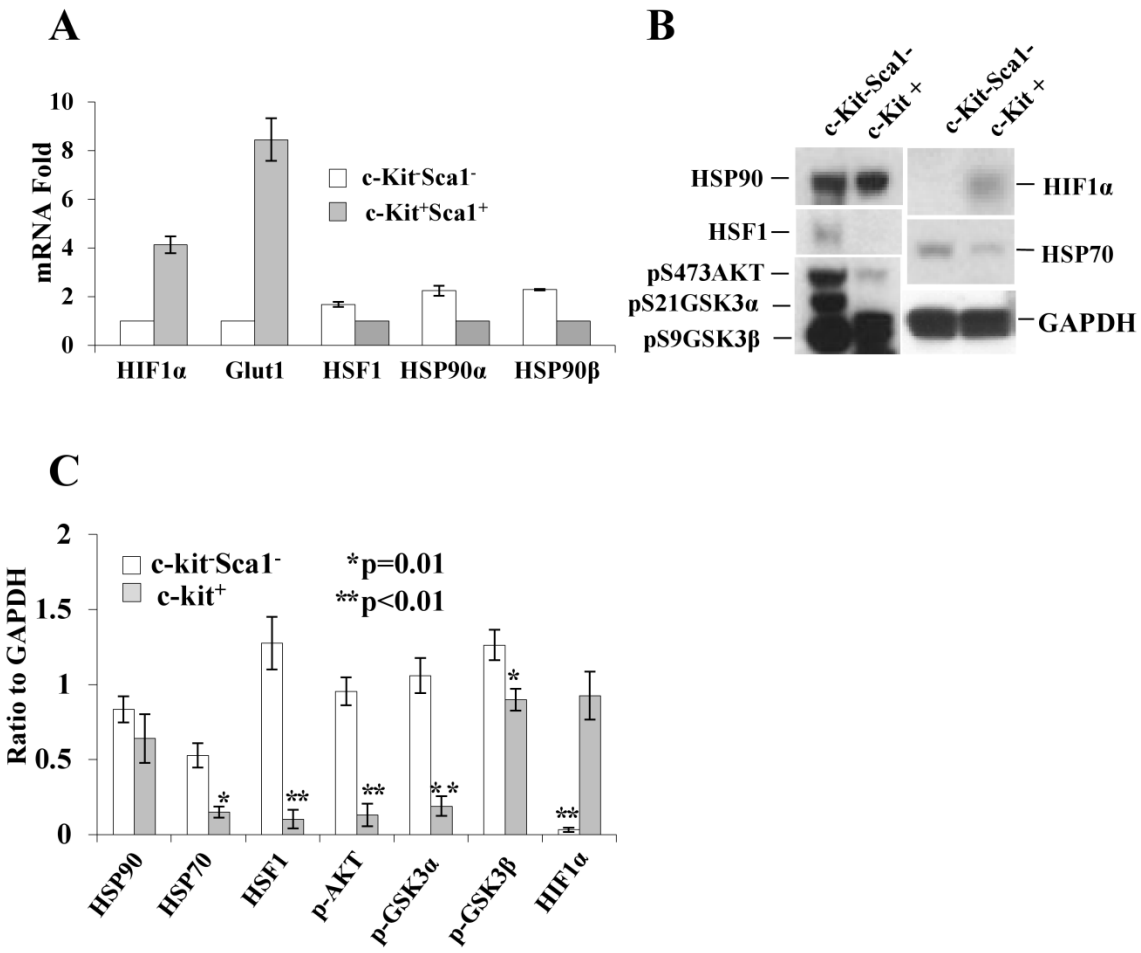

Figure 3.1 The Distinct Features of Lymphoma CSCs (c-Kit$^+$Sca1$^+$) and Differentiated Cells (c-Kit$^-$Sca1$^-$). Freshly isolated lymphoma cells from spleen tissues of TGB lymphoma mice were stained with c-Kit and Sca1 antibodies and sorted using a BD FACS/Aria system. **(**A) Quantitative RT-PCR showing the relative fold increase in mRNAs of indicated genes in the c-Kit$^-$Sca1$^-$ and c-Kit$^+$Sca1$^+$ subsets; the subset with lower mRNA levels is arbitrarily set to 1. (B) Western blot showing indicated proteins in the subsets of c-Kit$^-$Sca1$^-$ and c-Kit+ (c-Kit$^+$Sca1$^+$combined with c-Kit$^+$Sca1$^-$). (C) The relative ratios of protein bands to GAPDH in (B) were calculated by densitometry.

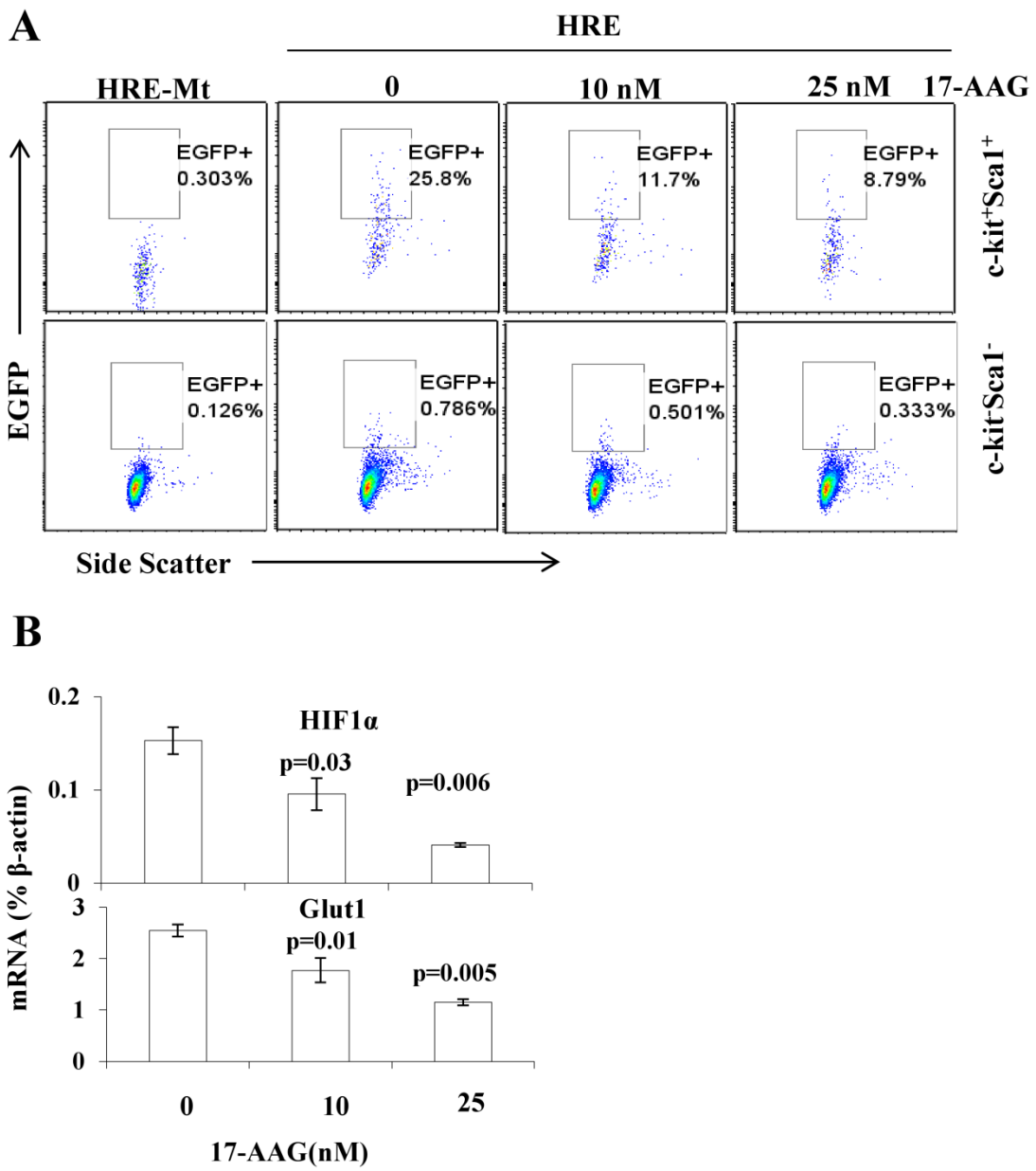

Figure 3.2 17-AAG Suppresses HIF1α Function and Expression. (A) TGB lymphoma cells were infected with a lentivirus containing HRE-EGFP or HRE-Mt (Mt, HIF1α binding site mutated) sequences. After 7 days of culture in 1% methylcellulose medium, the infected cells were treated with 17-AAG for 24 hours. The EGFP positive cells in the two subsets, relative to the negative control gate of HRE-Mt, were analyzed by flow cytometry. (B) After 17-AAG treatment, the lymphoma cells were subjected to mRNA extraction and quantitative RT-PCR using specific primers for HIF1α and Glut1. The percentage of mRNA relative to β-actin is shown. All data presented in this figure have been repeated at least twice.

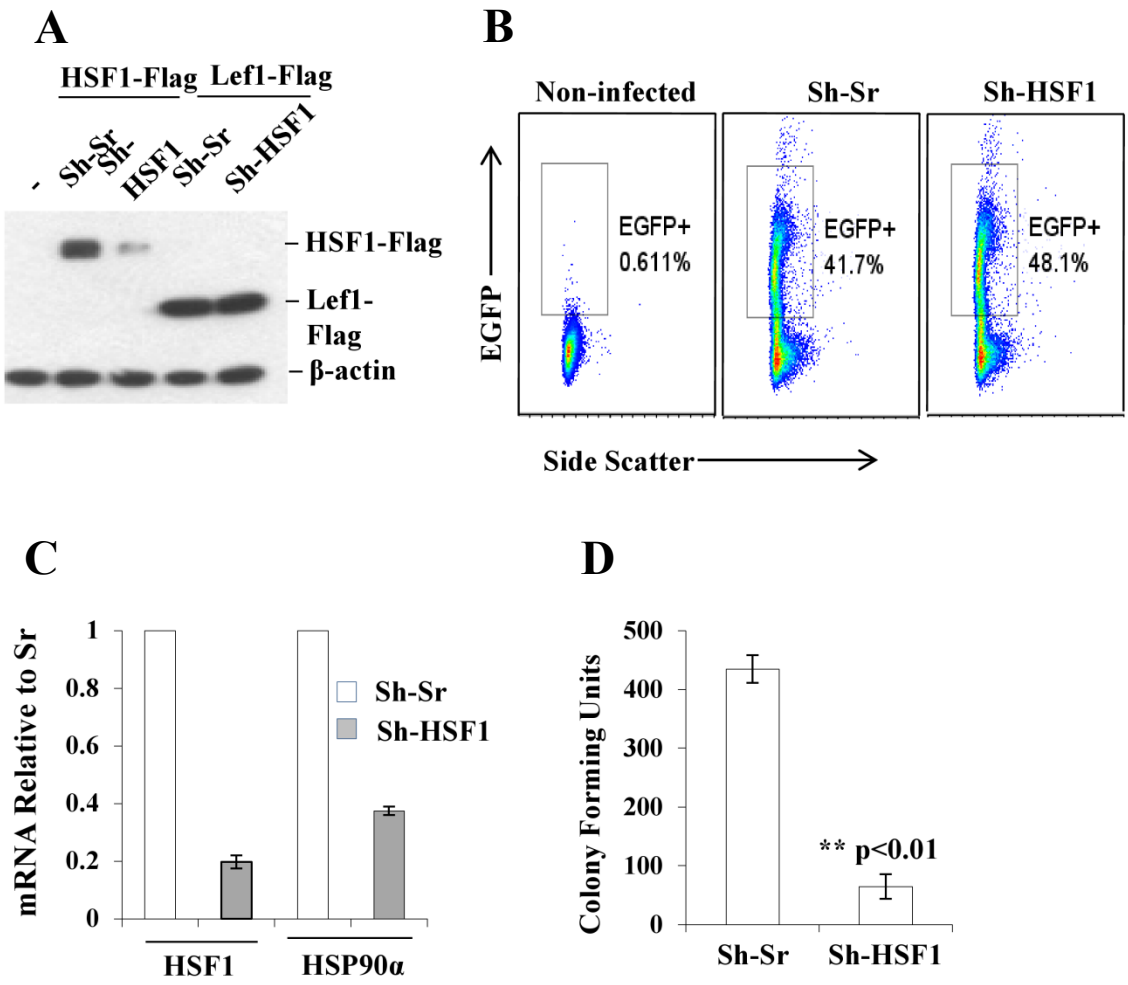

Figure 3.3 HSF1 is Required for the Maintenance of Lymphoma CSCs. (A) Knockdown efficiency of HSF1 by Sh-RNA. Twenty four hours after cotransfection with the plasmids for Sh-HSF1, Flag-tagged HSF1, or Flag-tagged Lef1 as indicated, the HEK293 cells were lysed for Western-blot to detect the HSF1-silencing efficiency using anti-Flag antibody. (B-D) Knockdown of HSF1 abrogated the colony formation ability of lymphoma CSCs. After infection with the lentivirus for Sh-HSF1 or scrambled control, infected cells were cultured in expansion medium for 48 hours to check the infection efficiency (B) Relative mRNA levels of HSF1 and HSP90α to scrambled control (Sr), which is arbitrarily set as 1, were determined in sorted EGFP-positive cells expressing Sh-HSF1 or Sh-Sr (C). Unsorted, infected cells were directly seeded in triplicate in 1% methylcellulose medium for CFUs assays (D). EGFP-positive colonies were counted under fluorescence microscope after 7 days of culture. All data presented in this figure have been repeated at least twice.

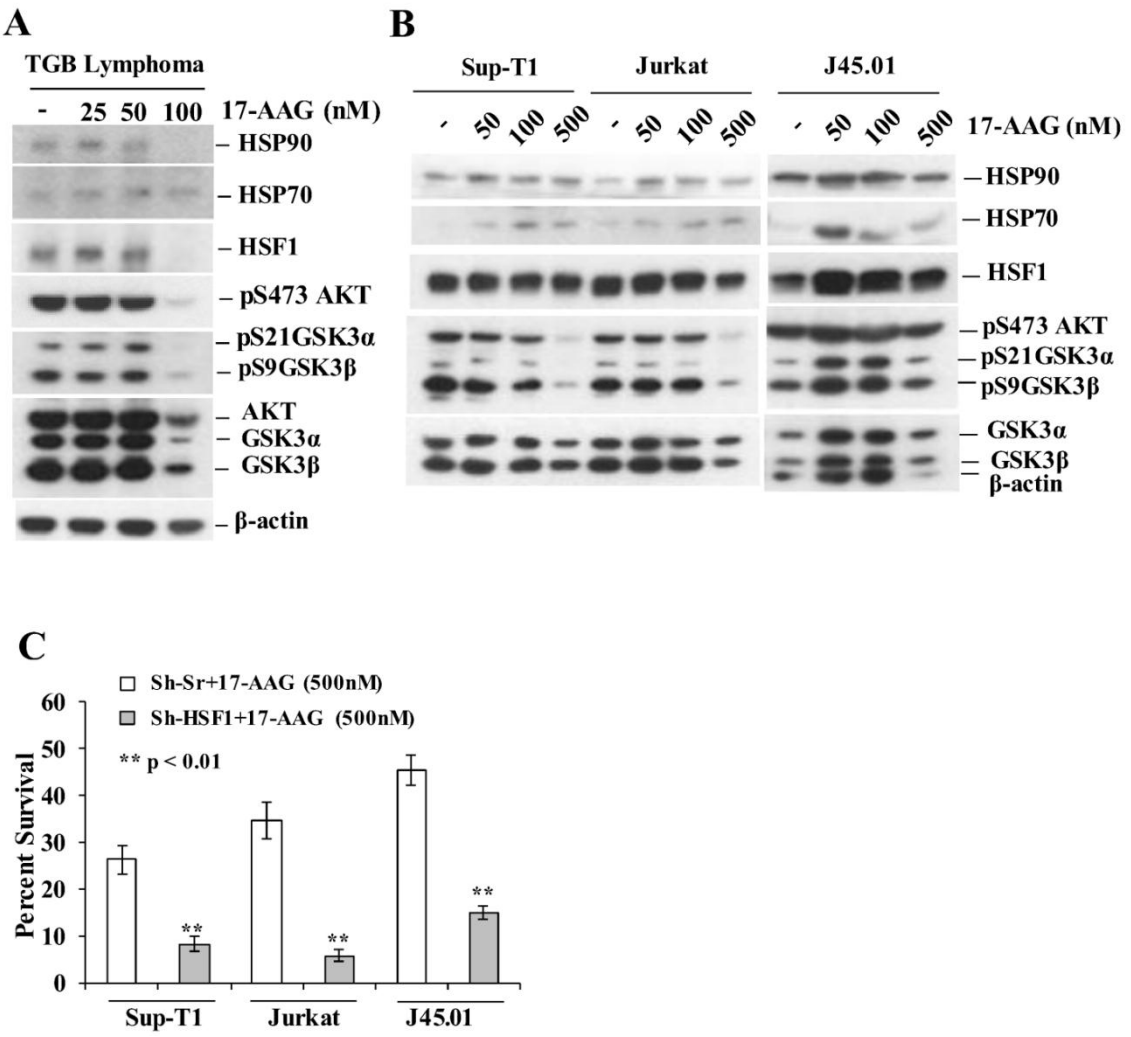

Figure 3.4 Non-CSCs Show HSF1-mediated Resistance to 17-AAG Treatment. (A) Lymphoma non-CSC cells are resistant to low doses of 17-AAG treatment. After treatment with 25 to 100 nM of 17-AAG for 24 hrs, the cultured lymphoma cells were lysed for Western-blot to detect the expression of chaperones, HSF1, and the AKT/GSK-3β pathway. (B) T-lymphoblastic lymphoma/leukemia cell lines resist high doses of 17-AAG. T-lymphoma/leukemia cell lines were treated with increasing concentrations of 17-AAG for 48 hours, and then lysed for western blots to detect the indicated proteins. (C) Knockdown of HSF1 rendered T-lymphoma/leukemia cell lines sensitive to 500 nM 17-AAG treatment. Forty eight hours after spinoculation with lentivirus for Sh-HSF1 or scrambled control, the cells were selected with 6.5 μg/ml blasticidin for one week. The drug-resistant cells (more than 95% GFP positive) were seeded in triplicate in 6-well plates and treated with 500 nM 17-AAG or vehicle for 72 hours. The percent ratio of the treated to untreated viable cells in each group is shown.

Figure 3.5 The Effects of HSF1 Knockdown in AML Cells. (A) The protein expression of chaperones and clients in human AML cells. Compared to normal mouse bone marrow (BM) cells, the four AML cells from patients and THP-1 (a human AML cell line) expressed increased levels of chaperones, HSF1, and the active AKT/GSK-3β pathway similarly as TGB lymphoma cells, as determined by Western-blot. (B) 17-AAG treatment reduces HIF1α mRNA expression in a dose-dependent manner. The mRNA levels of HIF1α relative to β-actin is shown. (C) Knockdown of HSF1 abrogated colony formation of AML CSCs. After lentiviral spinoculation, portions of AML cells were seeded directly in triplicate in 1% methylcellulose medium for CFUs assays (D) the remaining cells were cultured for 48 hours to detect the EGFP expression and determine the relative mRNA levels of HSF1 and HSP90α to scrambled control (Sr), which is arbitrarily set as 1, in sorted EGFP-positive cells expressing Sh-HSF1 or Sh-SrI (E). All data presented in this figure have been repeated at least twice.

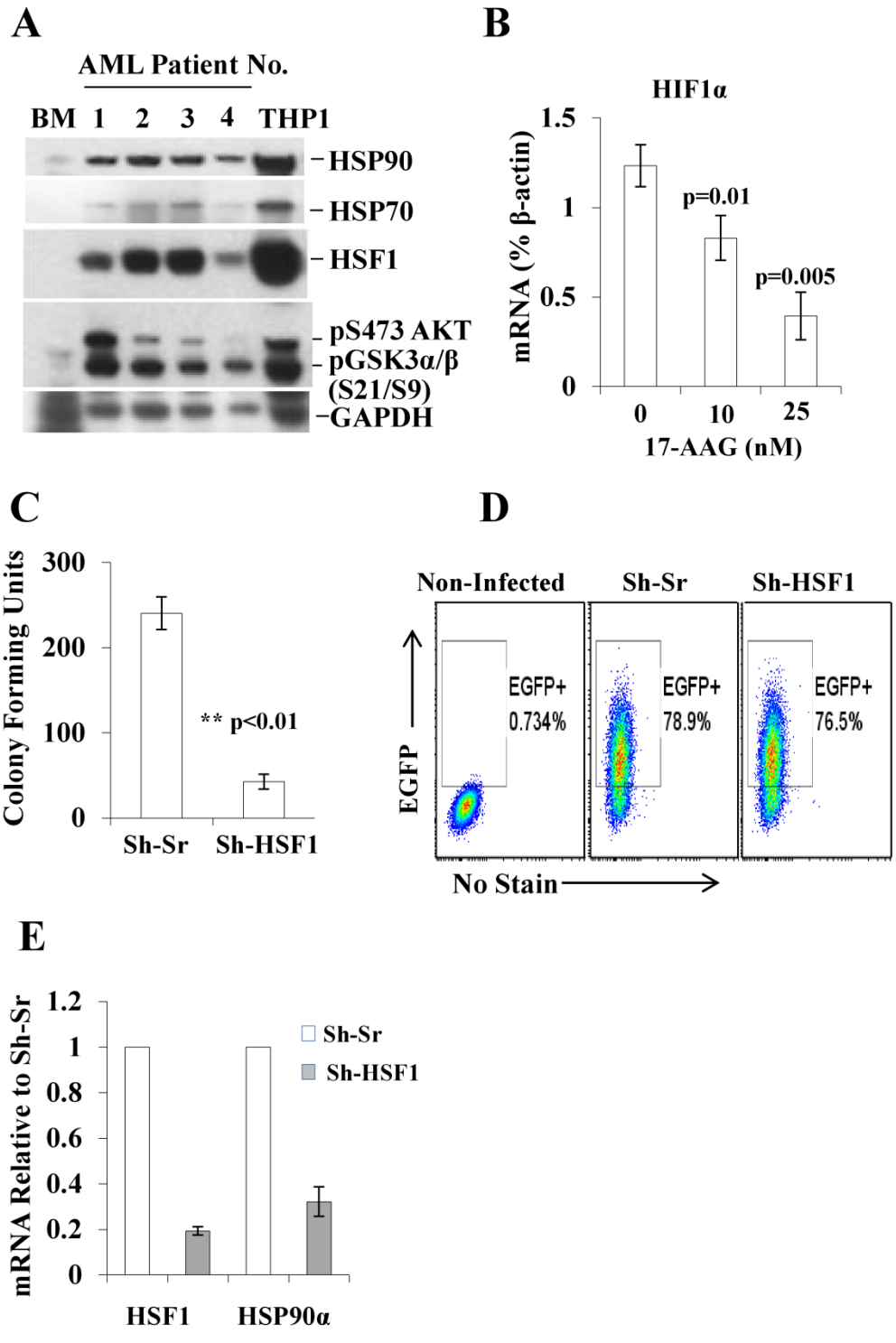
A
AML Patient No.
BM 1 2 3 4 THP1
HSP90
HSP70
HSF1
pS473 AKT
pGSK3α/β (S21/S9)
GAPDH
B
HIF1α
mRNA (% β-actin)
1.5
1
0.5
0
p=0.01
p=0.005
0 10 25
17-AAG (nM)
C
Colony Forming Units
300
200
100
0
** p<0.01
Sh-Sr Sh-HSF1
D
Non-Infected
Sh-Sr
Sh-HSF1
EGFP+ 0.734%
EGFP+ 78.9%
EGFP+ 76.5%
EGFP
No Stain
E
mRNA Relative to Sh-Sr
1.2
1
0.8
0.6
0.4
0.2
0
Sh-Sr
Sh-HSF1
HSF1
HSP90α

Chapter 4

A Combination Strategy for Sensitizing Breast Cancer Stem Cells to Conventional Therapy

Abstract

Ionizing radiation is a commonly used breast cancer therapy used to reduce the tumor bulk, and has been found to decrease local recurrence following surgical removal of breast tumors. However, some patients ultimately relapse. CSCs have been shown to be radioresistant, implicating a role for these cells in the recurrence of breast cancer following radiotherapy. Thus, a successful strategy to efficiently treat patients and reduce recurrences would be to combine a CSC-targeting agent with radiation. Our past work has shown 17-AAG can selectively eliminate CSCs from both a mouse T-lymphoma model and human AML. Here we demonstrate that 17-AAG can sensitize breast CSCs to ionizing radiation in vitro. SUM149 and MDA-MB-231 Aldefluor-positive cells, as well as T47D $CD44^+/CD24^-/ESA^+$ cells were reduced following fractionated radiation when treated with 17-AAG. Surprisingly, MDA-MB-231 $CD44^+/CD24^-/ESA^+$ cells did not show enhanced radiation-mediated killing when treated with 17-AAG, demonstrating heterogeneity in the CSC population within and between cell lines to HSP90 inhibition. Interestingly, resistance to radiation was not a universal feature of breast CSCs. HCC1937 Aldefluor-positive and $CD44^+/CD24^-/ESA^+$ cells were reduced following radiation in vitro. Similarly, SUM159 and MDA-MB-231 Aldefluor-positive cells grown as xenografts were also reduced by radiation.

Taken together, these results show that radioresistance, while not uniformly expressed in all breast CSCs, can be reversed with 17-AAG in certain cases.

Introduction

Despite continued advances in treating many solid and hematological cancers, tumor recurrence and effective prevention and control of metastatic spread remain unresolved problems. However, the discovery and identification of cancer stem cells (CSCs), and their contribution to relapse and metastasis, may provide a therapeutic target to effectively reduce these problems. CSC's critical reliance on activated self-renewal pathways makes them vulnerable to inhibitors that can adequately target this process. Unfortunately, targeting these pathways is difficult since the control of self-renewal involves multiple intrinsic and extrinsic signals, allowing for high levels of redundancy [1-4]. In this way, a single inhibitor blocking one self-renewal pathway may not suffice. Simultaneous inhibition of multiple self-renewal pathways through HSP90 inhibition may provide a suitable alternative to single inhibitors [5]. In particular, HSP90 inhibition has been shown to be effective at selectively targeting CSCs [6, 7]. Work presented in Chapter 2 corroborates these claims, as CSCs from our mouse T-cell lymphoma model and AML were found to be selectively sensitive to the HSP90 inhibitor 17-AAG. Higher concentrations of 17-AAG were necessary to achieve efficacy in the differentiated lymphoma cells in our model system. Our results together with other published reports suggest that the optimal use of 17-AAG may be as a CSC-targeting agent. Therefore, utilizing 17-AAG at a lower dose, in conjunction with an effective conventional therapy,

should provide a highly effective strategy at controlling both bulk tumor growth as well as relapse and metastasis.

Having already shown the validity of 17-AAG treatment in controlling T-cell lymphoma CSCs and their ability to reinitiate cancer both in vitro and in vivo, we chose to demonstrate a combination strategy in an alternate, solid tumor system. Similar to other solid and hematological cancers, recurrence and metastatic spread in breast cancer remain significant therapeutic challenges. Radiotherapy is often used in addition to surgery in breast cancer patients to prevent local recurrence. Studies examining the utility of adjuvant radiation following surgery, have shown that local recurrence rates are often dramatically reduced with the addition of radiation. When radiation was given after surgical removal of the tumor, local recurrence at 5-years and overall recurrence at 10-years were 7% and 19.3%, respectively [8, 9]. In contrast the 5-year local recurrence and 10-year overall recurrence was 26% and 35%, respectively, for patients who solely relied on surgery. While these analyses show substantial reductions in recurrence with adjuvant radiotherapy, some patients ultimately relapse. Therefore, new strategies for treatment are needed for patients to further reduce the risk of relapse and thus extend survival.

As with chemotherapy [10-12], CSCs have been shown to be intrinsically resistant to ionizing radiation [11, 13-21]. Breast CSCs that display the surface marker phenotype $CD44^{+}/CD24^{-}$ were shown to have lower levels of reactive oxygen at basal conditions, as well as following exposure to ionizing radiation. Thus, enrichment of CSCs as observed following radiotherapy is likely due to an anti-oxidant mechanism within CSCs [13]. Similarly, enhanced DNA repair from damage incurred from radiation has also been demonstrated in breast CSCs [13, 14, 22]. Furthermore, recent evidence

has even shown that radiation itself can potentially generate tumorigenic cells from the bulk population [23]. Therefore, residual and/or radiation-induced CSCs, having evaded radiotherapy, may provide an explanation for the persistent, albeit lower, rates of local and overall recurrence. If this is truly the case, a successful strategy for dealing with breast tumors would be to combine a CSC-targeting agent with conventional fractionated radiation. In this way, surviving or generated CSCs would be eliminated at the time of treatment, and potentially nullify the risk of local and overall recurrence.

In the study presented here, the efficacy of combining 17-AAG with fractionated radiation in treating both bulk breast cancer cells and the CSC subpopulation was examined. HSP90 inhibition has been suggested as a treatment strategy for breast cancer for a number of reasons. Similar to PTCL, elevated expression of HSP90 and HSF1 has been observed in breast cancer, and has been linked to poor patient survival [24-27]. Additionally, breast CSCs have been shown to rely on HSP90 clients (Her2, AKT) for regulation of self-renewal, indicating that they should be sensitive to 17-AAG HSP90 inhibition [28, 29]. Indeed, when human breast cancer cell lines were treated in vitro with 17-AAG, the tumorigenic Aldefluor-positive population was reduced (unpublished results). These effects were typically seen at concentrations lower than what was required to disrupt bulk breast cancer cells, demonstrating selective sensitivity similar to our lymphoma CSCs. Interestingly, while the in vitro enrichment and radioresistance of breast CSCs could be reduced with 17-AAG treatment, when treated in vivo, the CSCs were found to be sensitive to radiotherapy regardless of the addition of 17-AAG. This suggests that results from in vitro studies demonstrating radioresistance and generation of CSCs may not be entirely reflective of CSCs in vivo. Therefore, care must be taken

about generalizing in vitro findings for predicting in vivo responses. Lastly, our results show that combining 17-AAG with fractionated radiation is an effective strategy in certain tumor types, and warrants further study in vivo.

Material and Methods

Cell Lines and Reagents

Human breast cancer cell lines SUM159, SUM149, HCC1937, MDA-MB-231, and T47D were obtained from the Wicha Laboratory (University of Michigan, Ann Arbor, MI). The SUM159 and SUM149 cell lines were maintained in Ham's F12 medium supplemented with 5% fetal bovine serum (FBS), 5 µg/ml insulin, 1 µg/ml hydrocortisone, 1% Pen/Strep antibiotic (10,000 units/ml penicillin G sodium, 10,000 µg/ml streptomycin sulfate) and 20 µg/ml gentamycin. The MDA-MB-231, and HCC1937 cell lines were maintained in RPMI medium supplemented with 10% fetal bovine serum (FBS), and 1% Pen/Strep antibiotic. The T47D cell line was cultured using RPMI medium supplemented with 10% fetal bovine serum (FBS), 5 µg/ml insulin, and 1% Pen/Strep antibiotic. Cell lines were maintained in culture at 37°C and 10% CO2, except for HCC1937 which were maintained at 5% CO2. 17-AAG was purchased from LC Laboratories (Woburn, MA).

MTS Cell Proliferation Assay

Human breast cancer cell lines were seeded into 96-well microplates at a density of 3,000 cells per well. Cells were treated with increasing concentrations of 17AAG. After 72 hour incubation, cell viability was assessed by the MTS cell proliferation assay

(Promega, Madison, WI) according to the manufacturer's instruction. Cellular IC50 was displayed as the concentration necessary to decrease viability to 50% of control untreated cells.

Aldefluor Assay

The Aldefluor assay was carried out according to the manufacturer's protocol (Stemcell Technologies, Vancouver, British Columbia). For both in vivo and in vitro studies, the ALDH1 substrate bodipyaminoacetaldehyde (BAAA) was added to the single cell suspension at a concentration of 1.5 μM, which was then incubated for 40 min at 37°C. A portion of cells was incubated with a 10-fold molar excess of an ALDH1 enzyme inhibitor, diethylamino benzaldehyde (DEAB) in addition to BAAA and incubated similarly for 40 min. In the presence of DEAB, the ALDH1 enzyme is inhibited from metabolizing BAAA and therefore functions as a negative control, allowing us to distinguish Aldefluor-positive and Aldefluor-negative cells. At the end of BAAA-staining, cells were washed once with HBSS containing 2% FBS and subsequently stained with 1 μg/mL 4,2-diamidino-2-phenylindole dihydrochloride (DAPI) to exclude non-viable cells. Flow cytometry was performed at the University of Michigan Cancer Center Flow Cytometry Core. Data analysis was performed with the software program Weasel (Walter and Eliza Hall Institute of Medical Research).

Flow Cytometry with CD44/CD24/ESA

Following 17-AAG and/or radiation treatment, breast cancer cells are detached and counted using a Countess cell counter (Invitrogen). One million cells are transferred

to 5 mL FACS tubes and resuspended in 300 μL of HBSS containing 2% Fetal Bovine Serum. Five microliters mouse anti-human CD44-APC, mouse anti-human ESA-FITC, and mouse anti-human CD24-PE (BD Pharmingen) were given to each sample and incubated on ice, covered, for 30 min. Samples were then washed twice with HBSS containing 2% FBS. Finally, samples were resuspended in 500 μL HBSS 2% FBS containing 1 μg/mL DAPI for nuclear staining. Flow cytometry was performed at the University of Michigan Cancer Center Flow Cytometry Core. Data analysis was performed with the software program Weasel (Walter and Eliza Hall Institute of Medical Research).

Colony Formation

Sorted SUM149 Aldefluor-positive and Aldefluor-negative cells were seeded in triplicate in 60-mm dishes and treated with 17-AAG (10 and 20 nM) for 1 hour. After treatment, the cells were exposed to 0, 1, 2 and 4 Gy of radiation (Philips RT250, Kimtron Medical) and incubated for 24 hours for cellular attachment. 17-AAG was washed away following exposure to radiation, and the cells were cultured at 37C for 10-12 days. Colonies were stained with crystal violet and counted, and the survival curves were fitted by linear-quadratic equation [30].

Irradiation of Cell Lines and Tumor Xenografts

Breast cancer cell lines and tumor xenografts were irradiated as described before [31]. Cell lines were plated and allowed to attach overnight. The following day, cells were treated with 17-AAG 6 hours prior to radiation treatment. Irradiation was

performed using a Philips RT250 (Kimtron Medical) in the University of Michigan Comprehensive Cancer Center Experimental Irradiation Core. Dosimetry was carried out using an ionization chamber connected to an electrometer system that is directly traceable to a National Institute of Standards and Technology calibration. Following treatment, cells were washed and given fresh medium containing 17-AAG at indicated doses. This was performed for three consecutive days, and Aldefluor and CD44/CD24/ESA staining was performed on the sixth day. For tumor irradiation, animals harboring SUM159, SUM149, or MDA-MB-231 xenografts were anesthetized with isoflurane and positioned such that the apex of each mammary fat pad tumor was at the center of a 2.4-cm aperture in the secondary collimator, with the rest of the mouse shielded from radiation.

Xenograft Tumor Model and Reimplantation

All experiments involving mice were approved by the University Committee on the Use and Care of Animals at the University of Michigan. For tumor implantation, at least 1 x 10^6 SUM159, SUM149, or MDA-MB-231 cells mixed with Matrigel (50%, v/v) were injected into the fourth mammary fat pads of 4-week-old NOD/SCID mice (Jackson Laboratories, Bar Harbor, ME) and allowed to form palpable tumors. When tumors reached approximately 50 mm^3 volume, mice were randomly put into control and treatment groups. Mice receiving 17-AAG (5 mg/kg 17-AAG dissolved in 10% DMSO + 40% Cremophor EL:Ethanol (3:1, v/v) + 50% PBS) were given drug by I.P. injection whereas control mice were given vehicle alone. For mice receiving the combination therapy, one treatment cycle (one week) consisted of 17-AAG given two days prior to radiation, followed by three days of 17-AAG plus 2 Gy/day radiation, then 2 days with

neither treatment for recovery. Mice receiving 17-AAG alone were given 5 days of 5 mg/kg 17-AAG consecutively, whereas mice receiving only radiation were given 2 Gy/day for 3 consecutive days. Tumors were measured with digital calipers at least once a week. Tumors were removed for analysis the day following the last dose of radiation. Tumor reimplantation was conducted as previously described [29, 32]. In brief, single cell suspensions were stained with the fluorescent nucleic acid dye DAPI for viability screening. Cells were also stained with either mouse anti-H2Kd-APC/CY7 or mouse anti-HLA-APC/CY7 antibodies (BD Pharmingen) to distinguish human tumor cells from mouse cells. Viable cells (5×10^2) derived from primary tumors treated with vehicle, 17-AAG, radiation, or the combination were injected into mammary fat pads of secondary NOD/SCID mice (n=4 for each condition).

Tumor Tissue Dissociation

Tissue was mechanically and enzymatically dissociated to obtain single cell suspensions, as previously described [30]. In brief, tumors were minced finely with scalpels and incubated in 10% collagenase/hyaluronidase (Stem Cell Technologies, Vancouver, British Columbia) in Medium 199 at 37 °C for 60 minutes. Single cell suspensions were obtained by filtering the digested tumor through a 40 μm filter (BD Biosciences, San Jose, CA). Single cell suspensions were centrifuged at 1500 rpm at 4°C, and pellets were resuspended in HBSS containing 2% FBS for the Aldefluor assay, CD44/CD24/ESA staining, and tumor reimplantation.

Statistics

Statistical significance was determined using unpaired Student's t-test.

Results

Sensitivity to 17-AAG Mediated HSP90 Inhibition is Varied in Breast Cancer Lines

Elevated expression of chaperones and their related proteins (HSP90, HSF1) has been correlated with poor prognosis in breast cancer patients [24-27]. Therefore, it has been hypothesized that breast cancer cells would be sensitive to HSP90 inhibition. To confirm that 17-AAG could reduce growth rate and viability in breast cancer cell lines, SUM149 and MDA-MB-231 cells were cultured with increasing concentrations of 17-AAG and the MTS assay performed. Both cell lines had reduced viability with 17-AAG treatment (Figure 4.1). However, there was a large difference in the effective 17-AAG concentration range between the two cell lines. SUM149 breast cancer cells had a similar sensitivity to HSP90 inhibition (IC50 approximately 93 nM) as other breast cancer lines previously tested in our lab (SUM159, IC50 approximately 35 nM; MCF-7, IC50 approximately 100 nM; unpublished data). In agreement with reports in the literature [33], MDA-MB-231 cells were dramatically more resistant to HSP90 inhibition (IC50 approximately 17 μM). These results highlight that the efficacy achieved by HSP90 inhibition may not be solely based on the presence of oncogenic clients within a cancer cell type. Rather the efficacy may be determined by whether the cancer cells are critically reliant on the pathway in which the clients function.

In Vitro Response to Radiotherapy Combined with 17-AAG in Breast CSCs is Cell Line Dependent

Identification of breast CSCs can be conducted using various techniques. Breast CSCs were originally identified by their surface marker expression of $CD44^+/CD24^-/Lin^-$ [34]. However, in basal breast cancer lines, greater than 90% of the cell population has this phenotype. Further studies later demonstrated that $CD44^+/CD24^-/ESA^+$ expression can identify tumorigenic stem cells better in basal breast cancer cell lines [12]. Lastly, stem and CSCs in a number of solid and hematological cancers have been identified by their elevated expression of the Aldehyde Dehydrogenase enzyme [32, 35-37]. In some instances, surface markers have been combined with Aldehyde Dehydrogenase activity to identify tumorigenic stem cells [38-40]. We first utilized the Aldefluor assay to discern breast CSCs from the tumor bulk when examining the efficacy of 17-AAG. Both SUM149 and SUM159 breast cancer cells were treated with 17-AAG for 3 days before performing the Aldefluor assay (Figure 4.2A-C). The percentage of Aldefluor-positive cells in SUM159 and SUM149 cell lines were reduced by 68% and 42%, respectively, following 17-AAG treatment (10 nM). Similar to the previously studied lymphoma CSCs, these Aldefluor-positive cells were selectively sensitive to HSP90 inhibition compared to the tumor bulk. To assess whether these Aldefluor-positive cells also tolerated ionizing radiation more than the non-CSCs, Aldefluor-positive and Aldefluor-negative cells were isolated for use in a clonogenic survival assay (Figure 4.3A,B). For this assay, small numbers of SUM149 cells were plated onto culture dishes, treated with radiation, and allowed to form colonies. Cells that are more resistant (such as CSCs) generate more colonies, which can be used to calculate the survival fraction [41]. At a dose of 2 Gy, 80% of the Aldefluor-positive cells survived, compared to only 50% of the

Aldefluor-negative cells. This resistance was abrogated with 17-AAG treatment (20 nM), as approximately 40% of the Aldefluor-positive cells survived after 2 Gy of radiation (Figure 4.3B). This sensitization to radiation with 17-AAG was not seen with the Aldefluor-negative cells, demonstrating the selective sensitivity to HSP90 inhibition in the breast CSCs.

Having demonstrated that Aldefluor-positive cells display greater resistance to a single dose of radiation compared to the Aldefluor-negative cells, it was subsequently examined if this also holds true for fractionated doses of radiation. Dose fractionation has been previously used to exploit the faulty cellular repair present in malignant cells [41]. Unfortunately, CSCs have been shown to be resistant to this method of treatment [13, 23, 42]. To determine if HSP90 inhibition can sensitize CSCs, both MDA-MB-231 and HCC1937 breast cancer cells were pretreated with 17-AAG before each dose of radiation, given consecutively for 3 days. On the sixth day, cells were analyzed for changes in the Aldefluor-positive population following treatment (Figure 4.4A,B). Similar to SUM149 cells, 17-AAG treatment alone was capable of reducing the number of Aldefluor-positive cells in both HCC1937 (61% absolute reduction) and, albeit less selectively, MDA-MB-231 (23% absolute reduction). Following radiation treatment alone, the percentage of MDA-MB-231 Aldefluor-positive cells rose from 0.99% to 2.13%, despite a ~50% reduction in absolute CSC number. This increase indicates that although the CSCs remain sensitive to radiation, they are more resistant than the non-CSCs. Similar to results with SUM149 cells, pre-treatment with 17-AAG prevented the enrichment of Aldefluor-positive cells in both MDA-MB-231 and HCC1937 cells following radiation. Strikingly, HCC1937 Aldefluor-positive cells were as sensitive to

radiation as the Aldefluor-negative cells, as indicated by the lack of increase in the percentage of Aldefluor-positive cells following radiation (Figure 4.4B). These results suggest that CSC radioresistance may be relative to cancer subtype. Alternatively, since cancers often harbor multiple subtypes of CSCs, which vary phenotypically, these subtypes may also vary in radioresistance.

To examine if an alternate CSC phenotype harbors radioresistance in breast cancer cell lines, further studies were carried out to determine if $CD44^+/CD24^-/ESA^+$ CSCs also vary in their ability to survive treatment. The breast cancer cell lines HCC1937, MDA-MB-231, and T47D were treated with fractionated doses of radiation and 17-AAG as described above before being assayed for changes in the $CD44^+/CD24^-/ESA^+$ subpopulation. Similar to the decrease seen in Aldefluor-positive cells, $CD44^+/CD24^-/ESA^+$ HCC1937 cells were significantly sensitive to fractionated doses of 4 Gy radiation (94% reduction) (Figure 4.5A). These cells were also sensitive to 17-AAG treatment alone (29% Absolute CSC reduction). However, when combined with radiation, 17-AAG treatment did not result in a further reduction of CSCs. As seen with the MDA-MB-231 Aldefluor-positive cells, the $CD44^+/CD24^-/ESA^+$ cells were markedly increased (19-fold) following fractionated doses of 4 Gy radiation (Figure 4.5B). However, these CSCs were unaffected by 17-AAG treatment, which instead sensitized the non-CSCs rather than the CSCs to radiation. This is shown by the increase in CSC percentage but not absolute number. Lastly, the ability of 17-AAG to sensitize breast CSCs was shown most convincingly with T47D $CD44^+/CD24^-/ESA^+$ cells (Figure 4.5C). When T47D cells were treated with fractionated doses of 3 Gy and 5 Gy, we observed a 3.8-fold and 6.3-fold increase in $CD44^+/CD24^-/ESA^+$, respectively. Treatment with 17-

AAG was able to reduce the absolute number of CSCs, and cause a dose-dependent reduction in CSC enrichment following radiation. Taken together, these results indicate that radioresistance in CSCs, as well as efficacy with 17-AAG, can vary between not only tumor type, but also CSC phenotype.

Sensitivity of Breast CSCs to Radiotherapy and 17-AAG In Vivo

The variable level of radioresistance in breast CSCs observed may be attributed to the culturing methods used in the experiments above. Previous studies have shown that chemoresistance varies greatly between cells grown in 2-dimensional and 3-dimentional culture [43]. This has been postulated to result from environmental and/or conformational cues that cells encounter in 3-dimensional growth (i.e. growth in vivo) [44]. For instance, interaction of the α6β1 integrin receptor with the extracellular matrix protein laminin can induce AKT-mediated survival mechanisms, leading to resistance of conventional therapy [44, 45]. Having first validated radioresistance and radiosensitization with 17-AAG treatment in SUM149 Aldefluor-positive cells in vitro, subsequent studies were carried out to assess the response to radiation and 17-AAG treatment in vivo. Unsorted SUM149 cells were implanted in the mammary fat pads of NOD/SCID mice and were allowed to form palpable tumors before beginning treatment. In order to provide a clinically relevant radiotherapy regimen, fractionated doses of radiation (2 Gy) were given consecutively over 3 days per week. Since we have previously shown that Aldefluor-positive cells are more sensitive to HSP90 inhibition than the bulk population, a significantly lower dose than what other preclinical studies have tested was chosen to be used in combine with radiation. Indeed, a 17-AAG dosage

regimen as low as 5 mg/kg was previously found to efficiently eliminate Aldefluor-positive cells in both a breast cancer cell line (SUM159) and a primary human xenograft (MC1) in vivo (unpublished data). The SUM149 tumors were treated with four cycles of radiation, 5 mg/kg 17-AAG, or a combination of the two treatments before tumors were removed for Aldefluor analysis. As shown in Figure 4.6A, the growth of SUM149 tumors was modestly inhibited with 17-AAG treatment. This validates our strategy for combining a CSC-targeted agent with conventional therapy, as CSC-specific treatment will have little effect on bulk tumor cells, requiring an additional therapy to eliminate the differentiated population. As expected, radiation resulted in a large reduction in bulk tumor volume, while the combination strategy similarly repressed the tumor growth throughout the study. Interestingly, when tumors were analyzed for changes in the Aldefluor-positive population, neither 17-AAG nor radiation yielded a change in percentage of CSCs relative to control tumors (Figure 4.6B). Since 17-AAG-treated tumors were reduced solely in the number (Figure 4.6C), and not percentage of CSCs, this indicates that HSP90 inhibition does not selectively target the CSCs but rather affects both CSCs and non-CSCs simultaneously. Likewise, the number of CSCs were reduced in radiation-treated tumors, despite the radioresistance displayed by these cells in vitro. Finally, combining 17-AAG with radiation treatment significantly reduced the number of Aldefluor-positive cells as compared to control. However, there was no statistical difference between the combination strategy and either treatment given alone. Taken together, the data indicates that breast CSCs, while affected by radiation in vivo, can be further sensitized by 17-AAG mediated HSP90 inhibition.

To assess if the remaining CSCs in SUM149 tumors were impaired in their capacity to self-renew following treatment, 500 cells from each treatment group were implanted into healthy recipient mice and allowed to form tumors (Figure 4.6D). In contrast to reimplantation results from our lab which showed 17-AAG treatment impairs reinitiation of tumors in secondary recipient mice, cells from 17-AAG treatment showed similar tumor reinitiation as untreated control mice. This suggests that the level of self-renewal impairment engendered by 17-AAG may also vary across different cell lines. In addition, cells from both radiation and the combination therapy were slightly less capable of tumor reinitiation. Thus, while impairment of self-renewal of SUM149 CSCs can be achieved with radiotherapy, improving the level of impairment will likely require higher 17-AAG doses than used in this study.

As the in vitro results indicated differences in radioresistance between cell lines, we performed similar in vivo experiments with SUM159 and MDA-MB-231 xenografts to assess efficacy in combining low doses of 17-AAG with fractionated radiation. After 2 cycles of treatment, SUM159 tumors were removed and analyzed for changes in the Aldefluor-positive population. On average, tumors treated with radiation or a 17-AAG + radiation combination were beginning to show signs of regression compared to the control tumors (Figure 4.7A). Despite receiving fewer treatment cycles than SUM149 tumors, SUM159 tumors exhibited an even greater reduction in the absolute number of Aldefluor-positive cells following radiation (77%) or the combination (32%) (Figure 4.7B). Interestingly, combining 17-AAG with radiation increased the percentage of Aldefluor-positive cells relative to radiation alone (Figure 4.7C). This suggests that 17-AAG is sensitizing the differentiated cells rather than the CSCs to radiation. The results

were replicated in MDA-MB-231 xenografts treated with radiation, 17-AAG, and the combination of both therapies. MDA-MB-231 tumor growth was reduced to a greater extent following radiation or radiation combined with 17-AAG, than in tumors treated with 17-AAG alone (Figure 4.8A). In contrast to in vitro results, radiation decreased the percentage of Aldefluor-positive cells by 24% (Figure 4.8B). As with SUM159, combining 17-AAG with radiation increased the percentage of Aldefluor-positive cells while reducing their absolute number, suggesting sensitization of the differentiated population to radiotherapy (Figure 4.8C). Finally, to examine if differences in CSC phenotype can explain the radiosensitivity seen with the Aldefluor-positive MDA-MB-231 cells, we analyzed changes in the $CD44^+/CD24^-/ESA^+$ population following these treatments (Figure 4.8D). MDA-MB-231 $CD44^+/CD24^-/ESA^+$ cells were reduced following all treatments in a similar manner as the Aldefluor-positive population. These results indicate CSC radioresistance observed in vitro may not always predict in vivo radioresistance.

Discussion

As with peripheral T-cell lymphoma (PTCL), increased patient survival in breast cancer through the reduction in relapse and metastatic progression requires identification and validation of novel agents that can target tumorigenic stem cells [1, 46]. These CSCs harbor resistance to both chemotherapy and radiation, making them the likely mediators of recurrence following therapy. Successful strategies for targeting CSC have primarily revolved around disruption of their capacity to self-renew [1]. However, the self-renewal process is governed by multiple factors, relying on signals originating from both within

the cells as well as their microenvironment [1-3]. Thus, the likelihood for redundancy within these signaling pathways suggests that multiple inhibitors may be required to fully ablate self-renewal. In contrast, disruption of self-renewal via HSP90 inhibition is a more suitable strategy, as multiple self-renewal signals can be blocked without the need for more than one inhibitor. The work presented here with CSCs from mouse lymphoma, AML, and breast cancer cells have validated this claim, showing often potent and selective elimination of these tumorigenic subpopulations by targeting HSP90. While the use of CSC-targeting agents may be necessary for improving overall patient survival, use of these compounds as a single therapy will likely be an ineffective strategy, due to the continued (albeit limited) proliferative potential within the tumor bulk. Thus, an effective strategy for using CSC-targeting agents is through combination with a conventional strategy that can adequately remove the bulk of the tumor cells. This strategy was tested in the current study by combining the CSC-targeting agent (17-AAG) with an effective conventional treatment (radiation), which when used alone is ineffective against the CSC subpopulation [3, 47-49].

17-AAG was first confirmed to eliminate breast CSCs defined by their expression of the Aldehyde Dehydrogenase (ALDH) enzyme. Both SUM159 and SUM149 Aldefluor-positive cells were reduced following treatment with 17-AAG at concentrations well below their bulk tumor cell IC50. In agreement with reports in the literature [42, 50], breast CSCs from the SUM149, MDA-MB-231, and T47D cell lines were shown to have higher resistance to radiation in vitro, as assessed via clonogenic and Aldefluor assays. However, this was not a universal feature of breast CSCs, as HCC1937 CSCs identified either by ALDH activity or surface marker expression were reduced

following radiation. This observation is in agreement with similar reports describing heterogeneity within CSC subtypes to radiation. Given a single dose of 8 Gy, UM2 xenografts became enriched $CD44^+/CD24^-$ cells, whereas this population was depleted in MC1 xenografts [51]. Also, $CD24^-/ESA^+$ MDA-MB-231 cells showed higher survival following radiation than this population in MDA-MB-468 cells [3, 50]. These results indicate the presumption of CSC radioresistance may not hold true for all stem cell subtypes. Some reports have attributed radioresistance to the high levels of antioxidants present in CSCs [48]. In this way, there may be differences in the amount of antioxidants between CSCs from different cell types. However, Zielske et al found that despite a low oxidation profile in MC1 CSCs, these cells ultimately succumbed to radiation, indicating that other factors beyond antioxidant levels can account for radioresistance [51].

Radiosensitization by 17-AAG treatment was also found to vary between CSC subpopulations both within the same cell line and between cell lines. Aldefluor-positive cells from SUM149 and MDA-MB-231 cell lines were sensitized to radiation when combined with 17-AAG, albeit at very different doses. Interestingly, MDA-MB-231 $CD44^+/CD24^-/ESA^+$ cells did not appear sensitized to radiation with 17-AAG treatment. In contrast, T47D showed a dose-dependent decrease in $CD44^+/CD24^-/ESA^+$ cells with 17-AAG treatment following radiation. Several potential reasons may explain these observed differences in sensitization. First, while both Aldefluor and surface marker expression have been used to characterize CSCs in breast cancer cell lines, they may identify subpopulations which are distinct from each other. Using xenografts of primary human breast cancers, overlap between the Aldefluor-positive and $CD44^+/CD24^-/Lin^-$ cells was approximately 1% [32]. In this way, reliance on signaling pathways which

drives tumorigenicity and self-renewal may be different between these two subpopulations. Indeed, Aldefluor-positive breast cancer cells have been shown to rely on the PTEN/AKT/β-catenin network [29], whereas $CD44^+/CD24^-/Lin^-$ cells require Erbb3/PI3K/AKT/NF-kB signaling activity [52]. As discussed above, phenotypically similar CSCs from different cell types may respond differently to treatment [50, 51]. $CD44^+/CD24^-/Lin^-$ cells from MDA-MB-231 and T47D had differed in their response to 17-AAG when given radiation. This discrepancy may result from the expression level of NQO1, an enzyme necessary for the conversion of 17-AAG to its more potent intracellular form [53]. MDA-MB-231 cells have been shown to have very low levels of NQO1, whereas this enzyme is expressed in T47D cells [33, 54]. Additionally, T47D cells exhibit a lower level of induction of HSC70 and HSP72 following 17-AAG treatment, in contrast to the elevated expression seen in MDA-MB-231 cells with 17-AAG treatment [33, 55]. Thus, reduced intracellular levels of converted 17-AAG coupled with heightened expression of other heat shock proteins in response to treatment may dampen the efficacy of HSP90 inhibition in the MDA-MB-231 $CD44^+/CD24^-/Lin^-$ cells, rendering them more radioresistant compared to T47D CSCs.

Interestingly, despite observing radioresistance in the majority of cell lines tested in vitro, repeated cycles of fractionated radiation were capable of reducing the number of CSCs present in SUM149, SUM159, and MDA-MB-231 xenografts in vivo. These results appear to contradict previous reports which show that tumors treated with radiation experience enrichment of CSCs [47-49, 51]. It is important to note, however, that previous published studies often utilized only a short radiation treatment of tumors a few days prior to analysis. In the present study, consecutive fractionated doses were

given for at least two cycles (two weeks), and analysis was performed the day following the last dose of treatment, more closely mimicking dosing regimens used in patients [56]. Therefore, both the time allotted for the CSCs to potentially repopulate, and the amount of total radiation received, may provide some reasoning for these discrepancies. Cancer stem cells which are radiation resistant compared to bulk population may be able to survive single or short cycles of radiation, as has been shown [3]. However, as our study indicates, repeated cycles of radiation may be able to overcome a CSC threshold for resistance, leading to a decrease in this population. This suggests care must be taken to prevent suboptimal dosing in patients with tumors harboring radioresistant CSCs. It is also possible that enrichment of CSCs following radiation requires more time before analyzing tumor samples than was given in the study presented here. However, a recent report has shown that reprogramming of differentiated cells into a more stem-like phenotype following radiation occurs faster than the CSC doubling time [23], and so the CSC enrichment process should be detectable a short time after therapy. In addition, Zielske et al showed that two weeks after receiving a single high dose (8 Gy), MC1 CSCs decreased while UM2 CSCs were resistant and enriched for by the radiation [51]. Therefore, reduction in CSCs following radiation is less likely to be dependent on the amount of time before analysis, but rather reflects a heterogeneous response in various CSC populations following treatment.

As with the variable sensitization of CSCs to radiation with 17-AAG treatment described in vitro, CSCs in tumor xenografts also showed varied responses to HSP90 inhibition. When combined with 5 mg/kg 17-AAG, SUM149 Aldefluor-positive cells were further reduced, showing sensitization with HSP90 inhibition. In contrast,

Aldefluor-positive cells from MDA-MB-231 and SUM159 were higher in percentage following the combination therapy, suggesting sensitization of the differentiated cells rather than the CSCs. One potential explanation for this difference could be that CSCs respond differently to drug treatment depending on signals they receive from their microenvironment. Thus, in vitro responses may not accurately predict efficacy in vivo. For example, breast cancer cells display greater chemoresistance when grown in a three dimensional culture, more closely reflecting the in vivo environment [2, 43]. In this setting, cues from the microenvironment can provide added survival signals which may reduce the efficacy of 17-AAG, and thus eliminate any additive effects to radiation treatment. However, the efficacy seen in SUM149 Aldefluor-positive cells when 17-AAG is added to cycles of fractionated radiation indicates this strategy can be effective. Taken together, the effectiveness of HSP90 inhibition in sensitizing breast CSCs to radiation can be achieved in certain cell lines. While some CSC subpopulations appear sensitive to radiotherapy, care must be taken to ensure adequate levels of radiation are provided to prevent possible transient enrichment/reprogramming of resistant CSCs, which can influence recurrence and metastasis.

References

1. Cheng, L., et al., *The clinical and therapeutic implications of cancer stem cell biology.* Expert Rev Anticancer Ther, 2011. **11**(7): p. 1131-43.
2. Scadden, D.T., *The stem-cell niche as an entity of action.* Nature, 2006. **441**(7097): p. 1075-9.
3. Brunner, T.B., et al., *Cancer stem cells as a predictive factor in radiotherapy.* Semin Radiat Oncol, 2012. **22**(2): p. 151-74.
4. LaBarge, M.A., et al., *Human mammary progenitor cell fate decisions are products of interactions with combinatorial microenvironments.* Integr Biol (Camb), 2009. **1**(1): p. 70-9.
5. Neckers, L. and P. Workman, *Hsp90 molecular chaperone inhibitors: are we there yet?* Clin Cancer Res, 2012. **18**(1): p. 64-76.
6. Sauvageot, C.M., et al., *Efficacy of the HSP90 inhibitor 17-AAG in human glioma cell lines and tumorigenic glioma stem cells.* Neuro Oncol, 2009. **11**(2): p. 109-21.
7. Peng, C., et al., *Inhibition of heat shock protein 90 prolongs survival of mice with BCR-ABL-T315I-induced leukemia and suppresses leukemic stem cells.* Blood, 2007. **110**(2): p. 678-85.
8. Clarke, M., et al., *Effects of radiotherapy and of differences in the extent of surgery for early breast cancer on local recurrence and 15-year survival: an overview of the randomised trials.* Lancet, 2005. **366**(9503): p. 2087-106.
9. Darby, S., et al., *Effect of radiotherapy after breast-conserving surgery on 10-year recurrence and 15-year breast cancer death: meta-analysis of individual patient data for 10,801 women in 17 randomised trials.* Lancet, 2011. **378**(9804): p. 1707-16.
10. Schatton, T., et al., *Identification of cells initiating human melanomas.* Nature, 2008. **451**(7176): p. 345-9.
11. Eramo, A., et al., *Chemotherapy resistance of glioblastoma stem cells.* Cell Death Differ, 2006. **13**(7): p. 1238-41.
12. Fillmore, C.M. and C. Kuperwasser, *Human breast cancer cell lines contain stem-like cells that self-renew, give rise to phenotypically diverse progeny and survive chemotherapy.* Breast Cancer Res, 2008. **10**(2): p. R25.
13. Phillips, T.M., W.H. McBride, and F. Pajonk, *The response of CD24(-/low)/CD44+ breast cancer-initiating cells to radiation.* J Natl Cancer Inst, 2006. **98**(24): p. 1777-85.
14. Woodward, W.A., et al., *WNT/beta-catenin mediates radiation resistance of mouse mammary progenitor cells.* Proc Natl Acad Sci U S A, 2007. **104**(2): p. 618-23.
15. Bao, S., et al., *Glioma stem cells promote radioresistance by preferential activation of the DNA damage response.* Nature, 2006. **444**(7120): p. 756-60.
16. Chiou, S.H., et al., *Identification of CD133-positive radioresistant cells in atypical teratoid/rhabdoid tumor.* PLoS One, 2008. **3**(5): p. e2090.
17. Blazek, E.R., J.L. Foutch, and G. Maki, *Daoy medulloblastoma cells that express CD133 are radioresistant relative to CD133- cells, and the CD133+ sector is enlarged by hypoxia.* Int J Radiat Oncol Biol Phys, 2007. **67**(1): p. 1-5.

18. Chang, C.J., et al., *Enhanced radiosensitivity and radiation-induced apoptosis in glioma CD133-positive cells by knockdown of SirT1 expression.* Biochem Biophys Res Commun, 2009. **380**(2): p. 236-42.
19. Holtz, M.S., S.J. Forman, and R. Bhatia, *Nonproliferating CML CD34+ progenitors are resistant to apoptosis induced by a wide range of proapoptotic stimuli.* Leukemia, 2005. **19**(6): p. 1034-41.
20. Lu, K.H., et al., *Evaluation of radiotherapy effect in resveratrol-treated medulloblastoma cancer stem-like cells.* Childs Nerv Syst, 2009. **25**(5): p. 543-50.
21. Lomonaco, S.L., et al., *The induction of autophagy by gamma-radiation contributes to the radioresistance of glioma stem cells.* Int J Cancer, 2009. **125**(3): p. 717-22.
22. Diehn, M. and M.F. Clarke, *Cancer stem cells and radiotherapy: new insights into tumor radioresistance.* J Natl Cancer Inst, 2006. **98**(24): p. 1755-7.
23. Lagadec, C., et al., *Radiation-induced reprogramming of breast cancer cells.* Stem Cells, 2012. **30**(5): p. 833-44.
24. Yano, M., et al., *Expression of hsp90 and cyclin D1 in human breast cancer.* Cancer Lett, 1999. **137**(1): p. 45-51.
25. Pick, E., et al., *High HSP90 expression is associated with decreased survival in breast cancer.* Cancer Res, 2007. **67**(7): p. 2932-7.
26. Santagata, S., et al., *High levels of nuclear heat-shock factor 1 (HSF1) are associated with poor prognosis in breast cancer.* Proc Natl Acad Sci U S A, 2011. **108**(45): p. 18378-83.
27. Calderwood, S.K., *Elevated levels of HSF1 indicate a poor prognosis in breast cancer.* Future Oncol, 2012. **8**(4): p. 399-401.
28. Korkaya, H., et al., *HER2 regulates the mammary stem/progenitor cell population driving tumorigenesis and invasion.* Oncogene, 2008. **27**(47): p. 6120-30.
29. Korkaya, H., et al., *Regulation of mammary stem/progenitor cells by PTEN/Akt/beta-catenin signaling.* PLoS Biol, 2009. **7**(6): p. e1000121.
30. Wei, D., et al., *Radiosensitization of human pancreatic cancer cells by MLN4924, an investigational NEDD8-activating enzyme inhibitor.* Cancer Res, 2012. **72**(1): p. 282-93.
31. Morgan, M.A., et al., *Mechanism of radiosensitization by the Chk1/2 inhibitor AZD7762 involves abrogation of the G2 checkpoint and inhibition of homologous recombinational DNA repair.* Cancer Res, 2010. **70**(12): p. 4972-81.
32. Ginestier, C., et al., *ALDH1 is a marker of normal and malignant human mammary stem cells and a predictor of poor clinical outcome.* Cell Stem Cell, 2007. **1**(5): p. 555-67.
33. Zajac, M., et al., *Molecular signature of response and potential pathways related to resistance to the HSP90 inhibitor, 17AAG, in breast cancer.* BMC Med Genomics, 2010. **3**: p. 44.
34. Al-Hajj, M., et al., *Prospective identification of tumorigenic breast cancer cells.* Proc Natl Acad Sci U S A, 2003. **100**(7): p. 3983-8.
35. Armstrong, L., et al., *Phenotypic characterization of murine primitive hematopoietic progenitor cells isolated on basis of aldehyde dehydrogenase activity.* Stem Cells, 2004. **22**(7): p. 1142-51.

36. Hess, D.A., et al., *Functional characterization of highly purified human hematopoietic repopulating cells isolated according to aldehyde dehydrogenase activity.* Blood, 2004. **104**(6): p. 1648-55.
37. Corti, S., et al., *Identification of a primitive brain-derived neural stem cell population based on aldehyde dehydrogenase activity.* Stem Cells, 2006. **24**(4): p. 975-85.
38. Clay, M.R., et al., *Single-marker identification of head and neck squamous cell carcinoma cancer stem cells with aldehyde dehydrogenase.* Head Neck, 2010. **32**(9): p. 1195-201.
39. Kim, M.P., et al., *ALDH activity selectively defines an enhanced tumor-initiating cell population relative to CD133 expression in human pancreatic adenocarcinoma.* PLoS One, 2011. **6**(6): p. e20636.
40. Silva, I.A., et al., *Aldehyde dehydrogenase in combination with CD133 defines angiogenic ovarian cancer stem cells that portend poor patient survival.* Cancer Res, 2011. **71**(11): p. 3991-4001.
41. Pajonk, F., E. Vlashi, and W.H. McBride, *Radiation resistance of cancer stem cells: the 4 R's of radiobiology revisited.* Stem Cells, 2010. **28**(4): p. 639-48.
42. Lagadec, C., et al., *Survival and self-renewing capacity of breast cancer initiating cells during fractionated radiation treatment.* Breast Cancer Res, 2010. **12**(1): p. R13.
43. Tredan, O., et al., *Drug resistance and the solid tumor microenvironment.* J Natl Cancer Inst, 2007. **99**(19): p. 1441-54.
44. Aoudjit, F. and K. Vuori, *Integrin signaling in cancer cell survival and chemoresistance.* Chemother Res Pract, 2012. **2012**: p. 283181.
45. Cordes, N., et al., *Fibronectin and laminin increase resistance to ionizing radiation and the cytotoxic drug Ukrain in human tumour and normal cells in vitro.* Int J Radiat Biol, 2003. **79**(9): p. 709-20.
46. Liu, S. and M.S. Wicha, *Targeting breast cancer stem cells.* J Clin Oncol, 2010. **28**(25): p. 4006-12.
47. Atkinson, R.L., et al., *Thermal enhancement with optically activated gold nanoshells sensitizes breast cancer stem cells to radiation therapy.* Sci Transl Med, 2010. **2**(55): p. 55ra79.
48. Diehn, M., et al., *Association of reactive oxygen species levels and radioresistance in cancer stem cells.* Nature, 2009. **458**(7239): p. 780-3.
49. Zhang, M., R.L. Atkinson, and J.M. Rosen, *Selective targeting of radiation-resistant tumor-initiating cells.* Proc Natl Acad Sci U S A, 2010. **107**(8): p. 3522-7.
50. Al-Assar, O., et al., *Radiation response of cancer stem-like cells from established human cell lines after sorting for surface markers.* Int J Radiat Oncol Biol Phys, 2009. **75**(4): p. 1216-25.
51. Zielske, S.P., et al., *Ablation of breast cancer stem cells with radiation.* Transl Oncol, 2011. **4**(4): p. 227-33.
52. Hinohara, K., et al., *ErbB receptor tyrosine kinase/NF-kappaB signaling controls mammosphere formation in human breast cancer.* Proc Natl Acad Sci U S A, 2012. **109**(17): p. 6584-9.

53. Guo, W., et al., *Formation of 17-allylamino-demethoxygeldanamycin (17-AAG) hydroquinone by NAD(P)H:quinone oxidoreductase 1: role of 17-AAG hydroquinone in heat shock protein 90 inhibition.* Cancer Res, 2005. **65**(21): p. 10006-15.
54. Han, Y., et al., *NAD(P)H:quinone oxidoreductase-1-dependent and -independent cytotoxicity of potent quinone Cdc25 phosphatase inhibitors.* J Pharmacol Exp Ther, 2004. **309**(1): p. 64-70.
55. Powers, M.V., P.A. Clarke, and P. Workman, *Dual targeting of HSC70 and HSP72 inhibits HSP90 function and induces tumor-specific apoptosis.* Cancer Cell, 2008. **14**(3): p. 250-62.
56. *NIH consensus conference. Treatment of early-stage breast cancer.* JAMA, 1991. **265**(3): p. 391-5.

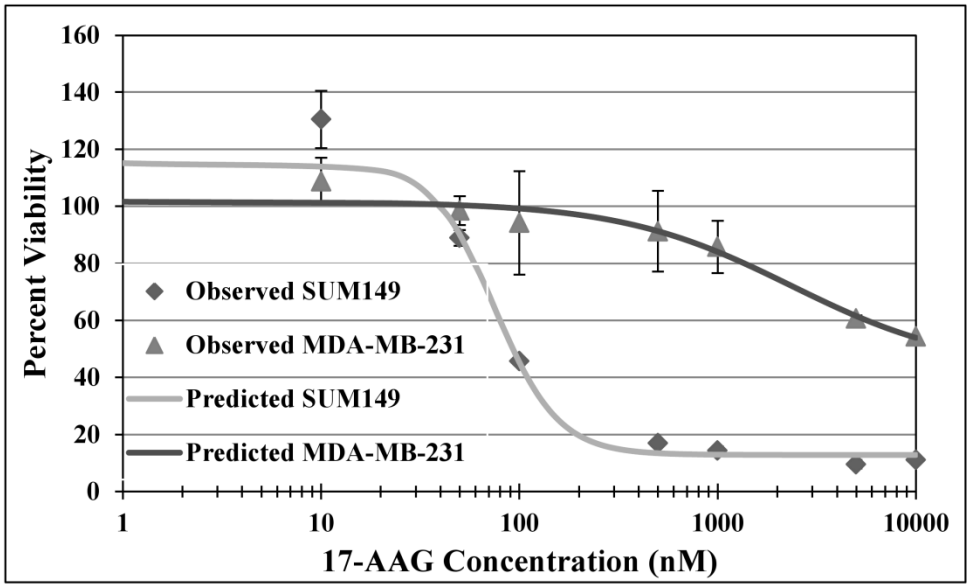

Figure 4.1 17-AAG Decreases Viability in Breast Cancer Cell Lines. Both SUM149 and MDA-MB-231 breast cancer cell lines were seeded into 96-well plates and treated with increasing concentrations of 17-AAG for 3 days. After this treatment period, cells were tested using the MTS assay. SUM149 cells were dramatically more sensitive to 17-AAG-mediated HSP90 inhibition than MDA-MB-231 cells.

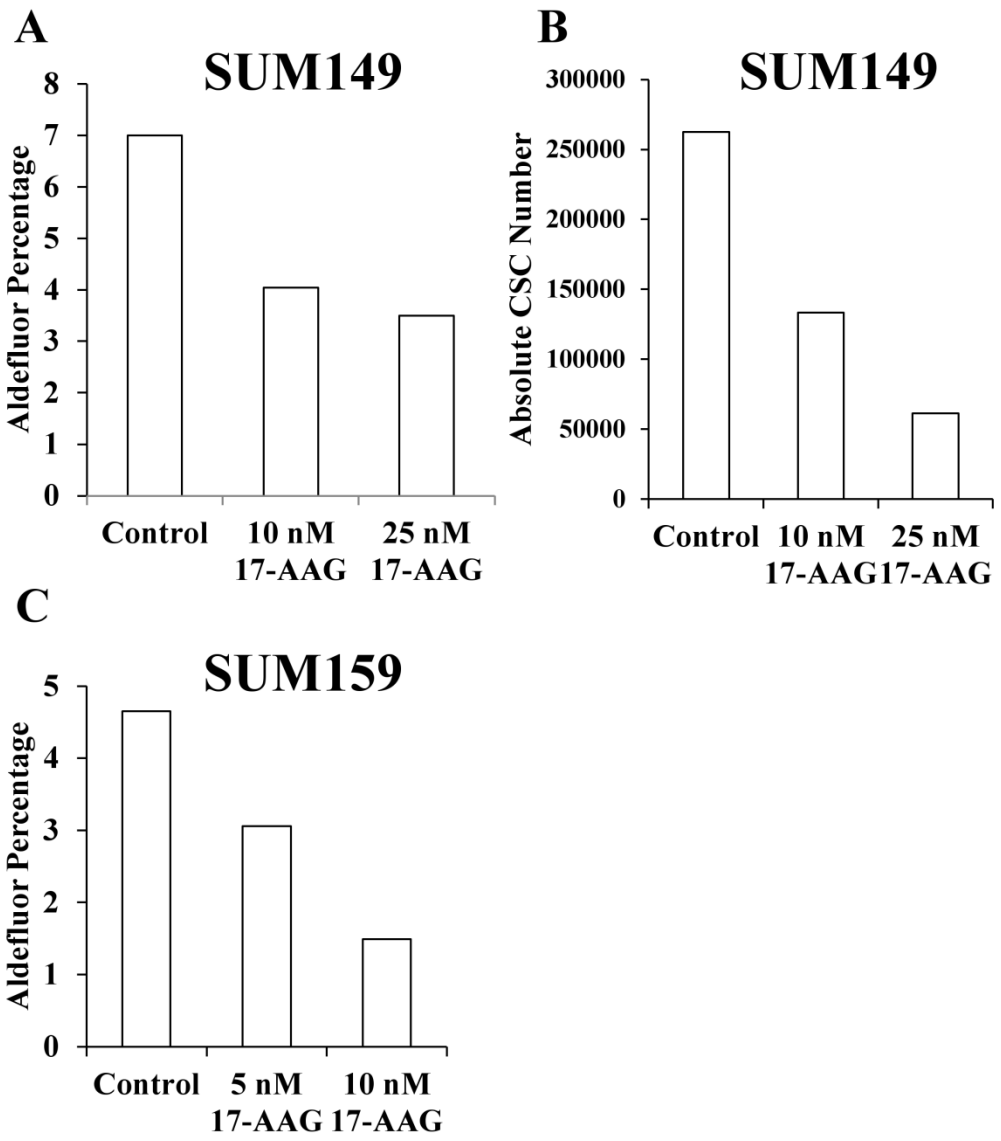

Figure 4.2 Breast CSCs are Eliminated Following 17-AAG Treatment. To validate that 17-AAG treatment can effectively eliminate breast CSCs, we treated breast cancer cells from the SUM149 and SUM159 cell lines with 17-AAG for three days before analyzing for changes in Aldefluor expression. (A and B) SUM149 Aldefluor-positive cells were reduced with 17-AAG, with higher concentrations also affecting the non-CSCs, as indicated by the less dramatic decrease in the percentage of Aldefluor-positive cells (A) compared to the decrease in absolute number (B). (C) SUM159 Aldefluor-positive cells were similarly reduced with 17-AAG. In contrast to SUM149, treatment with low concentrations of 17-AAG primarily effected the CSC population.

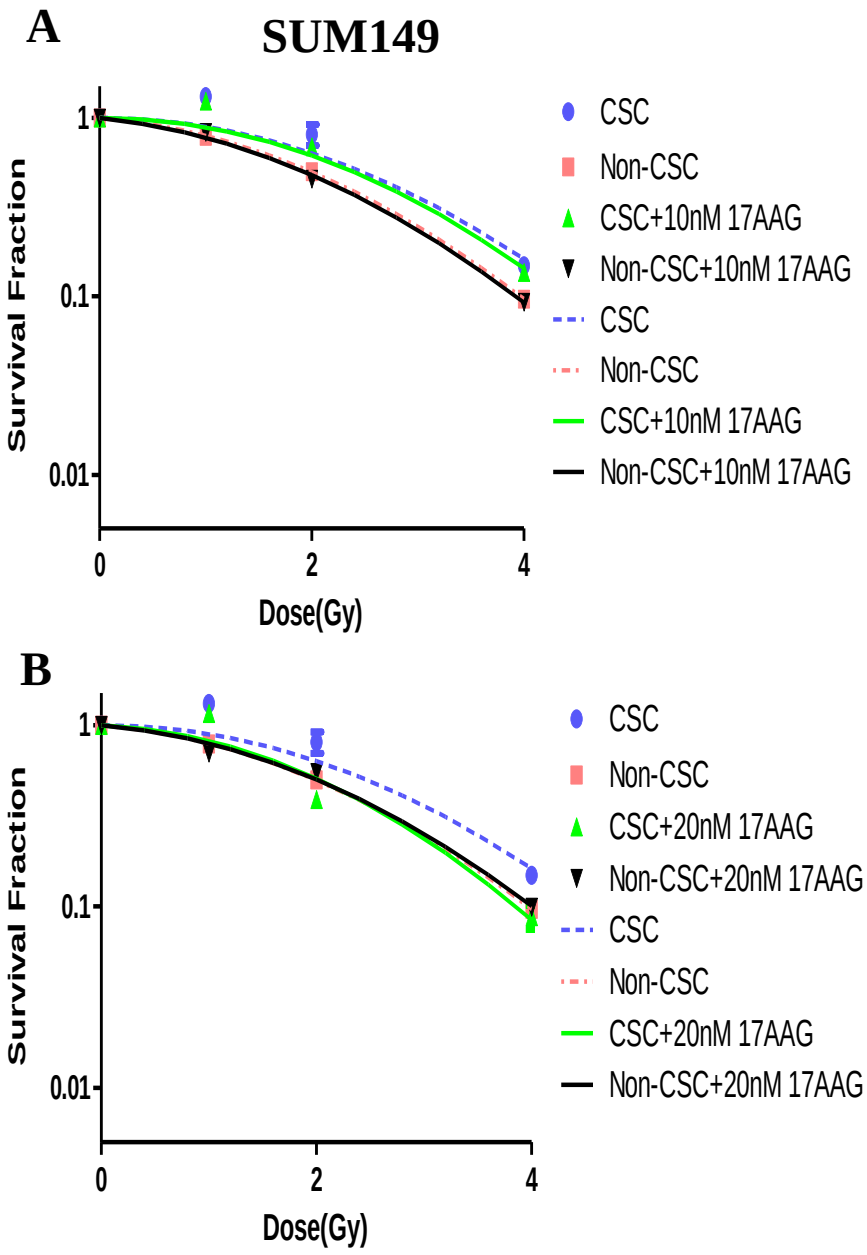

Figure 4.3 Breast CSCs are Sensitized to Radiation Following 17-AAG Treatment. To determine if 17-AAG could sensitize breast CSCs to radiation, SUM149 Aldefluor-positive and –negative cells were sorted by FACS to obtain pure populations, and both populations were treated with 17-AAG or vehicle before exposure to a single dose of radiation, as indicated in (A and B). CSCs exhibited higher survival following radiation compared to non-CSCs. This radioresistance was eliminated with a 20 nM 17-AAG pre-treatment (B), demonstrating sensitization of CSCs to radiation.

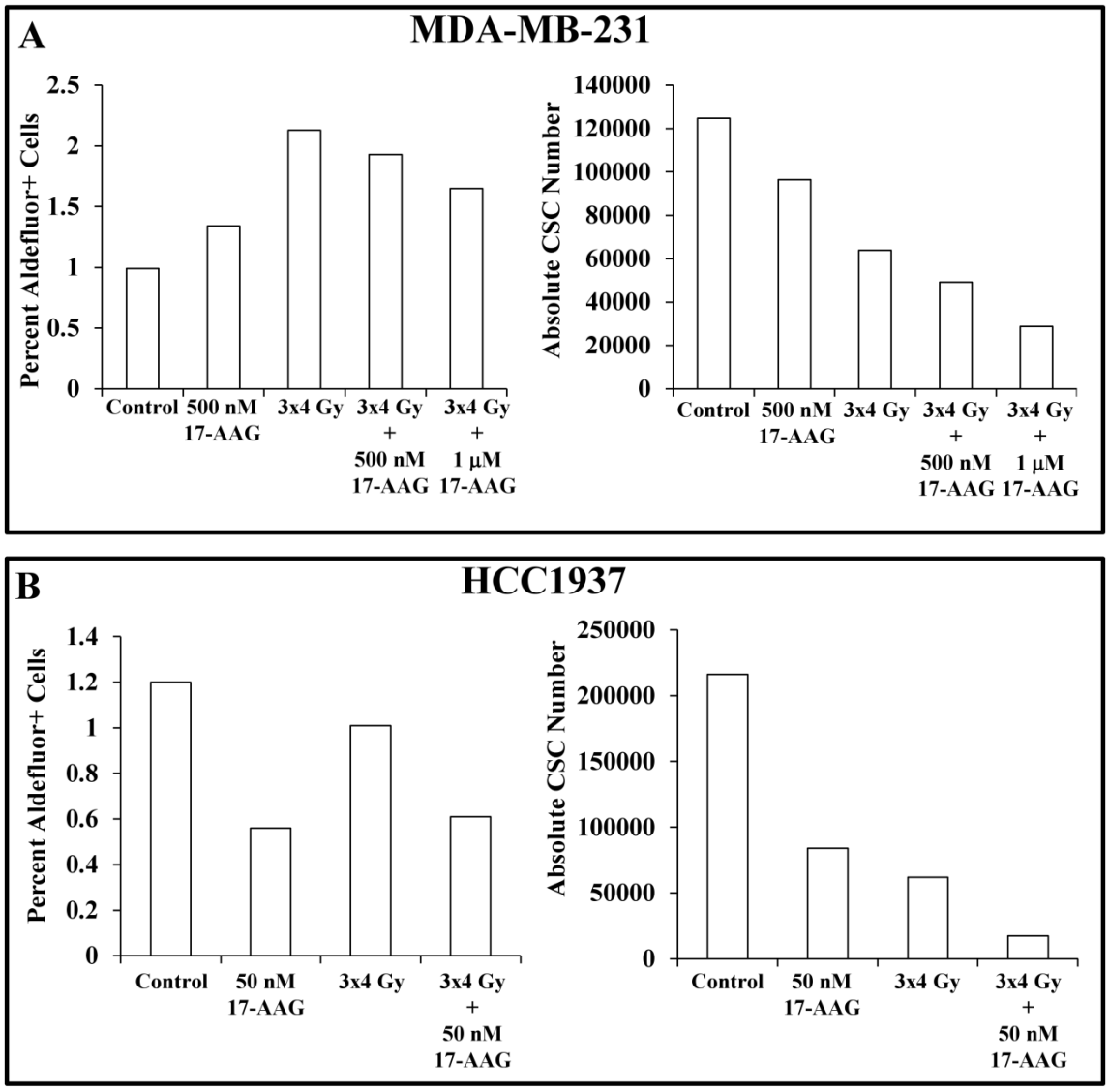

Figure 4.4 MDA-MB-231 and HCC1937 Aldefluor-positive Cells are Sensitized to Radiation via 17-AAG Treatment. In order to determine if 17-AAG can sensitize breast CSCs from other cell lines, MDA-MB-231 (A) and HCC1937 (B) cancer cells were pre-treated with 17-AAG before each exposure to radiation. Fractionated doses of radiation (4 Gy) were given to each cell line for 3 consecutive days. On the sixth day following the initial dose of radiation, cells were analyzed for changes in their Aldefluor expression. 17-AAG treatment was capable of sensitizing the Aldefluor-positive cells from both cell lines to radiation.

Figure 4.5 Radioresistance and Sensitization with 17-AAG is also Dependent on CSC Phenotype. To determine if differences in radioresistance also existed between CSC phenotypes within and between breast cancer cell lines, cells were given pre-treatment with 17-AAG or vehicle before each fractionated dose of radiation. MDA-MB-231 and HCC1937 cells were given 3 consecutive doses of 4 Gy, whereas T47D was given 3 consecutive doses of either 3 Gy or 5 Gy radiation. Cells were analyzed for changes in the number of $CD44^+/CD24^-/ESA^+$ expressing cells on the sixth day following initial treatment. (A) In contrast to MDA-MB-231 Aldefluor-positive cells, the $CD44^+/CD24^-/ESA^+$ population was not sensitized to radiation following pre-treatment with 17-AAG. HCC1937 $CD44^+/CD24^-/ESA^+$ cells were even more sensitive to radiation than the Aldefluor-positive population (B). While $CD44^+/CD24^-/ESA^+$ cells from the MDA-MB-231 cell line were unaffected by 17-AAG pre-treatment, T47D $CD44^+/CD24^-/ESA^+$ cells were sensitized to radiation when combined with 17-AAG. This suggests that radioresistance and 17-AAG sensitization are dependent on both the cell type and the particular CSC phenotype.

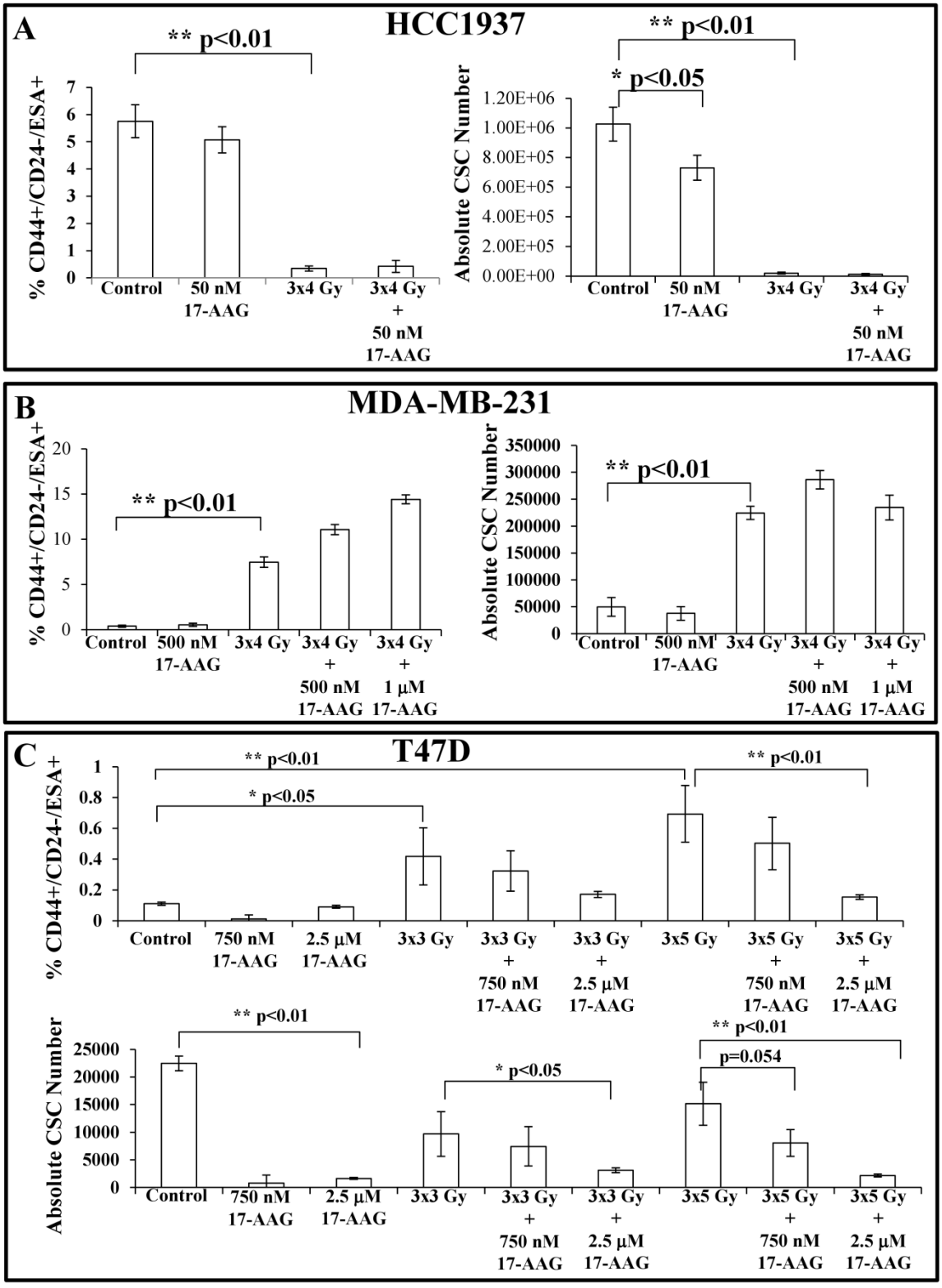
A
HCC1937
** p<0.01
% CD44+/CD24-/ESA+
Control
50 nM 17-AAG
3x4 Gy
3x4 Gy + 50 nM 17-AAG
** p<0.01
* p<0.05
Absolute CSC Number
B
MDA-MB-231
** p<0.01
500 nM 17-AAG
1 µM 17-AAG
C
T47D
* p<0.05
750 nM 17-AAG
2.5 µM 17-AAG
3x3 Gy
3x5 Gy
p=0.054

Figure 4.6 Breast CSCs are Sensitized to Radiation via 17-AAG Treatment. (A) Tumor xenografts of SUM149 cells in NOD/SCID mammary fat pads were treated with cycles of 5 mg/kg 17-AAG with or without 2 Gy radiation. Days when mice were given 17-AAG or 2 Gy radiation are indicated by the red and black brackets, respectively. At a dose of 5 mg/kg, 17-AAG modestly disrupted tumor growth, whereas both radiation and the combination therapy strongly impaired growth. At the end point, all treatments resulted in tumor sizes that were statistically different than the controls (**$p<0.01$). (B and C) Despite radioresistance and sensitivity of SUM149 cells to 17-AAG in vitro, Aldefluor analysis of the tumor samples showed that the CSCs were as sensitive to either radiation alone or 17-AAG alone as the tumor bulk. However, combining 17-AAG with radiation significantly reduced the Aldefluor-positive population. (D) Five hundred cells from previously treated tumors were implanted into secondary NOD/SCID mice to observe changes in tumor initiation following therapy. Only tumors treated with radiation or the combination treatment displayed modest inhibition of tumorigenicity, suggesting higher doses of 17-AAG than used in our study are required for improving the efficacy of 17-AAG/radiation combination strategy.

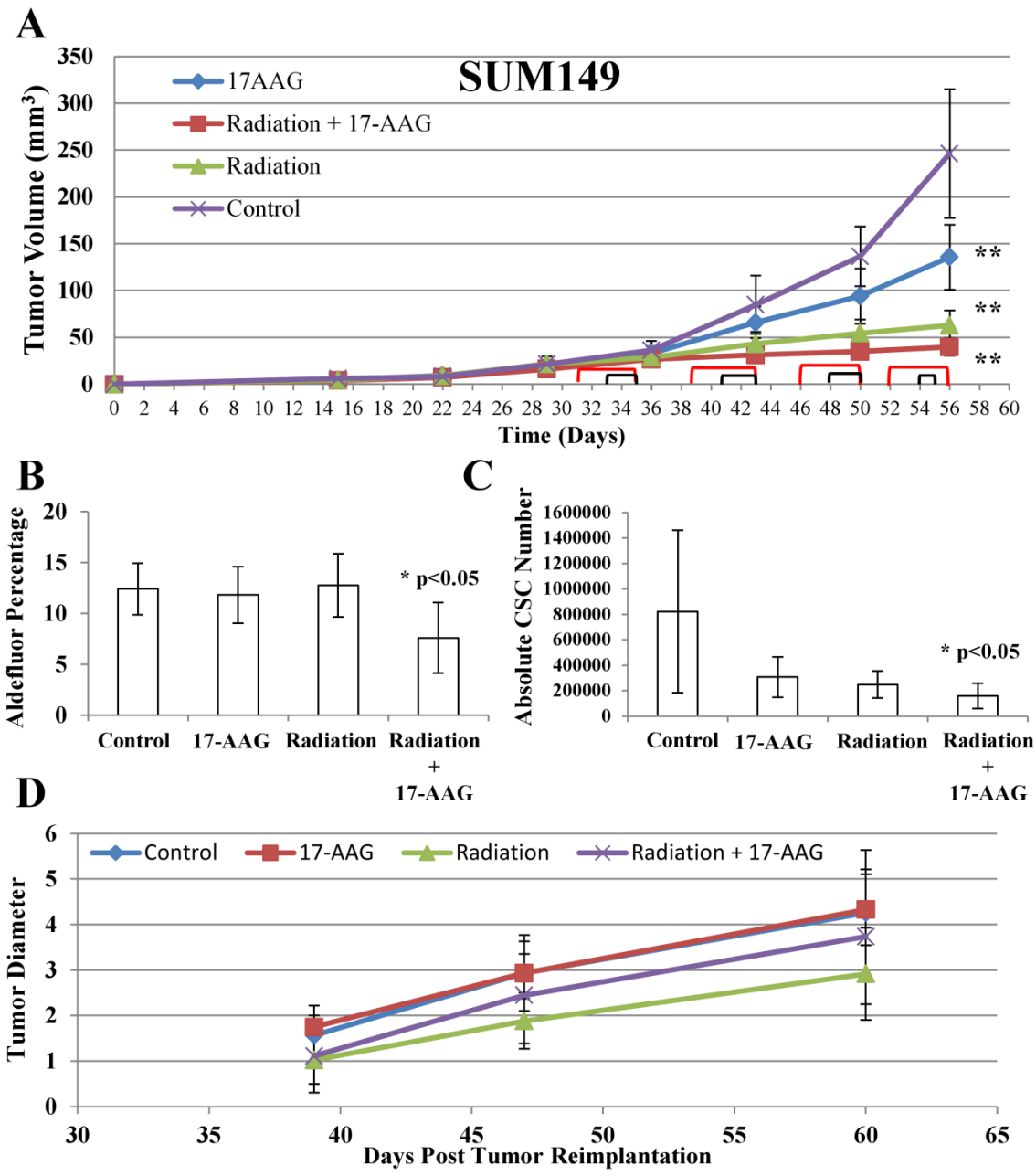
A
SUM149
17AAG
Radiation + 17-AAG
Radiation
Control
Tumor Volume (mm³)
Time (Days)
**
**
**
B
Aldefluor Percentage
* p<0.05
Control
17-AAG
Radiation
Radiation + 17-AAG
C
Absolute CSC Number
* p<0.05
Control
17-AAG
Radiation
Radiation + 17-AAG
D
Control
17-AAG
Radiation
Radiation + 17-AAG
Tumor Diameter
Days Post Tumor Reimplantation

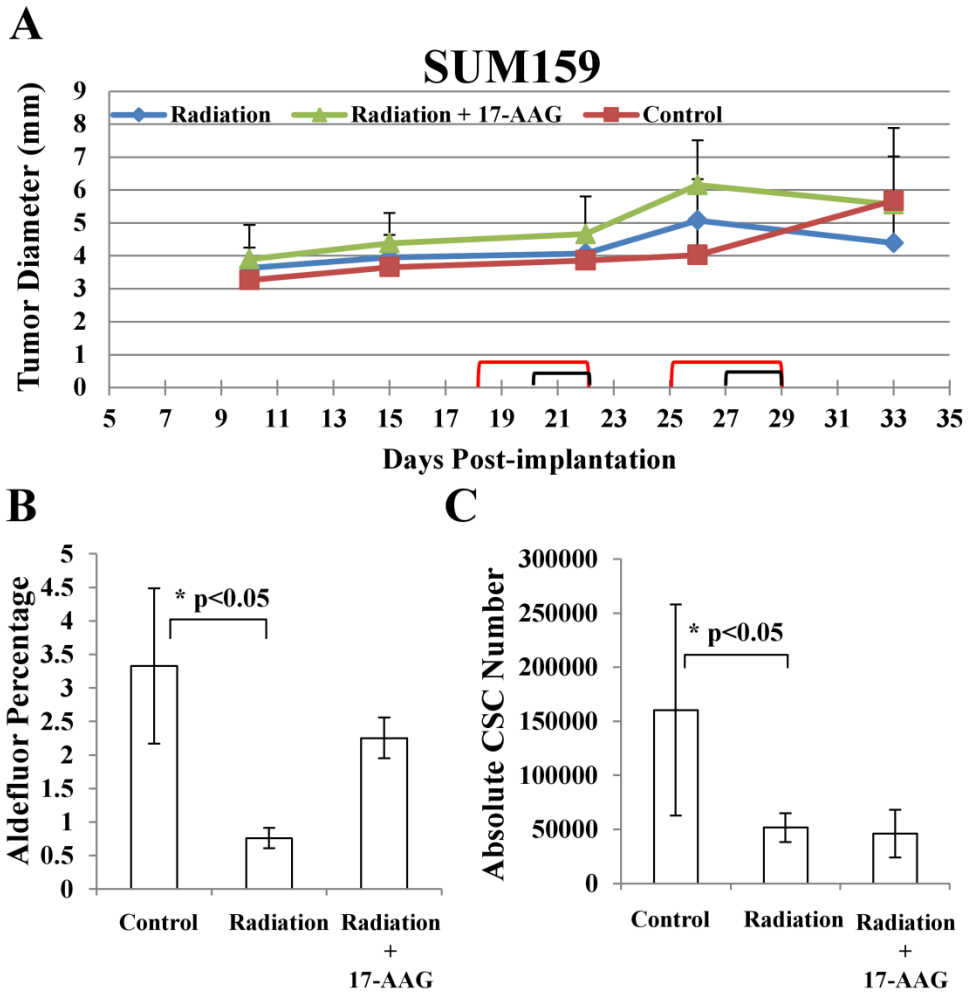

Figure 4.7 Efficacy of Radiation and 17-AAG Treatment in SUM159 Tumor Xenografts. SUM159 xenografts were treated with radiation (2 Gy) and 17-AAG (5 mg/kg) as done before. Days where mice were given 17-AAG or 2 Gy radiation are indicated by the red and black brackets, respectively. (A) Two cycles of treatment resulted in only modest reduction in tumor growth. (B and C) Radiation treatment significantly reduced the number of SUM159 Aldefluor-positive cells. Interestingly, 17-AAG treatment appeared to sensitize non-CSCs more than the CSCs, as shown by the increased percentage of Aldefluor-positive cells following the combination therapy.

Figure 4.8 MDA-MB-231 Xenograft Treatment with 17-AAG and Radiation. (A) MDA-MB-231 tumor xenografts were treated with radiation (2 Gy) and 17-AAG (5 mg/kg). Days where mice were given 17-AAG or 2 Gy radiation are indicated by the red and black brackets, respectively. 17-AAG treatment alone did not appear to influence tumor growth. MDA-MB-231 tumors treated with radiation or the combination strategy showed a significant reduction in tumor volume compared to control (**$p<0.01$). (B and C) Similar to SUM159, MDA-MB-231 Aldefluor-positive cells were reduced with radiation treatment, despite showing resistance in vitro. In addition, 17-AAG treatment appeared to sensitize the differentiated cells rather than the CSCs. (D) To determine if the radioresistant CSC are defined by $CD44^+/CD24^-/ESA^+$ expression rather than Aldefluor positivity, MDA-MB-231 tumor cells were stained for these markers for FACS. $CD44^+/CD24^-/ESA^+$ MDA-MB-231 cells were reduced following radiation, 17-AAG and the combination treatment. However, there was no significant difference between the treatment groups.

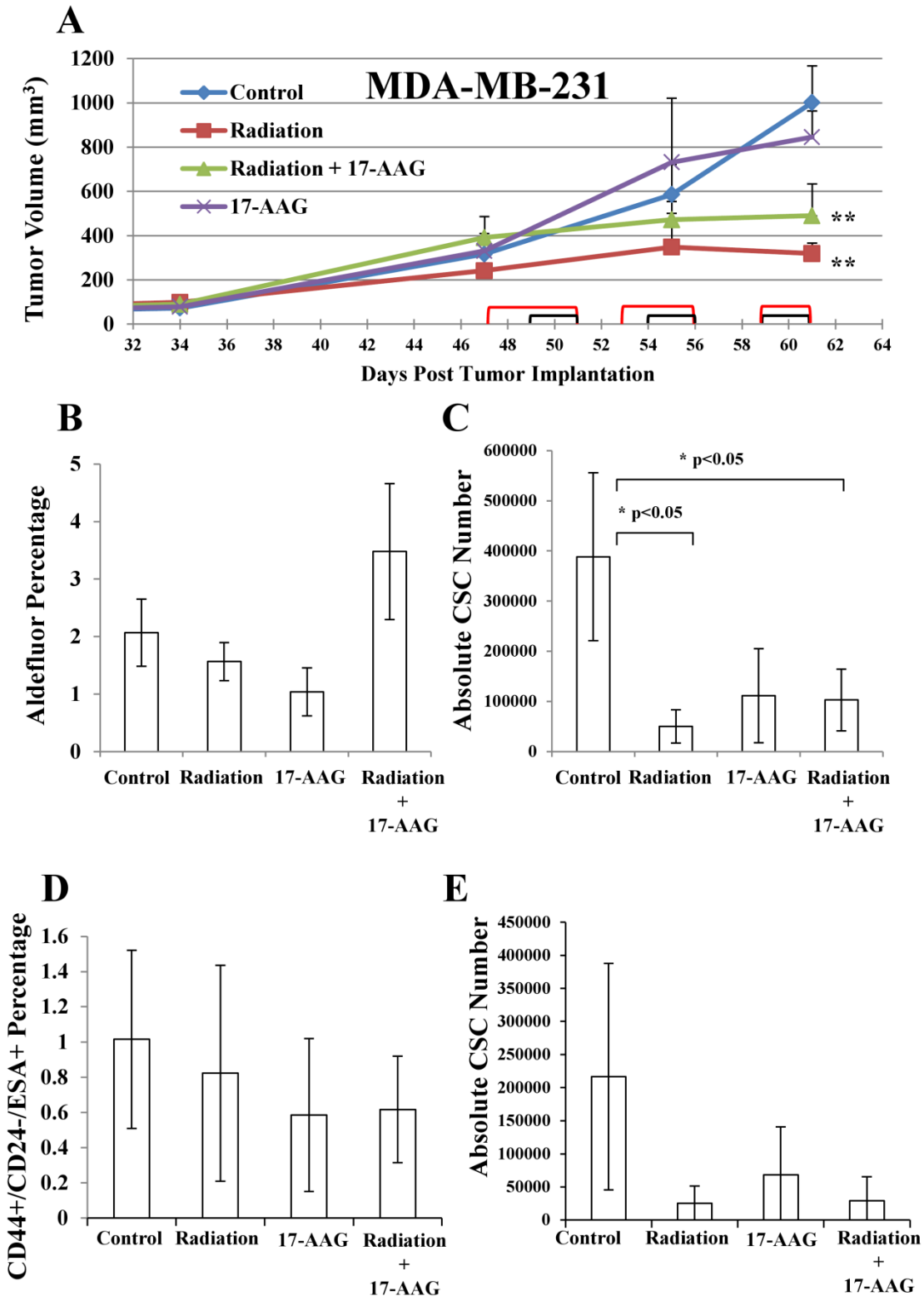
A
MDA-MB-231
Control
Radiation
Radiation + 17-AAG
17-AAG
Tumor Volume (mm³)
Days Post Tumor Implantation
**
**
B
Aldefluor Percentage
Control
Radiation
17-AAG
Radiation + 17-AAG
C
Absolute CSC Number
* p<0.05
* p<0.05
Control
Radiation
17-AAG
Radiation + 17-AAG
D
CD44+/CD24-/ESA+ Percentage
Control
Radiation
17-AAG
Radiation + 17-AAG
E
Absolute CSC Number
Control
Radiation
17-AAG
Radiation + 17-AAG

Chapter 5

Summary

Lacking effective treatments which can both reduce tumor burden and extend overall survival, patients diagnosed with peripheral T-cell lymphoma (PTCL) often have a poor prognosis [1, 2]. Over the past decade, research investigating the cancer stem cell (CSC) hypothesis has identified tumorigenic subpopulations in many hematological and solid tumors [3-10]. Postulated to originate from aberrantly activated pathways controlling self-renewal, CSCs have been implicated in a number of unsolved problems in cancer treatment. Having a greater propensity to survive many forms of conventional therapy, residual CSCs are believed to contribute to both local recurrence as well as facilitating metastasis [11, 12]. Because recurrence and metastasis impact the length of overall survival in patients, identifying CSC-targeting agents for PTCL treatment may provide a way to improve these patients prognosis. While inhibitors to CSC have been developed which target self-renewal pathways, redundancy in these signaling networks, along with additional cues from the microenvironment, may limit this approach [11, 13-15]. Therefore, HSP90 inhibition was examined as a potential strategy to target CSCs, as it can inhibit signaling pathways simultaneously. Several of the HSP90 clients have been shown to facilitate self-renewal signaling (Her2, AKT, and Hif1α) [16-19].

Utilizing our TGB mouse lymphoma cells as a model for PTCL, we found that the CSC population (c-Kit$^+$Sca1$^+$ cells) was selectively sensitive to 17-AAG mediated HSP90 inhibition. Doses as low as 10 nM were capable of reducing the number of CSCs

through apoptosis and also inhibited the self-renewal capacity of these cells. Cancer stem cells from acute myeloid leukemia (AML) were also found to be selectively sensitive to 17-AAG treatment. The effectiveness of our strategy was demonstrated to rely on the ablation of Hif1α function, an HSP90 client protein, which was previously shown to be necessary for maintenance of CSC subpopulations in TGB lymphoma and AML [20]. While the differentiated lymphoma cells from the TGB mouse model rely on sustained AKT/GSK-3β/β-catenin signaling, HSP90 inhibition was overall less effective in these cells, despite AKT being a HSP90 client. Interestingly, it was found that the non-CSCs contained elevated levels of chaperone proteins, as well as the HSF1 transcription factor, which can directly regulate chaperone expression. Knockdown of HSF1 in CSCs eliminated their ability to form colonies, further demonstrating the necessity of HSP90/ Hif1α function in CSC maintenance. The overexpression of HSF1 also induced resistance of the non-CSCs to 17-AAG, as shown by the sensitization of other human T-cell lymphomas to 17-AAG following HSF1 knockdown. This is in agreement with other reports which found HSF1 decreased the efficacy of HSP90 inhibition by inducing chaperone transcription (i.e. HSP70) [21, 22]. These results validate the hypothesis that 17-AAG is an effective CSC-targeting agent, and identified HSF1 expression as a potential prognostic indicator for efficacy of HSP90 inhibition.

Having shown efficacy with 17-AAG against mouse lymphoma and AML CSCs, we next examined the utility of this strategy in a solid tumor setting. Breast CSCs have been shown to be resistant to radiation, and have been suggested as the cause for local recurrence following adjuvant radiation treatment [14, 23-25]. In the studies presented in Chapter 4, it was demonstrated that low doses of 17-AAG were capable of reducing

breast CSCs similar to lymphoma and AML CSCs. Using both Aldehyde dehydrogenase and $CD44^+/CD24^-/ESA^+$ expression as identifiers for breast CSCs, 17-AAG was found to sensitize both Aldefluor-positive (SUM149, HCC1937, and MDA-MB-231) and $CD44^+/CD24^-/ESA^+$ (T47D) cells to radiation in vitro. Resistance to radiation was not a universal feature of all CSCs, as demonstrated by the loss of both Aldefluor and $CD44^+/CD24^-/ESA^+$ HCC1937 cells following fractionated radiation. In addition, 17-AAG failed to sensitize MDA-MB-231 $CD44^+/CD24^-/ESA^+$ cells to radiation. These results corroborate other studies that suggest CSCs both within and between cell lines are heterogeneous, and thus may display differential responses to conventional therapies [26, 27]. Most strikingly, despite showing resistance to radiation in certain cell lines, CSCs in vivo failed to demonstrate radioresistance. Only when radiation was combined with 17-AAG treatment was there a significant decrease in CSC number. However, the combination strategy was not significantly different from either treatment given alone. SUM159 and MDA-MB-231 Aldefluor-positive cells also failed to show any additive reduction in their population following the combination strategy. While our study provide limited evidence to suggest 17-AAG can be used as a radiosensitizer for CSCs, the differential responses to either radiation or efficacy with HSP90 inhibition highlights the current limitations in our understanding of CSC biology. While functional assays can show similar characteristics for phenotypically different CSCs within a given cell line, signaling pathway regulation and therapeutic resistance are likely to vary between the two subpopulations, which may reflect contradictory reports in the literature. These differences likely contributed to the heterogeneity in response to stressors such as radiation and HSP90 inhibition. In terms of clinical implications, our in vivo data

suggests that enrichment of CSCs likely results from insufficient dosing with radiation of the tumor, as repeated cycles of treatment were capable of reducing these tumorigenic cells. While still susceptible to radiation over the long term, CSC radiosensitizers are also likely needed, as transient enrichment (or generation from reprogramming) of CSCs may still increase the likelihood of metastatic spread during the start of therapy.

Along with other reported studies [18, 28], our data further solidifies 17-AAG-mediated HSP90 inhibition as a viable strategy for targeting CSC populations. While numerous clinical trials have shown failures with 17-AAG [29-33], the criteria for successfully demonstrating patient response was not suited for identifying CSC inhibition. Indeed, in terms of solid tumors, use of the RECIST criteria is primarily focused on percentage of tumor reduction; a feature not likely influenced by CSC-targeting agents [34]. In addition, our results showed that CSCs were typically sensitive to 17-AAG at low concentrations, suggesting that 17-AAG treatment could be given at doses much lower than those which have been previously associated with serious toxicity [35]. The clinical trials that have shown some success with 17-AAG were those which combined the agent with conventional therapy [36, 37]. The success of these trials highlights potential criteria that yield the greatest efficacy from HSP90 inhibition [35, 38]. First, tumor cell survival must be critically reliant on a signaling pathway that is facilitated by a HSP90 client protein. Secondly, the client protein(s) must be substantially reliant on solely HSP90, whose function cannot be substituted with other chaperones. The self-renewal process for CSCs is critical for their maintenance and survival, thus explaining the potency of inhibitors for this process. Because of this, we feel that use of 17-AAG as a CSC-targeting agent may be a superior approach in place of

using this drug as a manner to solely reduce tumor size. In addition, verification of an HSF1-mediated resistance mechanism may provide for development of a screening method to identifying potentially resistant tumor types. The work here provides clear results validating the efficacy of a 17-AAG mediated CSC therapy, and builds a case for the clinical reevaluation of 17-AAG treatment in combination with conventional therapy.

References

1. Reiser, M., et al., *T-cell non-Hodgkin's lymphoma in adults: clinicopathological characteristics, response to treatment and prognostic factors.* Leuk Lymphoma, 2002. **43**(4): p. 805-11.
2. Evens, A.M. and R.B. Gartenhaus, *Treatment of T-cell non-Hodgkin's lymphoma.* Curr Treat Options Oncol, 2004. **5**(4): p. 289-303.
3. Holyoake, T., et al., *Isolation of a highly quiescent subpopulation of primitive leukemic cells in chronic myeloid leukemia.* Blood, 1999. **94**(6): p. 2056-64.
4. George, A.A., et al., *Detection of leukemic cells in the CD34(+)CD38(-) bone marrow progenitor population in children with acute lymphoblastic leukemia.* Blood, 2001. **97**(12): p. 3925-30.
5. Matsui, W., et al., *Characterization of clonogenic multiple myeloma cells.* Blood, 2004. **103**(6): p. 2332-6.
6. Al-Hajj, M., et al., *Prospective identification of tumorigenic breast cancer cells.* Proc Natl Acad Sci U S A, 2003. **100**(7): p. 3983-8.
7. Singh, S.K., et al., *Identification of a cancer stem cell in human brain tumors.* Cancer Res, 2003. **63**(18): p. 5821-8.
8. Singh, S.K., et al., *Identification of human brain tumour initiating cells.* Nature, 2004. **432**(7015): p. 396-401.
9. Stingl, J., et al., *Purification and unique properties of mammary epithelial stem cells.* Nature, 2006. **439**(7079): p. 993-7.
10. Collins, A.T., et al., *Prospective identification of tumorigenic prostate cancer stem cells.* Cancer Res, 2005. **65**(23): p. 10946-51.
11. Cheng, L., et al., *The clinical and therapeutic implications of cancer stem cell biology.* Expert Rev Anticancer Ther, 2011. **11**(7): p. 1131-43.
12. Wicha, M.S., *Cancer stem cells and metastasis: lethal seeds.* Clin Cancer Res, 2006. **12**(19): p. 5606-7.
13. Scadden, D.T., *The stem-cell niche as an entity of action.* Nature, 2006. **441**(7097): p. 1075-9.
14. Brunner, T.B., et al., *Cancer stem cells as a predictive factor in radiotherapy.* Semin Radiat Oncol, 2012. **22**(2): p. 151-74.
15. LaBarge, M.A., et al., *Human mammary progenitor cell fate decisions are products of interactions with combinatorial microenvironments.* Integr Biol (Camb), 2009. **1**(1): p. 70-9.
16. Korkaya, H., et al., *HER2 regulates the mammary stem/progenitor cell population driving tumorigenesis and invasion.* Oncogene, 2008. **27**(47): p. 6120-30.
17. Korkaya, H., et al., *Regulation of mammary stem/progenitor cells by PTEN/Akt/beta-catenin signaling.* PLoS Biol, 2009. **7**(6): p. e1000121.
18. Sauvageot, C.M., et al., *Efficacy of the HSP90 inhibitor 17-AAG in human glioma cell lines and tumorigenic glioma stem cells.* Neuro Oncol, 2009. **11**(2): p. 109-21.
19. Gallia, G.L., et al., *Inhibition of Akt inhibits growth of glioblastoma and glioblastoma stem-like cells.* Mol Cancer Ther, 2009. **8**(2): p. 386-93.
20. Wang, Y., et al., *Targeting HIF1alpha eliminates cancer stem cells in hematological malignancies.* Cell Stem Cell, 2011. **8**(4): p. 399-411.

21. Bagatell, R., et al., *Induction of a heat shock factor 1-dependent stress response alters the cytotoxic activity of hsp90-binding agents.* Clin Cancer Res, 2000. **6**(8): p. 3312-8.
22. Powers, M.V. and P. Workman, *Inhibitors of the heat shock response: biology and pharmacology.* FEBS Lett, 2007. **581**(19): p. 3758-69.
23. Atkinson, R.L., et al., *Thermal enhancement with optically activated gold nanoshells sensitizes breast cancer stem cells to radiation therapy.* Sci Transl Med, 2010. **2**(55): p. 55ra79.
24. Diehn, M., et al., *Association of reactive oxygen species levels and radioresistance in cancer stem cells.* Nature, 2009. **458**(7239): p. 780-3.
25. Zhang, M., R.L. Atkinson, and J.M. Rosen, *Selective targeting of radiation-resistant tumor-initiating cells.* Proc Natl Acad Sci U S A, 2010. **107**(8): p. 3522-7.
26. Zielske, S.P., et al., *Ablation of breast cancer stem cells with radiation.* Transl Oncol, 2011. **4**(4): p. 227-33.
27. Al-Assar, O., et al., *Radiation response of cancer stem-like cells from established human cell lines after sorting for surface markers.* Int J Radiat Oncol Biol Phys, 2009. **75**(4): p. 1216-25.
28. Peng, C., et al., *Inhibition of heat shock protein 90 prolongs survival of mice with BCR-ABL-T315I-induced leukemia and suppresses leukemic stem cells.* Blood, 2007. **110**(2): p. 678-85.
29. Bagatell, R., et al., *Phase I pharmacokinetic and pharmacodynamic study of 17-N-allylamino-17-demethoxygeldanamycin in pediatric patients with recurrent or refractory solid tumors: a pediatric oncology experimental therapeutics investigators consortium study.* Clin Cancer Res, 2007. **13**(6): p. 1783-8.
30. Weigel, B.J., et al., *A phase I study of 17-allylaminogeldanamycin in relapsed/refractory pediatric patients with solid tumors: a Children's Oncology Group study.* Clin Cancer Res, 2007. **13**(6): p. 1789-93.
31. Ronnen, E.A., et al., *A phase II trial of 17-(Allylamino)-17-demethoxygeldanamycin in patients with papillary and clear cell renal cell carcinoma.* Invest New Drugs, 2006. **24**(6): p. 543-6.
32. Solit, D.B., et al., *Phase II trial of 17-allylamino-17-demethoxygeldanamycin in patients with metastatic melanoma.* Clin Cancer Res, 2008. **14**(24): p. 8302-7.
33. Heath, E.I., et al., *A phase II trial of 17-allylamino-17-demethoxygeldanamycin in patients with hormone-refractory metastatic prostate cancer.* Clin Cancer Res, 2008. **14**(23): p. 7940-6.
34. Eisenhauer, E.A., et al., *New response evaluation criteria in solid tumours: revised RECIST guideline (version 1.1).* Eur J Cancer, 2009. **45**(2): p. 228-47.
35. Neckers, L. and P. Workman, *Hsp90 molecular chaperone inhibitors: are we there yet?* Clin Cancer Res, 2012. **18**(1): p. 64-76.
36. Modi, S., et al., *HSP90 inhibition is effective in breast cancer: a phase II trial of tanespimycin (17-AAG) plus trastuzumab in patients with HER2-positive metastatic breast cancer progressing on trastuzumab.* Clin Cancer Res, 2011. **17**(15): p. 5132-9.

37. Richardson, P.G., et al., *Tanespimycin and bortezomib combination treatment in patients with relapsed or relapsed and refractory multiple myeloma: results of a phase 1/2 study*. Br J Haematol, 2011. **153**(6): p. 729-40.
38. Kim, Y.S., et al., *Update on Hsp90 inhibitors in clinical trial*. Curr Top Med Chem, 2009. **9**(15): p. 1479-92.

Appendix I

Potent Inhibition of Breast Cancer Stem Cells by a Novel Sesquiterpene Lactone MCL

Abstract

Drug discovery for cancer therapy has resulted in a wide range of new compounds, which work well in targeting the growth of the majority of tumor cells. Despite these advances, tumor relapse and metastatic progression still lack effective treatment strategies. Evidence stemming from many tumor types suggest that a subpopulation of cancer cells, termed cancer stem cells (CSCs), play a pivotal role in reinitiation of tumor growth and formation of metastatic lesions. While parthenolide and its water soluble analogue LC-1 have shown the potential of CSC targeting compounds in hematological malignancies, these compounds are rapidly eliminated from the body, and questions remain on their effectiveness in other solid tumors. Using parthenolide as a basis for new drug discovery, this study describes MCL, a novel sesquiterpene lactone, and its effectiveness against breast cancer and cancer stem cells. Treatment with MCL was effective at eliminating breast CSCs from both basal and luminal cell lines, as assayed by Aldefluor or $CD44^{+}/CD24^{-}$ expression. Additionally, tumorsphere initiation was dramatically reduced when SUM159 ALDH+ cells were cultured in 5 μM MCL. However, tumorsphere formation from ALDH+ cells treated with MCL was only slightly reduced, suggesting transient inhibition of self-renewal. Inhibition of breast CSCs was reversed with N-acetylcysteine pretreatment, suggesting a role of reactive oxygen in the activity of MCL. Unlike parthenolide, MCL was shown to directly block NF-kB activity rather than inhibit its nuclear translocation.

Building off the strengths of parthenolide and LC-1, MCL offers a new treatment strategy for breast cancer and its tumorigenic CSCs.

Introduction

Because cancer persists as a dominating health problem today, our increased understanding of the molecular mechanisms that govern tumor cells has produced a wide range of new and successful therapies. All but a few malignancies have established treatments that are capable of ameliorating tumor burden. However, while our current treatments can for the most part reduce tumor cells, relapse and metastatic progression still confound even our most sophisticated techniques. Many reports have suggested that a subpopulation of tumor cells known as cancer stem cells (CSCs), are potentially responsible for relapse and metastasis. CSCs have been shown to be highly resistant to conventional therapies,, due to their enhanced ability to repair damage and resist apoptosis. Tumors from patients that have undergone chemotherapy contain enriched populations of cells that display CSC phenotypes. It is therefore apparent that cancer treatments in the future will require the targeted elimination of these tumorigenic cells in addition to removing the tumor bulk [1-5].

Current efforts in drug discovery includes focusing on compounds which can target and eliminate CSCs, reducing the occurrence of relapse. Similar to discoveries in conventional treatments, natural products offer a starting point for identifying drugs that target CSCs. Sesquiterpene lactones are a class of drugs which have been shown to reduce inflammation and inhibit tumor cell growth [6, 7]. Parthenolide is one of the better known sesquiterpene lactones because of its ability to preferentially target CSCs over their normal equivalents [8]. This is a particularly important trait, as drugs that target

CSCs might also affect normal adult stem cells which reside in the majority of our tissues. Clinical development of parthenolide, however, was short lived due to a very low solubility in serum [9]. Later development of parthenolide analogues led to a water soluble form, LC-1. Although currently in Phase I trials for disseminated cancers, LC-1 suffers from a short half-life, which could potentially limit its efficacy [10]. The shortcomings of parthenolide and its known derivatives provide opportunities to discover novel sesquiterpene lactones which build off of the favorable characteristics of parthenolide and LC-1.

Our study addresses this opportunity and describes a novel sesquiterpene lactone (MCL) which can inhibit both breast cancer cell growth, and eliminate the tumorigenic CSC population. Cancer stem cells treated with MCL had a transient impairment of self-renewal, requiring the presence of MCL for its inhibitory effect. Interestingly, in contrast to parthenolide's known mechanism of action, MCL was found to block the activity of NF-kB directly, rather than facilitate its cytoplasmic sequestration.

Materials and Methods

Cell Lines and Reagents.

The SUM159 and SUM149 cell lines were maintained in Ham's F12 medium supplemented with 5% FBS, 5 µg/ml insulin, 1 µg/ml hydrocortisone, 1% antibiotic/antimycotic (10,000 units/ml penicillin G sodium, 10,000 µg/ml streptomycin sulfate, 25 µg/ml amphotericin B) and 20 µg/ml gentamycin. MDA-MB-231 and MCF-7 cells were maintained in RPMI 1640 medium with 10% FBS and 1%

antibiotic/antimycotic. MDA-MB-453 cells were maintained in DMEM medium supplemented with 10% FBS and 1% antibiotic/antimycotic. Cells were maintained in culture at 37°C and 10% CO2. The Aldefluor assay was purchased from Stemcell Technologies.

MTS Cell Proliferation Assay

Breast cancer cell lines were seeded into 96-well microplates at a density of 3,000 cells per well. Cells were treated with increasing concentrations of MCL (0.2–10 μM). After 72 hrs incubation, cell viability was assessed by the MTS cell proliferation assay (Promega, Madison, WI) according to the manufacturer's instruction. IC50 values were determined using the software WinNONlin (Pharsight), and was defined as the concentration necessary to decrease viability to 50% of control untreated cells.

Cancer Stem Cell Identification and Flow Cytometry Analysis

Breast cancer cell lines cells were seeded and allowed to attach overnight. Cells were then treated with increasing concentrations of MCL for three days. Next, cells were trypsinized and used for the Aldefluor assay, according to the manufacturer's protocol. For Aldefluor staining, the ALDH1 substrate bodipyaminoacetaldehyde (BAAA) was added to the single cell suspension at a concentration of 1.5 μM, which was then incubated for 40 min at 37°C. Additionally, a portion of cells was incubated with a 10-fold molar excess of an ALDH1 enzyme inhibitor, diethylamino benzaldehyde (DEAB) in addition to BAAA and incubated similarly for 40 min. For CD44/CD24 staining, single cell suspensions of MCF-7 cells were incubated for 30 minutes with CD44-APC

and CD24-PE antibodies (BD Biosciences). After the incubation, cells were washed once with HBSS containing 2% FBS. Subsequently, cells were stained with 1 μg/mL DAPI to exclude non-viable cells. Flow cytometry was performed at the University of Michigan Cancer Center Flow Cytometry Core. Data analysis was performed with the software program Weasel (Walter and Eliza Hall Institute of Medical Research).

Apoptosis Assay

Two hundred thousand SUM159 cells were seeded onto plates and allowed to attach overnight. For parthenolide treatment, cells were treated with a 5 μM concentration for 24 and 48 hours before analysis. For MCL treatment, cells were treated with either 5 μM or 8 μM for 48 hours only. After the allotted incubation time, both floating and attached cells were collected and stained with 1:20 Annexin V-APC antibody for 30 minutes on ice. Immediately before analysis, 1 μg/mL propidium iodide was added to each sample. Flow cytometry was performed at the University of Michigan Cancer Center Flow Cytometry Core. Data analysis was performed with the software program Weasel (Walter and Eliza Hall Institute of Medical Research).

Tumorsphere Formation

SUM159 ALDH+ cells were plated onto ultralow-attachment 96-well plates (Corning, Corning, NY) at a density of one cell per well. To promote the formation of tumorspheres, these single cells were grown in a serum-free mammary epithelial basal medium (MEBM) (Cambrex Bio Science Walkersville, Inc,) supplemented with B27 (Invitrogen, Carlsbad, CA,), 20 ng/mL EGF (BD Biosciences, San Jose, CA), antibiotic-

antimycotic (100 unit/ml penicillin G sodium, 100 ug/ml streptomycin sulfate and 0.25 μg/ml amphotericin B), 20 μg/ml Gentamycin, 1 ng/ml Hydrocortisone, 5 μg/ml Insulin, and 100 μM beta-mercaptoethanol (Gibco Invitrogen, Carlsbad, CA) in a humidified incubator (10% CO2, 37°C). For drug treatment, single ALDH+ cells were given MEBM medium containing supplements and 5 μM MCL or DMSO for 7 days. Primary tumorspheres were then counted and mechanically and enzymatically dissociated into single cell suspensions for the second and third passage. Single cell suspensions were plated onto ultralow-attachment 96-well plates at a low cellular density of less than 5 cells per well, and cultured in the absence of drug treatment. Tumorsphere formation rate was calculated as the ratio of the number of tumorspheres to the number of seeded cells.

N-acetylcysteine Treatment

SUM159 cells were plated and allowed to attach overnight. Cells were given 5 mM N-acetylcysteine and placed in a humidified incubator (10% CO2, 37°C) for 3 hours. After the pretreatment, the medium containing NAC was aspirated and each plate was washed with PBS. Medium was then replenished with the addition of MCL, parthenolide or vehicle control. After 72 hours, cells were trypsinized and used for the Aldefluor assay, as described above.

Immunocytochemistry

Two thousand SUM159 cells were seeded into black 96-well plates with optically clear bottoms and allowed to attach overnight. Cells were then treated with parthenolide or MCL for 24, 48, and 72 hours. At the end of each treatment, cells were treated with 10

ng/mL of TNFα for 30 minutes. After the TNFα treatment, medium was aspirated and cells were washed once with PBS. Next, PBS was aspirated and the cells were fixed in -20°C chilled methanol:acetone mixture (50:50 v/v). Fixative was then removed and cells were allowed to air dry before being blocking with 5% normal goat serum. After blocking, cells were incubated with blocking solution containing rabbit anti-p65 NF-kB antibody (Santa Cruz) for 1 hour. Cells were then washed twice with PBS, followed by incubation in blocking buffer with Alexa Fluor 488-conjugated goat anti-rabbit antibody. After washing with PBS, cells were treated with 1 ug/mL DAPI for nuclear staining and pictures were taken.

Lentiviral Transfection and Luciferase Assay

SUM159 and MDA-MB-231 breast cancer cells were plated and grown to 75% confluency. These cells were then washed with PBS and treated with medium containing a GreenFire Protein and firefly luciferase lentivirus which was under the control of either NF-kB response elements (RE), or the MCMV promoter for a control (Systems Biosciences). After culturing the cancer cells for 24 hours at 37 degrees C, an equal volume of normal culture medium was combined with the lentivirus medium, and the cells were grown for an additional 3 days. To ensure near 100% infection efficiency, SUM159 and MDA-MB-231 cells treated with lentivirus were sorted with a flow cytometer, using GFP expression as a marker for successful infection. To perform the luciferase assay, 2,500 SUM159 or MDA-MB-231 transfected with either the NF-kB RE or MCMV promoter lentivirus were plated into a white 96-well plate (Nunc) and allowed to attach overnight. These cells were then treated with parthenolide or MCL for 5 hours

prior to stimulation with 10 ng/ml TNFα for an additional 6 hours. Following stimulation with TNFα, cells were given One-Glo (Promega) reagent and allowed to sit at room temperature for 4 minutes before being read on Biotek Synergy 2 plate reader.

Statistics

The Student t-test was used to perform statistical analysis.

Results

MCL Eliminates both Differentiated and CSC Populations

In order to determine the ability of MCL to effect viability of breast cancer cells, several different breast cancer cell lines were used. One claudin-low (SUM159), two basal (SUM149, MDA-MB-231) and two luminal breast cancer cell lines (MCF-7, luminal A; MDA-MB-453, luminal B) were treated with increasing concentrations of MCL for three days before determining cell viability with the MTS assay (Figure I.1) [11]. The basal breast cancer cells were more susceptible to MCL mediated inhibition (IC50 7-8.4) as compared to the luminal cell lines (IC50 10.6-10.9). We next determined if MCL affects CSCs present within each cell line. Cells that display stem cell properties can be isolated from normal human breast tissue, breast carcinomas and cancer cell lines, by virtue of their increased expression of aldehyde dehydrogenase (ALDH) activity as assessed by the Aldefluor assay [12]. Additionally, ALDH+ cells have been shown to be highly tumorigenic as compared to ALDH- cells, and elevated expression of ALDH gene in patience has been correlated with a poorer prognosis in IBC [12, 16]. Therefore, we measured the CSC population within several cell lines by using the Aldefluor assay, as

well as with antibodies for the CSC-identifying surface markers CD44 and CD24. Breast cancer cells (SUM159, SUM149, MDA-MB-231, and MDA-MB-453) treated with increasing concentrations of MCL exhibited a reduction in the ALDH+ population (Figure I.2A,B). SUM159 and MDA-MB-231 ALDH+ cells were the most sensitive to MCL treatment, with 5 μM MCL reducing the percentage of ALDH+ cells by 82% and 77%, respectively. SUM149 ALDH+ cells, while increased in percentage with 5 μM MCL, were reduced in absolute number by 33.6%. Interestingly, CSCs present in the luminal cell lines MCF-7 ($CD44^+/CD24^-$ cells) and MDA-MB-453 (ALDH+ cells) required a higher concentration (8 μM) for inhibition, relative to the basal cell effective concentrations (5 μM) (Figure I.2B,C). This suggests that CSCs from the more basal like cell lines (SUM159, SUM149, MDA-MB-231) were more sensitive to the effects of MCL than the luminal cell lines.

Parthenolide has been shown to preferentially induce apoptosis in CSCs [17]. This was confirmed in SUM159 breast cancer cells, as ALDH+ cells were preferentially induced into apoptosis over the ALDH- cells with increasing incubation time with parthenolide (Figure I.3A). When SUM159 cells were treated with increasing concentrations of MCL, 8 μM was found to preferentially induce apoptosis in ALDH+ cells over the ALDH- cells by 2-fold (Figure I.3B). However, 5 μM MCL failed to induced apoptosis in ALDH+ cells after a 48 hour incubation. As this concentration was capable of reducing the number of CSCs, MCL likely relies on a separate mechanism for bringing about this effect on CSCs at a lower concentration.

MCL Can Transiently Reduce CSC Self-Renewal

Stem and cancer stem cells maintain their numbers through a process of asymmetric cell division, called self-renewal. Through a tightly controlled process, this division generates an identical stem cell and a daughter cell, with only the former having the full ability for further self-renewal. By keeping this ratio of stem and daughter cells the same, normal tissues can maintain a low number of stem cells which potentially reduces the risk of an aberrant outgrowth. It is widely believed that a failure in the control mechanisms for self-renewal is a likely instigator of CSC formation [18]. Therefore, one approach for treating CSCs would be to interfere with self-renewal, and thereby reduce the proliferation of these cells. Quantifying breast CSC self-renewal can be done through observing changes in the number of formed spheroid colonies, called tumorspheres. It is believed that formation of tumorspheres is governed by the CSC, and during the growth of the tumorsphere, the number of CSCs within the tumorsphere can change depending on their self-renewal capacity [19]. To test if MCL can impair breast CSC self-renewal, single SUM159 ALDH+ cells were plated into ultra-low attachment plates at a density of one cell per well, treated with MCL or vehicle, and allowed to form tumorspheres. After a seven day incubation, 5μM of MCL reduced the tumorsphere formation by 74% ($p<0.01$) (Figure I.4A). Tumorspheres from either condition were then dissociated into single cells and replated at 5 cells/well under drug free conditions. Observing the level of tumorsphere formation without MCL provides a method to determine if impairment of self-renewal with MCL is either permanent or transient. After seven days, tumor cells that were previously incubated with MCL formed 26% ($p<0.05$) fewer tumorspheres than tumor cells from vehicle-treated tumorspheres. Additionally, in

the third passage of tumorspheres, the number of formed tumorspheres between the previously treated and control groups were indistinguishable. Lastly, tumorsphere size (believed to reflect the proliferation rate of progenitor cells) was not largely affected by the presence of MCL (Figure I.4B) [19, 20]. These data suggest that disruption of self-renewal by MCL is transient, and requires the presence of MCL to exhibit inhibition on CSCs.

MCL May Increase Oxidative Stress Through Inhibition of NF-kB

One of the mechanisms parthenolide uses to kill tumor and CSCs is the production of oxidative stress (ROS). As a potent inhibiter of NF-kB, parthenolide disrupts this key signaling pathway which functions to protect cells from oxidative stress induced damage. The majority of sesquiterpene lactones appear to share this characteristic ability to inhibit NF-kB [7, 21]. Additionally, an epoxide contained within the parthenolide structure promotes ROS formation, further exacerbating the damage which the tumor cells accumulate and eventually succumb to [22]. The requirement for ROS formation for parthenolide toxicity can be illustrated with the use of a potent antioxidant N-acetylcysteine (NAC). Pretreating tumor cells with NAC can abolish the effects of parthenolide by providing a free radical sink to absorb formed ROS [17]. To determine if NAC could disrupt the CSC killing effect of parthenolide or MCL, SUM159 breast cancer cells were first pretreated with either 5 mM NAC or PBS for 3 hours. After the allotted time, the cells were washed and treated with 5 μM parthenolide or MCL. Parthenolide treatment reduced the percentage of ALDH+ cells by 92%. However, pretreatment with NAC partially attenuated parthenolide cytotoxicity, reducing ALDH+

cells by only 51% (Figure I.5). Similar results were seen with MCL. SUM159 cells treated with MCL had a 67% reduction in ALDH+ cells. This reduction in CSCs was completely abolished in cells pretreated with NAC. These results suggest reactive oxygen may be a potential facilitator of parthenolide and MCL cytotoxicity in breast CSCs.

As stated above, parthenolide elicits most of its activity through the disruption of NF-kB signaling. In a normal cell, NF-kB is sequestered in the cytoplasm by IkB, which upon cell stimulation or oxidative stress, is phosphorylated and degraded. This releases NF-kB, allowing it to translocate to the nucleus to promote transcription of repair genes. Parthenolide facilitates the accumulation of oxidative damage by disrupting the kinase which helps degrade IkB and the release of NF-kB. To determine if parthenolide mediated cytoplasmic retention of NF-kB holds true for breast cancer cells, SUM159 cells were plated into 96-well plates and allowed to attach overnight. These cells were then pretreated with 5 μM parthenolide before stimulation with TNFα, a cytokine known to stimulate NF-kB nuclear translocation. Using an immunofluorescent stain for the p65 subunit of NF-kB, SUM159 cells not stimulated with TNFα show a distinctive cytoplasmic staining for NF-kB (Figure I.6A). Upon TNFα stimulation, NF-kB staining produces a very strong nuclear signal, as TNFα drives the release of IkB and translocation to the nucleus. In contrast, pretreatment with parthenolide blocked NF-kB nuclear translocation at all time points, as typically seen in other studies [23, 24]. Interestingly, MCL did not block NF-kB translocation, even with a 72 hour pretreatment (Figure I.6B). Only when SUM159 cells were pretreated with 20 μM of MCL before TNFα stimulation was NF-kB retained in the cytoplasm (data not shown). As this level

of drug is four times the amount necessary to kill ALDH+ cells, it is evident that blockade of NF-kB nuclear transport is not the principle mechanism of CSC elimination.

Although transcriptional activity is often inferred from NF-kB nuclear translocation, this is not a direct measurement of its effect on target genes. While MCL failed to block the translocation of NF-kB, we wished to examine whether t MCL could directly interact with NF-kB, regardless of its cellular location, and thereby block its transcriptional activity. A similar interaction has been previously reported with helenalin, a sesquiterpene lactone which blocks NF-kB directly, while failing to prevent NF-kB nuclear translocation [25]. To determine if MCL mimicked this phenomena, a lentiviral construct consisting of a luciferase reporter under the control of NF-kB binding sites within its promoter was transfected into SUM159 and MDA-MB-231 breast cancer cells. Similar to the immunofluorescence results, luciferase signal was only detected after NF-kB stimulation with TNFα (Figure I.7). In accord with its ability to block NF-kB translocation, luciferase signal was completely abolished in SUM159 and MDA-MB-231 cells pretreated with parthenolide. However, while failing to block NF-kB translocation in SUM159 cells, MCL pretreatment reduced the TNFα induced luciferase signal in a dose dependent manner. These results suggest MCL is also capable of NF-kB inhibition, albeit through a direct mechanism, and provides a possible target for eliciting its inhibition on both the cancer and CSCs.

Discussion

Conventional cancer treatments have shown to be limited in their ability to reduce the rates of recurrence and metastatic progression. While capable of alleviating some level of tumor burden for many cancers, conventional therapies fail to reduce tumor-initiating CSCs, which studies have shown to be likely contributors to both tumor relapse and metastasis [1-5]. Fortunately, our growing knowledge of CSCs has yielded some potential drug candidates which have shown promising efficacy [26]. Parthenolide, in particular, has shown to not only potently inhibit AML stem cells, but do so selectively by sparing normal hematopoietic stem cells [8]. This is a tremendously desirable trait, as normal tissues harbor resident adult stem cells which play a vital role in tissue function. Interest in parthenolide promoted further development, leading to an orally bioavailable, water soluble form LC-1. While successfully circumventing parthenolide's poor solubility, LC-1 is rapidly eliminated from the body, potentially limiting its use to circulating cancers in the blood. In order to identify new compounds which, like parthenolide and LC-1, can kill CSCs, we screened novel derivatives of parthenolide and identified MCL as an effective inhibitor of CSCs.

We first examined the effects of MCL on breast cancer cells and stem cells in vitro, using the MTS and Aldefluor assays. In our study, we demonstrated that MCL not only reduced breast cancer cell viability, but also the percentage of breast CSCs present in both basal and luminal cell lines. While preferential induction of apoptosis in breast CSCs by parthenolide has been validated in our study, only high doses of MCL generated apoptosis in SUM159 ALDH+ cells. To determine if the effects of MCL were

produced through disruption of CSC self-renewal, Aldefluor+ cells were allowed to generate tumorspheres in the presence of MCL. The first generation of tumorspheres was markedly reduced under these conditions, compared to the number generated from our vehicle treated controls. Additionally, we replated single cells obtained from the MCL and vehicle treated first generation tumorspheres in drug-free medium in order to observe if self-renewal was disrupted permanently. While there did appear to be a reduction in tumorsphere formation from the previously treated MCL cells, the level of self-renewal inhibition was lower than what was observed when the CSCs were exposed to the drug. These results show that while MCL is a potent inhibitor of both the bulk population of breast cancer cells and CSCs, the effects are governed only partially through disruption of self-renewal, and rely on cell death mechanisms other than apoptosis at lower concentrations.

One of the mechanisms by which parthenolide is believed to function through is the production of reactive oxygen [21]. ROS formation is highly toxic to living cells as these free radicals can covalently modify nearly any molecule they encounter [27]. Cellular defenses rely on the high concentration of glutathione produced inside the cell, which absorb ROS and keep damage away from vital cellular components [28]. Pretreating cells with N-acetylcysteine, a precursor to glutathione that can also reverse cysteine modifications, is capable of reversing parthenolide's effects, demonstrating the requirement for ROS formation [17]. Likewise, our pretreatment of NAC on SUM159 breast cancer cells before exposure to MCL also reversed our compound's ability to reduce the CSC population. Similar to parthenolide, MCL potentially requires ROS for mediating its inhibition on CSCs. Another mechanism by

which sesquiterpene lactones like parthenolide inhibit cancer and CSCs is through a blockade of NF-kB mediated gene regulation. Parthenolide inhibits NF-kB nuclear translocation by disrupting a kinase that releases NF-kB from its cytoplasmic tether IkB [22]. Using immunofluorescence, we tracked NF-kB translocation after pretreatment of MCL followed by stimulation with TNFα. Unlike parthenolide, MCL failed to block NF-kB translocation. However, other sesquiterpene lactones, such as Helenalin, have shown that disruption of NF-kB translocation is not a necessary requirement for its inhibition [25]. In line with this reasoning, more recent studies with parthenolide have shown blockade of NF-kB nuclear translocation may not be the predominate mechanism for drug activity, instead relying on direct alkylation of cysteine 38, an NF-kB amino acid crucial for DNA binding [29]. Using a NF-kB mediated luciferase reporter, we demonstrated that, like Helenalin, pretreatment with MCL could prevent NF-kB activity, regardless of failing to prevent nuclear translocation. This raises the possibility that MCL disrupts NF-kB directly, thereby blocking its ability to regulate gene expression.

It is tempting to speculate that the differences in sensitivity observed between the cancer cells in the different cell lines with MCL treatment could be explained by their dependence on NF-kB gene regulation. Indeed, constitutive NF-kB activity was found to be higher in basal breast cancer cells than luminal cell lines, and was preferentially involved in their proliferation [30]. In agreement with this study are reports that EZH2, a Polycomb protein crucial for self-renewal and expansion of breast CSCs, has been shown to enhance NF-kB activity in basal breast cancer cells, while repressing NF-kB activity in luminal breast cancer cells [31, 32]. IL-6, a cytokine with known involvement in CSC self-renewal, was reduced in MDA-MB-231 and increased in MCF-7 cells following

EZH2 knockdown, further illustrating the dichotomy in NF-kB regulation between breast cancer subtypes. It could be possible that luminal cells and their suspected stem cell component, having reduced NF-kB activity, rely less on this signaling pathway for a driving force, and so would exhibit a subdued response to MCL mediated NF-kB inhibition. In this regard, future studies with MCL should focus on NF-kB reliant breast cancers, such as those arising from aggressive ER-/PR-/Her2- basal-like cells.

Our study describes a novel derivative of parthenolide that shares in the ability to target breast cancer cells and stem cells. As more studies acknowledge the problem CSCs pose on successful cancer therapy, it is important to scrutinize newly introduce inhibitors for their ability to target this cancer subpopulation. By choosing parthenolide as a starting point for our drug discovery, our compound has shown to be effective against both breast cancer and the CSC subpopulation. As more treatments that target CSCs are developed and incorporated with conventional therapy, the elimination of one of the oldest global health problems may finally be within reach.

References

1. Reya, T., et al., *Stem cells, cancer, and cancer stem cells.* Nature, 2001. **414**(6859): p. 105-11.
2. Gangemi, R., et al., *Cancer stem cells: a new paradigm for understanding tumor growth and progression and drug resistance.* Curr Med Chem, 2009. **16**(14): p. 1688-703.
3. Morrison, B.J., et al., *Breast cancer stem cells: implications for therapy of breast cancer.* Breast Cancer Res, 2008. **10**(4): p. 210.
4. Lawson, J.C., G.L. Blatch, and A.L. Edkins, *Cancer stem cells in breast cancer and metastasis.* Breast Cancer Res Treat, 2009.
5. Ischenko, I., et al., *Cancer stem cells: how can we target them?* Curr Med Chem, 2008. **15**(30): p. 3171-84.
6. Hall, I.H., et al., *Anti-inflammatory activity of sesquiterpene lactones and related compounds.* J Pharm Sci, 1979. **68**(5): p. 537-42.
7. Ghantous, A., et al., *What made sesquiterpene lactones reach cancer clinical trials?* Drug Discov Today. **15**(15-16): p. 668-78.
8. Guzman, M.L., et al., *An orally bioavailable parthenolide analog selectively eradicates acute myelogenous leukemia stem and progenitor cells.* Blood, 2007. **110**(13): p. 4427-35.
9. Sweeney, C.J., et al., *The sesquiterpene lactone parthenolide in combination with docetaxel reduces metastasis and improves survival in a xenograft model of breast cancer.* Mol Cancer Ther, 2005. **4**(6): p. 1004-12.
10. Grant, S., *New agents for AML and MDS.* Best Pract Res Clin Haematol, 2009. **22**(4): p. 501-7.
11. Herschkowitz, J.I., et al., *Identification of conserved gene expression features between murine mammary carcinoma models and human breast tumors.* Genome Biol, 2007. **8**(5): p. R76.
12. Ginestier, C., et al., *ALDH1 is a marker of normal and malignant human mammary stem cells and a predictor of poor clinical outcome.* Cell Stem Cell, 2007. **1**(5): p. 555-67.
13. Charafe-Jauffret, E., et al., *Aldehyde dehydrogenase 1-positive cancer stem cells mediate metastasis and poor clinical outcome in inflammatory breast cancer.* Clin Cancer Res. **16**(1): p. 45-55.
14. Guzman, M.L., et al., *The sesquiterpene lactone parthenolide induces apoptosis of human acute myelogenous leukemia stem and progenitor cells.* Blood, 2005. **105**(11): p. 4163-9.
15. O'Brien, C.A., A. Kreso, and C.H. Jamieson, *Cancer stem cells and self-renewal.* Clin Cancer Res. **16**(12): p. 3113-20.
16. Dontu, G., et al., *In vitro propagation and transcriptional profiling of human mammary stem/progenitor cells.* Genes Dev, 2003. **17**(10): p. 1253-70.
17. Korkaya, H., et al., *HER2 regulates the mammary stem/progenitor cell population driving tumorigenesis and invasion.* Oncogene, 2008. **27**(47): p. 6120-30.

18. Pajak, B., B. Gajkowska, and A. Orzechowski, *Molecular basis of parthenolide-dependent proapoptotic activity in cancer cells.* Folia Histochem Cytobiol, 2008. **46**(2): p. 129-35.
19. Hehner, S.P., et al., *Sesquiterpene lactones specifically inhibit activation of NF-kappa B by preventing the degradation of I kappa B-alpha and I kappa B-beta.* J Biol Chem, 1998. **273**(3): p. 1288-97.
20. Hehner, S.P., et al., *The antiinflammatory sesquiterpene lactone parthenolide inhibits NF-kappa B by targeting the I kappa B kinase complex.* J Immunol, 1999. **163**(10): p. 5617-23.
21. Kwok, B.H., et al., *The anti-inflammatory natural product parthenolide from the medicinal herb Feverfew directly binds to and inhibits IkappaB kinase.* Chem Biol, 2001. **8**(8): p. 759-66.
22. Lyss, G., et al., *The anti-inflammatory sesquiterpene lactone helenalin inhibits the transcription factor NF-kappaB by directly targeting p65.* J Biol Chem, 1998. **273**(50): p. 33508-16.
23. Takebe, N., et al., *Targeting cancer stem cells by inhibiting Wnt, Notch, and Hedgehog pathways.* Nat Rev Clin Oncol. **8**(2): p. 97-106.
24. Wei, Y.H., et al., *Oxidative damage and mutation to mitochondrial DNA and age-dependent decline of mitochondrial respiratory function.* Ann N Y Acad Sci, 1998. **854**: p. 155-70.
25. Pani, G., T. Galeotti, and P. Chiarugi, *Metastasis: cancer cell's escape from oxidative stress.* Cancer Metastasis Rev. **29**(2): p. 351-78.
26. Garcia-Pineres, A.J., et al., *Cysteine 38 in p65/NF-kappaB plays a crucial role in DNA binding inhibition by sesquiterpene lactones.* J Biol Chem, 2001. **276**(43): p. 39713-20.
27. Yamaguchi, N., et al., *Constitutive activation of nuclear factor-kappaB is preferentially involved in the proliferation of basal-like subtype breast cancer cell lines.* Cancer Sci, 2009. **100**(9): p. 1668-74.
28. Chang, C.J., et al., *EZH2 promotes expansion of breast tumor initiating cells through activation of RAF1-beta-catenin signaling.* Cancer Cell. **19**(1): p. 86-100.
29. Lee, S.T., et al., *Context-specific regulation of NF-kappaB target gene expression by EZH2 in breast cancers.* Mol Cell. **43**(5): p. 798-810.

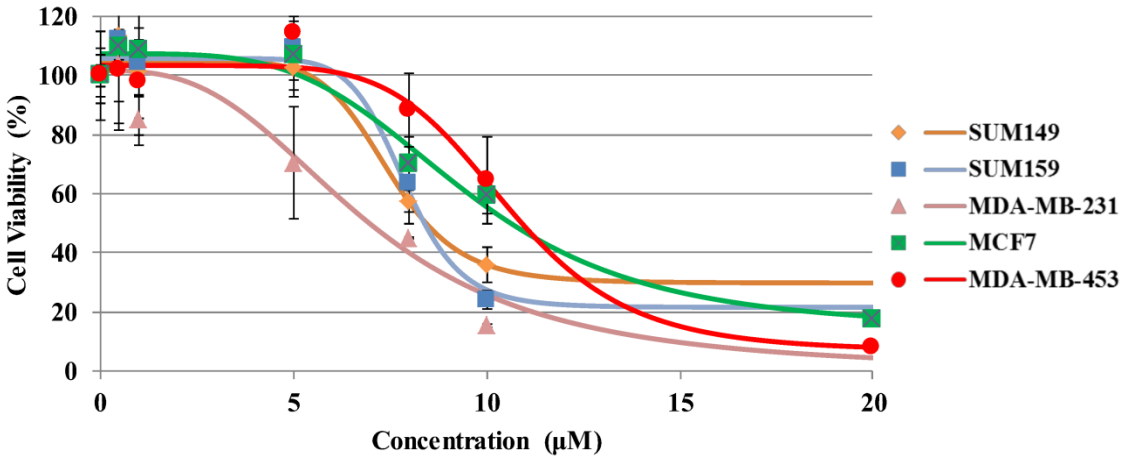

Figure I.1. Breast cancer cell sensitivity to MCL. Breast cancer cells were treated with increasing concentrations of MCL, and assessed for viability using the MTS assay. Basal and Claudin-low cell lines were more sensitive to MCL (IC50 7-8.4) than luminal cell lines (IC50 10.6-10.9).

Figure I.2 Effect of MCL on breast cancer stem cells. (A) Treatment of SUM159 cells with MCL decreased the percentage of ALDH+ in a dose dependent manner. (B) Basal breast cancer lines SUM149 and MDA-MB-231 saw reduction in ALDH+ beginning at 5 μM MCL. The luminal cell line MDA-MB-453 required a higher concentration (8 μM) of MCL to reduce its ALDH+ population. (C) $CD44^{+}/CD24^{-}$ MCF-7 cells were the least sensitive CSCs to MCL treatment.

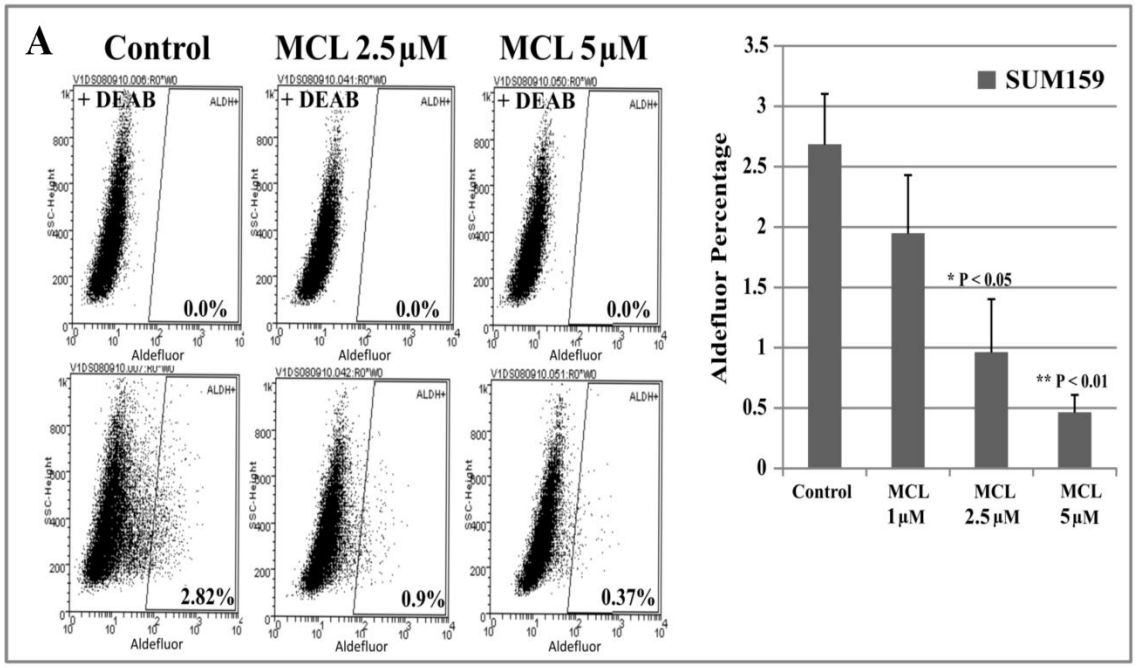
A
Control
MCL 2.5μM
MCL 5μM
+ DEAB
ALDH+
0.0%
2.82%
0.9%
0.37%
SSC-Height
Aldefluor
SUM159
Aldefluor Percentage
* P < 0.05
** P < 0.01
Control
MCL 1μM
MCL 2.5μM
MCL 5μM

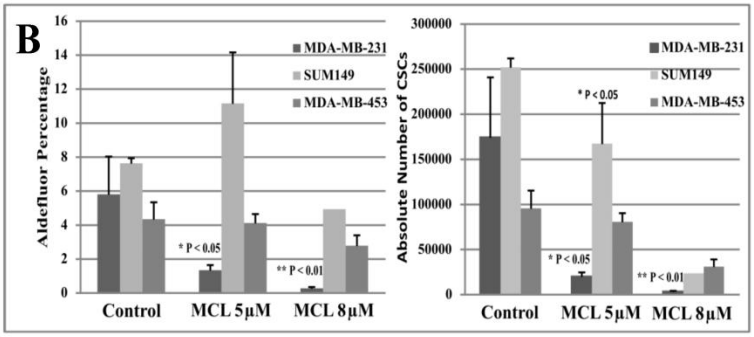
B
MDA-MB-231
SUM149
MDA-MB-453
Aldefluor Percentage
Absolute Number of CSCs
* P < 0.05
** P < 0.01
Control
MCL 5μM
MCL 8μM

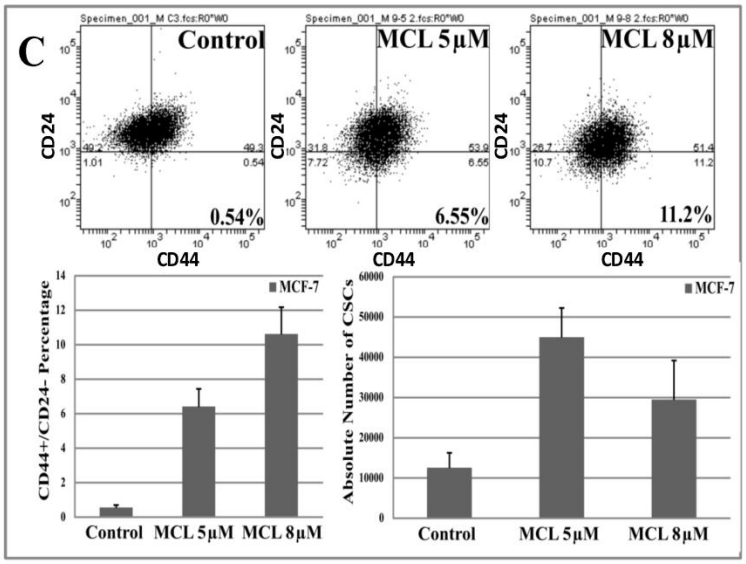
C
Control
MCL 5μM
MCL 8μM
CD24
CD44
0.54%
6.55%
11.2%
MCF-7
CD44+/CD24- Percentage
Absolute Number of CSCs
Control
MCL 5μM
MCL 8μM

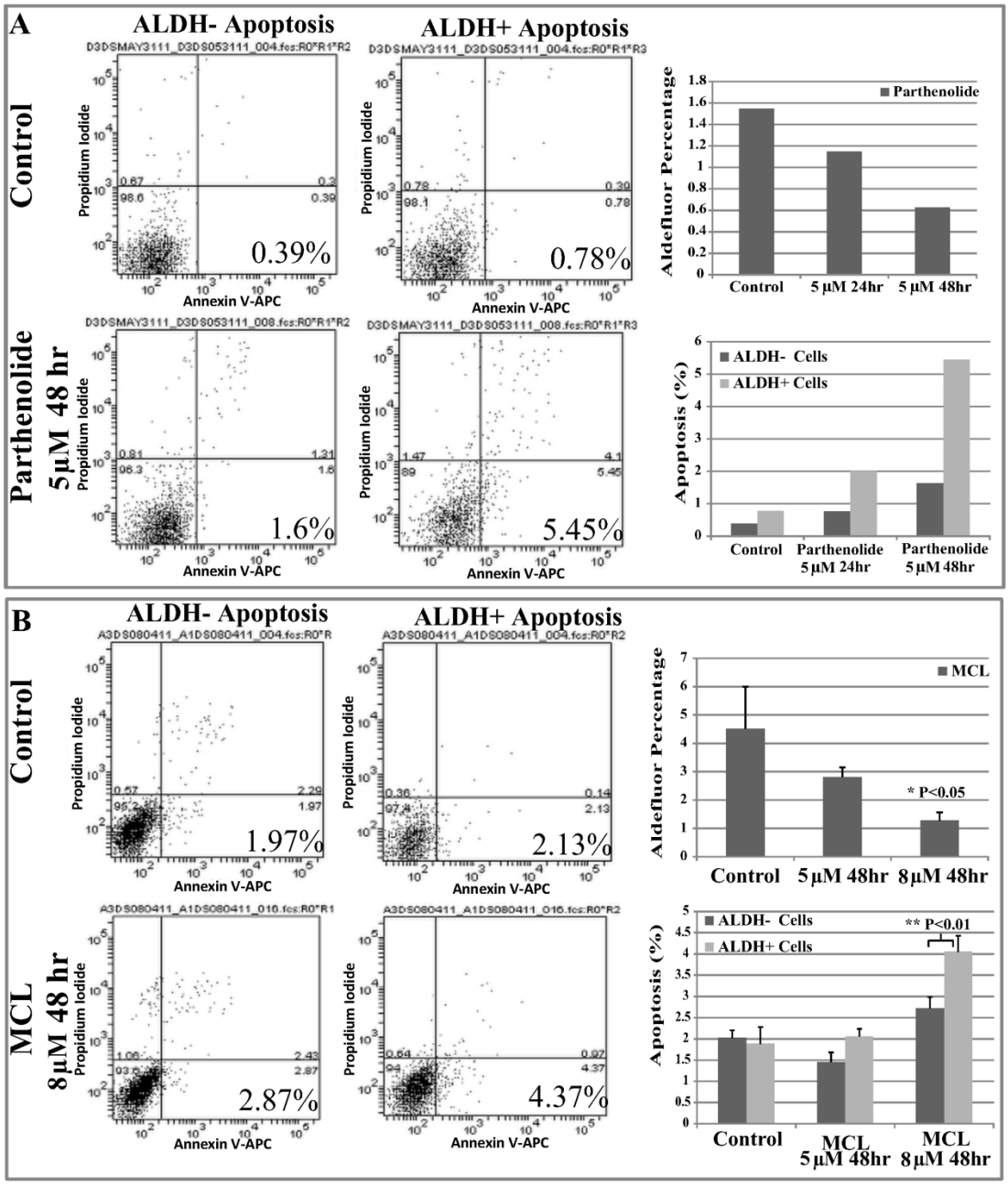

Figure I.3 Induction of apoptosis with parthenolide and MCL. (A) SUM159 cells treated with 5 µM parthenolide for 24 and 48 hours showed selective induction of apoptosis within the CSC population. (B) In contrast to parthenolide, induction of apoptosis was only observed after a 48 hour incubation with high concentration (8 µM) MCL.

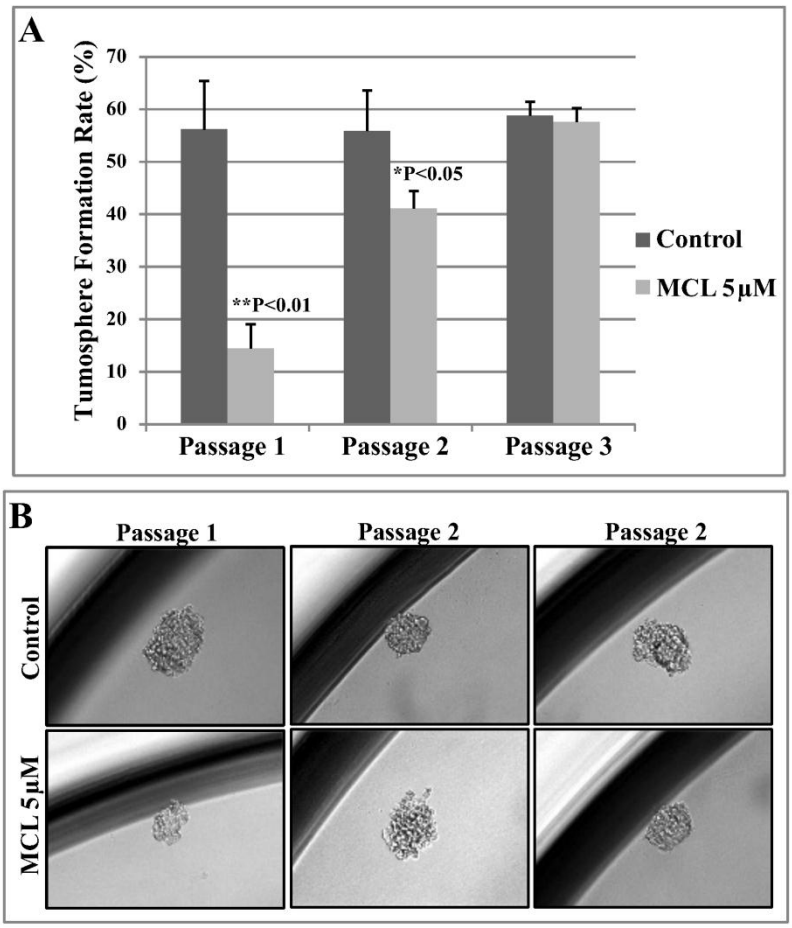

Figure I.4 Effects of MCL on breast CSC self-renewal. (A) The ratio of the number of spheres to the number of seeded ALDH+ cells represents the tumorsphere formation rate (%). Single ALDH+ SUM159 cells treated with 5 μM MCL had a diminished capacity to form tumorspheres. Under drug-free conditions, replated cells from MCL treated tumorspheres showed a modest inhibition on self-renewal, as compared to the control. (B) No significant differences were seen in tumorsphere size between cells treated with MCL or vehicle.

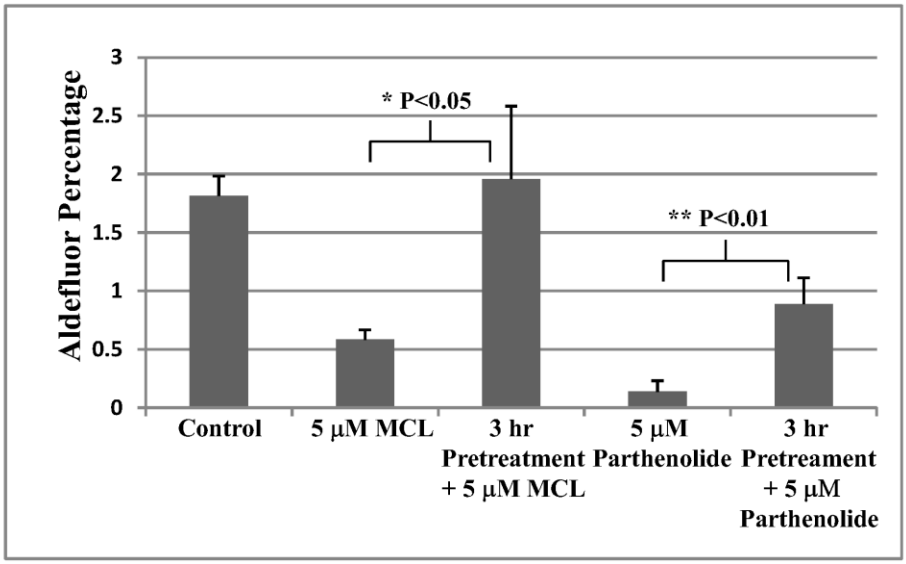

Figure I.5 The role of reactive oxygen species (ROS) in MCL's efficacy. Parthenolide is known to facilitate generation of ROS, leading to cell death. Pretreating SUM159 cells with 5 mM N-acetylcysteine (NAC), a precursor to glutathione, reduced the efficacy of parthenolide against ALDH+ cells. Similarly, NAC pretreatment abolished MCL's ability to eliminate ALDH+ cells.

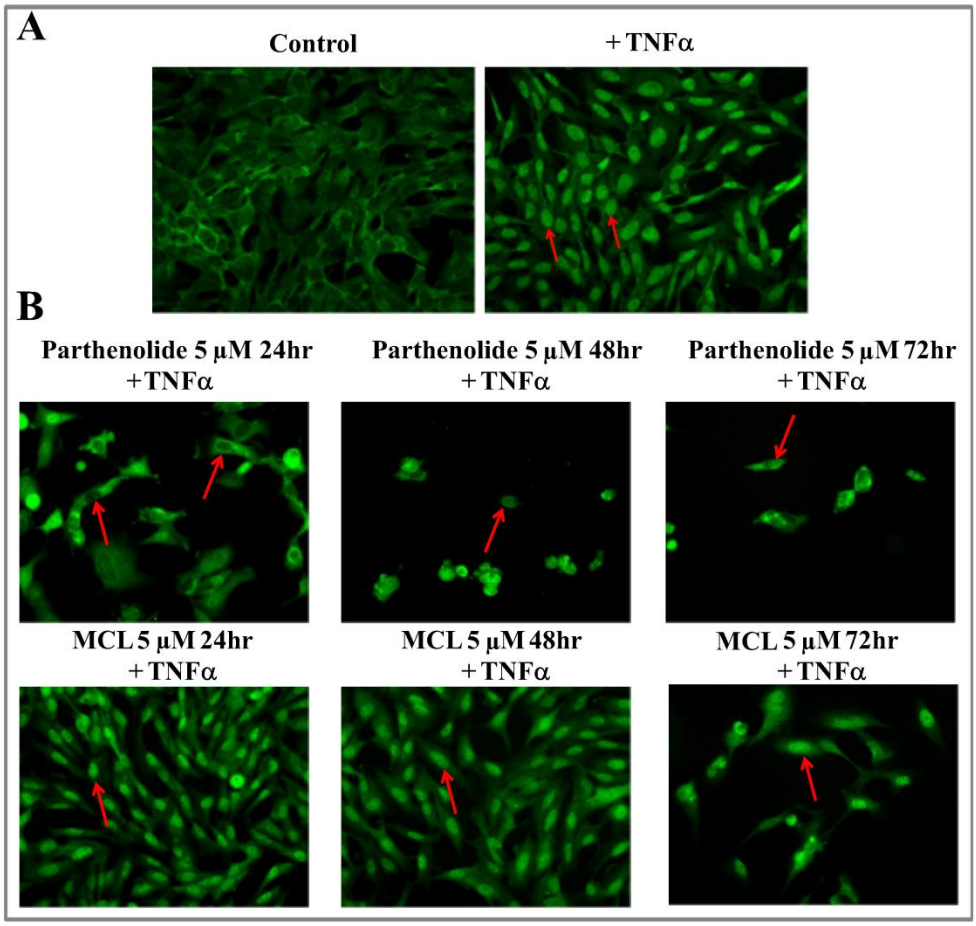

Figure I.6 Regulation of NF-kB translocation. (A) Staining of fixed SUM159 cells for the p65 subunit of NF-kB showed the typical cytoplasmic pattern. Upon stimulation with TNFα, NF-kB can be seen translocating to the nucleus for gene regulation. (B) Parthenolide is a well-known inhibitor of NF-kB translocation. Twenty four hour pretreatment of SUM159 cells with parthenolide prevented NF-kB translocation after TNFα stimulation. In contrast, MCL pretreatment failed to block NF-kB translocation after stimulation, at all time points.

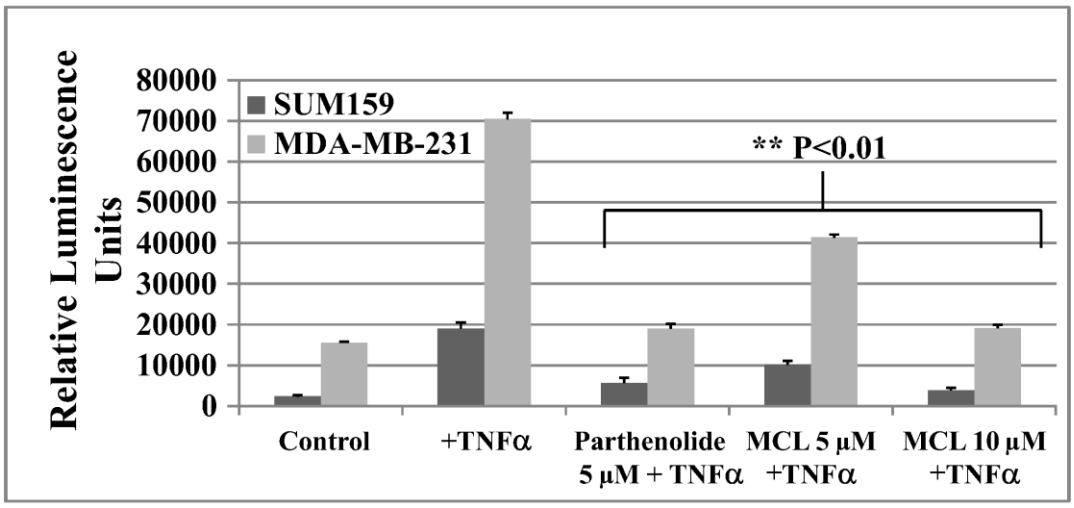

Figure I.7 Regulation of NF-kB Activity. SUM159 and MDA-MB-231 cells were transfected with a lentivirus harboring firefly luciferase downstream a NF-kB (or MCMV as a control) regulated promoter. Stimulation with TNFα induced luciferase activity of both SUM159 and MDA-MB-231 cells. Pretreatment with parthenolide before TNFα stimulation prevented the induction of luciferase. While failing to block NF-kB translocation, pretreatment of MCL before TNFα stimulation also blocked induction of luciferase, suggesting direct inhibition of the NF-kB protein.